Structural and mechanistic insights into ABC-type ECF transporters for vitamin uptake

Dosz-Majsnerowska, Maria

Structural and mechanistic insights into ABC-type ECF transporters for vitamin uptake

Maria Dosz-Majsnerowska

Cover design: Jadwiga Majsnerowska and Maria Dosz-Majsnerowska
Printed & Lay Out by:Proefschriftmaken.nl | | Uitgeverij BOXPress
Published by:Uitgeverij BOXPress, 's-Hertogenbosch

ISBN: 978-90-367-6692-0

This Ph.D. study was carried out in the Biochemistry Department of the Groningen Biomolecular Sciences and Biotechnology Institute of the University of Groningen and was financially supported by the Netherlands Organization for Scientific Research (NWO).

rijksuniversiteit
groningen

Structural and mechanistic insights into ABC-type ECF transporters for vitamin uptake

PhD thesis

to obtain the degree of PhD at the
University of Groningen
on the authority of the
Rector Magnificus, Prof. E. Sterken
and in accordance with
the decision by the College of Deans.
This thesis will be defended in public on
Friday 17 January 2014 at 11:00

by

Maria Dosz-Majsnerowska
born on 8 August 1984
in Wrocław, Poland

Supervisor:
Prof. D.J. Slotboom

Assessment committee:
Prof. M. W. Fraaije
Prof. E.J. Boekema
Prof. A.M. van Oijen

Rodzicom, Maćkowi, Rodzeństwu i Mamie Gabrysi

CONTENT

Chapter 1

Introduction

Parts of this chapter are based on:
Guus B. Erkens,
Maria Majsnerowska,
Josy ter Beek
and Dirk Jan Slotboom.

Energy Coupling Factor - Type ABC transporters
for Vitamin Uptake in Prokaryotes (2012).
Biochemistry 51 4390-4396

ABSTRACT

Energy Coupling Factor (ECF) transporters are a subgroup of ATP-Binding Cassette (ABC) transporters involved in the uptake of vitamins and micronutrients in prokaryotes. In contrast to classical ABC importers, ECF transporters do not make use of water-soluble substrate binding proteins or domains (SBPs or SBDs), but instead employ integral membrane proteins for substrate binding (named S-components). S-components form active translocation complexes with the ECF module, an assembly of two nucleotide-binding domains (NBDs, or EcfA) and a second transmembrane protein (EcfT). In some cases the ECF module is dedicated to a single S-component, but in many cases the ECF module can interact with several different S-components which are unrelated in sequence and bind diverse substrates. The modular organization with exchangeable S-components on a single ECF module enables the transport of chemically different substrates via a common route. The determination of the crystal structures of the S-components that recognize thiamin (ThiT), biotin (BioY) and riboflavin (RibU) have provided the first clue about the mechanism of S-component exchange. The recent crystal structures of two complete ECF-S-component complexes revealed that the orientation of the S-components in the membrane is highly unusual. Whereas in the absence of the ECF module S-components consist of six membrane-spanning α-helices, and the substrate-binding site is located close to the outer surface, in the presence of ECF module the S-components topple over, with the α-helices lying almost parallel to the membrane plane, exposing the binding site to the cytoplasm. This unexpected ability of the S-components suggests a unique mechanism that allows ECF transporters to translocate solutes across the membrane. This chapter describes the recent advances and the current views on the mechanism of transport by ECF transporters.

Architecture of ABC transporters

All cells separate their inside from the surrounding environment by the cell membrane which doesn't allow water soluble molecules to pass through. Hydrophobic, membrane embedded proteins facilitate an import and export of a broad range of compounds. ATP Binding Cassette (ABC) transporters form one of the largest superfamily of membrane protein complexes involved in the transport of a wide variety of substrates at the expense of ATP hydrolysis (Davidson et al., 2008). The architecture of ABC transporters is conserved and consists of a core of four subunits: two transmembrane domains (TMDs) through which the substrate is transported across the membrane and two nucleotide binding domains (NBDs) that provide the energy for substrate translocation by means of the ATP hydrolysis (figure 1). Both the amino acid sequence and tertiary structure of NBDs are well-conserved and for this reason NBDs are considered to be a hallmark of the ABC transporter family. The amino acid sequence and structure of the TMDs are not conserved in all ABC transporters and likely have a polyphyletic origin (Wang et al., 2009).

Depending on the direction of substrate translocation, ABC transporters are classified as importers or exporters. Exporters are found in prokaryotes as well as eukaryotes, whereas importers are present in prokaryotes only and have been classified into three types, based on the fold of the TMDs: (Type I, Type II, and Energy Coupling Factor transporters -ECF, figure 1) (Hollenstein et al., 2007; Rodionov et al., 2009). Type I and II importers rely on an additional substrate binding protein (SBP) for the recognition of their substrates (figure 1). In Gram-negative bacteria the SPBs are present in the periplasm as water-soluble proteins, but in Gram-positive bacteria the SBPs are associated with the membrane through a lipid anchor, or fused to the TMDs (Dassa and Bouige, 2001; van der Heide et al., 2001). ECF transporters (see below) and exporters do not make use of SBPs (see below).

ECF transporters have recently been discovered as a new class of ABC importers in prokaryotes (Rodionov et al., 2009). Like all ABC transporters they contain two identical or homologous NBDs (named EcfA/EcfA' in ECF transporters), which are associated with the transmembrane domains. The transmembrane assembly consists of two sequence-unrelated membrane proteins: the EcfT subunit and the S-component (Rodionov et al., 2009). Instead of employing SBPs, substrate binding in ECF transporters is exclusively performed by the S-component. The S-components are also stable as separate entities (not in complex with the other subunits), which suggests that they may also have a transporting function as solitary proteins (Duurkens et al., 2007; Erkens and Slotboom, 2010; Eudes et al., 2008; Hebbeln et al., 2007; Siche et al., 2010; Finkenwirth et al., 2013).

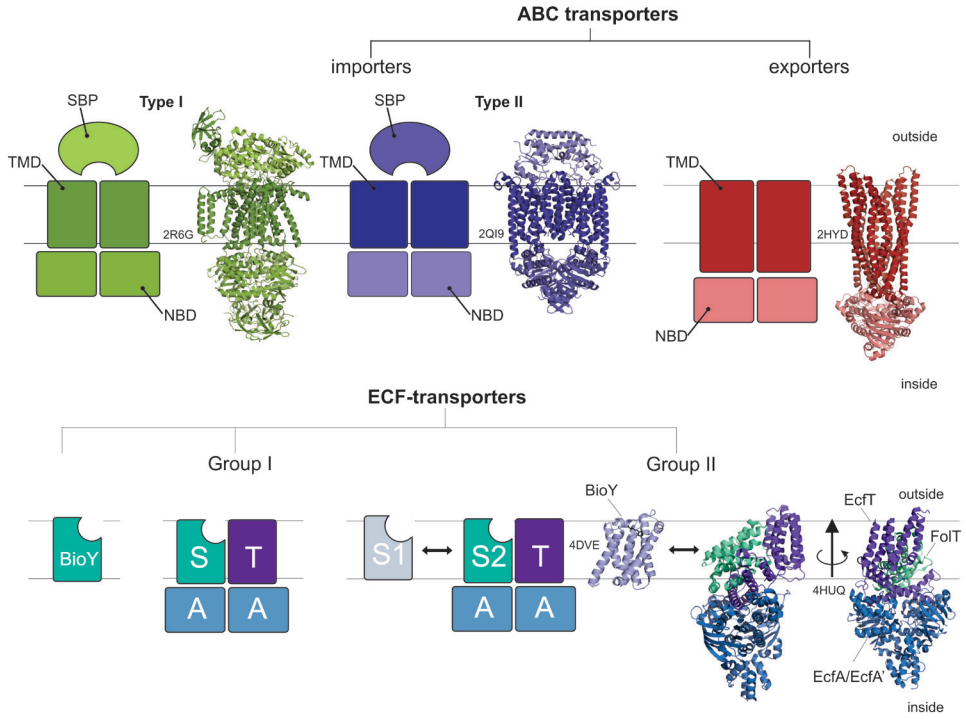

Figure 1: Subunit architecture of the different ABC transporter subclasses. The horizontal lines indicate the approximate position of the lipid bilayer. Top part: Next to the schematic representations, example structures of ABC transporters are depicted from left to right: the maltose transporter $MalFGK_2$ (PDB: 2R6G), the vitamin B12 transporter BtuCDF (PDB: 2QI9) and P-glycoprotein (PDB: 2HDY). Bottom part: ECF transporters from left to right: the biotin specific S-component lacking ECF module, Group I ECF transporters with ECF module dedicated to the S-component and Group II ECF transporters with S-components utilizing common ECF module - biotin specific S-component BioY (PDB: 4DVE) and folate specific S-component FolT in the complex with ECF module (PDB: 4HUQ).

Based on the organization of the genes coding for the subunits of ECF transporters, a distinction has been made between ECF transporters of Group I and Group II (figure 1). In the case of Group I ECF transporters, the genes for the subunits of an ECF module are organized in an operon that also codes for one S-component. It has been suggested that Group I transporters form a "dedicated" complex: the ECF module and the S-component encoded in the same operon exclusively interacts with each other (Rodionov et al., 2009). The ECF transporters of Group II are characterized by a genetic separation between the operon encoding the ECF module and the genes for one or more S-components. There are usually more S-component genes (up to twelve, scattered around the genome) than ECF module

operons and the ECF module is shared by the different S-components (ter Beek et al., 2011). Many organisms encode Group I as well as Group II transporters in their genomes. Whether in Group I transporters the ECF modules indeed are dedicated to a single S-component remains to be determined. Moreover, it is worth noticing that several organisms having genes encoded for biotin specific S-components miss the operons for ECF module (figure 1) (Rodionov et al., 2009; Finkenwirth et al., 2013). These biotin-specific proteins appear to function as ECF-independent transporters (Finkenwirth et al., 2013).

The shared use of a single ECF module by multiple S-component subunits in Group II provides a mechanism for the translocation of chemically diverse substrates by the same ECF module. The molecular basis of the modular S-component/ECF module interactions is unclear because the S-components for different substrates lack significant sequence similarity (averaged amino acid identities between 10 and 20%). The elucidation of the crystal structures of three different S-components (RibU specific for riboflavin (Zhang et al., 2010b), ThiT specific for thiamin (Erkens et al., 2011) and BioY specific for biotin (Berntsson et al., 2012)) provided the first atomic-level insight in the architecture and substrate selectivity of this class of proteins, and two recent crystal structures of two complete ECF transporters (specific for folate (Xu et al., 2013) and hydroxylmethyl pyrimidine (Wang et al., 2013)) provided an insight in the complex architecture. The structures of the whole complexes show an unexpected feature: S-components appear to be able to radically change their orientation in the lipid bilayer during transport cycle. The structures provide information about the mechanism of the modular interaction of the S-components with the ECF module and allow speculations about the transport mechanism.

S-components are membrane proteins specialized in substrate scavenging

The substrate specificity of ECF transporters is determined by the S-component subunit. S-components are small (~20 kDa) membrane proteins that are not related to any other membrane protein of known function. There is a large variation in the chemical nature of the substrates that can be recognized by the S-components, which ranges from divalent cations (Siche et al., 2010; Rodionov et al., 2006) to vitamins (Erkens and Slotboom, 2010; Eudes et al., 2008; Hebbeln et al., 2007; Burgess et al., 2006) and amino acids (Rodionov et al., 2009). Based on an amino acid sequence analysis, 21 different S-component families have so far been defined but substrate specificity has only been confirmed for a subset. Table 1 gives an overview of the S-component families and their (predicted) substrate specificity.

The pairwise sequence identity between S-components from different families is on average only 10-20%. Despite the differences, S-components share a number of common characteristics. The consensus (predicted) membrane topology consists of six transmembrane helices with the C- and N-terminus located on the cytoplasmic

Table 1
An overview of S-components and their substrate specificity.

Protein name	Substrate	Confirmed Y/N	Reference
ThiT	Thiamin (vitamin B_1), TMP, TPP	Y	(Erkens and Slotboom, 2010; Eudes et al., 2008)
RibU	Riboflavin (vitamin B_2), FMN	Y	(Duurkens et al., 2007; Burgess et al., 2006)
FolT	Folic acid (vitamin B_9), (6S)-folinic acid	Y	(Eudes et al., 2008)
BioY	Biotin (vitamin B_7)	Y	(Hebbeln et al., 2007; Berntsson et al., 2012)
PanT	Pantothenic acid (vitamin B_5)	Y	(Neubauer et al., 2009)
QueT	Queuosine precursor	N	
NiaX	Niacin (vitamin B_3)	Y	(ter Beek et al., 2011)
HmpT	Pyridoxine related	N	
ThiW	Thiazole (thiamin precursor)	N	
MtsT	Methionine precursor	N	
TrpP	Tryptophan	N	
LipT	Lipoate	N	
CblT	Cobalamine (vitamin B_{12}) precursor	N	
CbrT	Cobalamine (vitamin B_{12}) precursor	N	
QrtT	Queuosine precursor	N	
PdxU	Pyridoxine (vitamin B_6)	N	
MtaT	Methylthioadenosine	N	
NikMN	Nickel ions	Y	(Rodionov et al., 2006)
CbiMN	Cobalt ions	Y	(Rodionov et al., 2006)
HtsT	unknown	-	

side of the membrane. Because of their relatively small size, S-components are thus particularly hydrophobic proteins.

In the absence of the ECF module, S-components are stable both in the membrane and in detergent solution. The stability of solitary S-components had already been noted long before the molecular identities of the proteins were known: the S-component for folate (FolT) could be purified from wild-type *Lactobacillus casei* cells grown under folate limiting conditions without apparent co-purification of the ECF module (Henderson et al., 1977). It seems reasonable to assume that there is a biological function associated with the presence of solitary S-components. Possibly, the lone S-components are high-affinity substrate scavengers (see below); once their substrates are bound, the ECF module can subsequently recognize the loaded S-component and translocation takes place.

A general feature of ECF transporter S-components is their high binding affinity. Picomolar to nanomolar dissociation constants have been reported for the S-components specific for riboflavin (Duurkens et al., 2007), folate (Eudes et al., 2008), thiamin (Erkens and Slotboom, 2010; Eudes et al., 2008) and biotin (Henderson and Potuznik, 1982; Berntsson et al., 2012). The occurrence of S-component genes in the genomes of bacteria has been linked to a lack of biosynthetic genes for their substrates (Rodionov et al., 2009; 2002). Many of the substrates of ECF transporters are compounds needed in small amounts (micronutrients), which often are present in low concentrations in the environment. Excess amounts of solitary S-components would allow bacteria to scavenge these valuable compounds when resources are limited. The expression of most S-components is regulated by the intracellular concentration of their substrates, for instance by riboswitches (Zhang et al., 2010a). As a consequence, the expression of S-components is increased when the intracellular concentration of their substrate decreases, thus ensuring an upregulation of those S-components is needed to meet the specific demands. The solitary S-components may keep their substrates tightly bound until a complex is formed with the ECF module to transport the substrate.

Two families of S-components appear to have additional features. First, some S-components form bipartite or tripartite complexes with extra membrane proteins, as has been observed for the Co^{2+} and Ni^{2+}-specific S-components CbiMN and NikMN, respectively (Siche et al., 2010). The exact function of those additional components is unknown, but they are required for substrate transport/binding in the absence of the ECF module. Second, the *bioY* gene (which codes for the biotin-specific S-component BioY) is present in several organisms that lack genes encoding an ECF module (Rodionov et al., 2009; Finkenwirth et al., 2013). Ability of the biotin transport by solitary BioY has been shown for eight representatives of

this subgroup of the ECF transporters (Finkenwirth et al., 2013). Intriguingly, BioY from *Rhodobacter capsulatus* ($BioY_{RC}$), which is an S-component encoded in an operon with the ECF module (Group I ECF transporter), has also been attributed a transport function in the absence of the ECF module (Hebbeln et al., 2007). It must be noted that besides BioY from *R. capsulatus* there is no other S-component from Group I or II transporters which has been shown to mediate transport without the ECF module (ter Beek et al., 2011; Zhang et al., 2010b; Erkens et al., 2011; Berntsson et al., 2012). The evidence for biotin transport by solitary BioY from *R. capsulatus* is based solely on *in vivo* translocation and growth assays. Importantly, *in vitro* transport assays with the purified protein reconstituted in liposomes did not show the transport function of the solitary S-component (Berntsson et al., 2012 and **Chapter 2**).

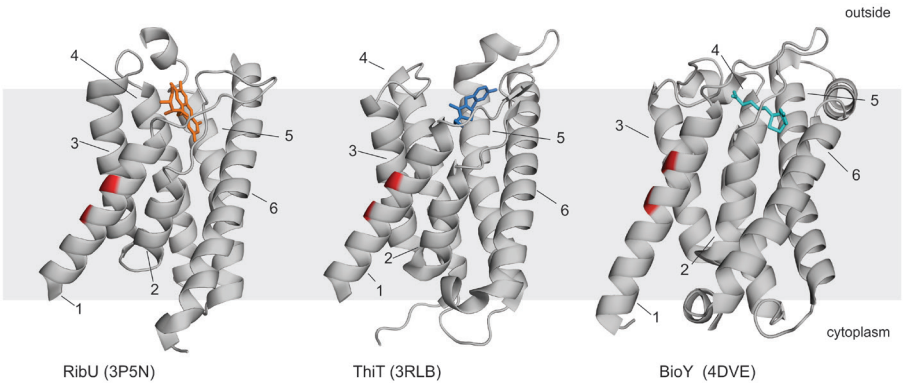

Figure 2: Structures of RibU (left, PDB: 3P5N), ThiT (center, PDB: 3RLB), BioY (right, PDB: 4DVE). The numbers indicate transmembrane helices 1-6. The bound substrates are depicted as orange (riboflavin), blue (thiamin) and cyan (biotin) sticks. The positions of the alanines in the AxxxA motif are colored red. The position of the lipid bilayer is represented in gray.

Structure-function relationships of solitary S-components

Recently, crystal structures have been determined of the S-components for riboflavin (RibU) from *Staphylococcus areus* (Zhang et al., 2010b) (PDB: 3P5B), thiamin (ThiT) (Erkens et al., 2011) (PDB: 3RLB) and biotin (Berntsson et al., 2012 and **Chapter 2**) (PDB: 4DVE) from *Lactococcus lactis*. With these structures available it has been possible to explain some of the functional characteristics associated with ECF transporters. The sequence similarity between ThiT, RibU and BioY is less than 20%, which is too low to establish homology (Sander and Schneider, 1991). Nevertheless, the three proteins have a similar fold (figure 2). In line with the membrane topology predictions, the

structures are built up of six transmembrane helices, but the lengths and the tilts of the helices are variable; helices 5 and 6 are long and cross the membrane at an angle of almost 45°, whereas helix 2 spans only half the membrane and is preceded by a hydrophobic loop (loop L1). The proteins were crystallized with their respective substrates bound. In RibU, ThiT and BioY a single substrate molecule was found at a site located near the extracellular face of the protein. The 1:1 substrate:protein binding stoichiometry is in line with biochemical experiments (Duurkens et al., 2007; Erkens and Slotboom, 2010; Berntsson et al., 2012 and **Chapter 2**). The resolution of the RibU structure (3.6 Å) did not allow a detailed analysis of the interactions between the substrate and the protein, but in the ThiT and BioY structure (2.0 and 2.1 Å resolution) these interactions can be traced, enabling a detailed description of the high-affinity binding site (Erkens et al., 2011; Berntsson et al., 2012 and **Chapter 2**). The substrate-protein interactions in BioY will be described in **Chapter 2**. In ThiT the substrate, thiamin, has a different conformation than the catalytic V-shape that is found in enzymes with thiamin-phosphates as a cofactor, which is consistent with the binding/transport function of ThiT. Thiamin is kept in place by numerous hydrogen bonds, as well as ionic and aromatic interactions. The abundance of interactions provides an explanation for the high binding affinity. The residues that interact with thiamin are located almost exclusively in the C-terminal half of the protein (comprising helices 4-6 and the loop between helices 5 and 6). Earlier mutagenesis studies on ThiT had already indicated that residues from helices 5 and 6 and the connecting loop were involved in substrate binding (Erkens and Slotboom, 2010). The only part from the N-terminal half of ThiT that interacts with the substrate is the loop L1 between helices 1 and 2. Based on all the currently available structures (of solitary S-components as well as ECF complexes) and an EPR study on solitary ThiT (Majsnerowska et al., 2013 and **Chapter 3**), the L1 loop has been shown to form a lid on the binding site and a relatively small displacement of this segment exposes the binding site to the external environment, allowing the substrate to bind. A similar open conformation of the loop in the context of the ECF module allows the substrate to leave the binding site on the inner side of the membrane (Xu et al., 2013; Wang et al., 2013) (see below).

There is some uncertainty about the oligomeric state of solitary S-components. Static light scattering coupled to refractive index measurements (SEC-MALLS) with the S-component for thiamin ThiT from *L. lactis* and BioY from *R. capsulatus* have unambiguously demonstrated that the proteins are monomeric in detergent solution (Erkens and Slotboom, 2010; Berntsson et al., 2012). In contrast, *in vivo* fluorescence (FRET lifetime) experiments on BioY from *R. capsulatus* ($BioY_{Rc}$) have indicated the possible existence of higher oligomers (Finkenwirth et al., 2010). It is not known

whether the proposed higher order oligomeric state of BioY is common to all S-components in a membrane environment, or whether it is related to the transport function that is associated with the solitary BioY. It is also possible that the detection of higher oligomers *in vivo* might reflect the presence of a small fraction of aggregated protein that is commonly observed upon membrane protein overexpression.

Structures of the ECF-S-component complexes

Recently, two crystal structures of complete ECF transporters were published. The two ECF complexes originate from the same organism (*Lactobaccillus brevis*), where the shared ECF module was crystalized with two different S-components: folate specific FolT and HmpT, which is predicted to be specific for hydroxylmethyl pyrimidine. The complexes were captured in the inward-facing, substrate- and nucleotide-free conformation. The global fold of the S-components in the context of the whole complex is the same as in solitary RibU, ThiT and BioY, but unexpectedly the S-components in the complex have a radically different orientation relative to the membrane: they lie almost parallel to the membrane plane, exposing the binding side to the inside of the cell (Xu et al., 2013; Wang et al., 2013). In the crystalized complexes, the S-components FolT and HmpT form extensive networks of interactions with the L-shaped EcfT subunit, which also binds to the EcfA and EcfA' subunits through two coupling helices. The coupling helices cross each other forming an X-shaped motif, which in the complex is situated between the S-component on one side and EcfA/EcfA' dimer on the other side. The C-terminus of each helix in the X-shaped motif contains xRx motif. Each of the xRx motif interacts with one ATPase domain. The importance of the arginine residues in this motifs for transport activity and complex formation had been shown before (Neubauer et al., 2009).

The coupling helices are not only involved in the interaction with EcfA and EcfA' but additionally make contacts with the helices of the S-component. One of the interaction point is formed by the AxxxA motif located in the first helix of the S-component. Although this helix spans the membrane in the solitary S-components, it lies parallel to the membrane in the context of the complex. The AxxxA motif was previously reported to play an important role in the formation of the active transporter (Erkens et al., 2011 and **Chapter 4**). The unexpected orientation of the S-component in the membrane results in the formation of the additional interaction region between the transmembrane helices of EcfT and extracytoplasmic loops of the S-component (L3 and L5).

The EcfA subunits associated with ECF transporters possess all the mechanistically important sequence motifs of the NBD superfamily. The structures of the isolated

EcfA/EcfA' dimers from *Thermotoga maritima* (PDB:2YZ2) and the subunits in the complexes from *Lactobaccillus brevis* confirm that EcfA proteins have the same fold as NBDs from the other ABC transporters. Superimposition of the latter with the NBD dimer of the maltose transporter reveals high similarity to the nucleotide-free, open conformation of MalK. Therefore, it is likely that the mechanism of ATP hydrolysis is similar to that of the classical ABC transporters.

Stoichiometry of the subunits in the ECF complex

The subunit stoichiometry of ECF transporter complexes is under debate. The ECF-FolT and ECF-HmpT complexes have four subunits present in a 1:1:1:1 stoichiometry. This stoichiometry had been shown by static light scattering/refractive index measurements (SEC-MALLS) of purified ECF complexes of the Group II transporters from *L. lactis* (ter Beek et al., 2011) and had been proposed based on information about genetic fusions of the genes for ECF transporter subunits in several genomes (Rodionov et al., 2009).

It should be noted that a different subunit stoichiometry has been proposed based on crosslinking studies of purified Group II ECF complexes (Karpowich and Wang, 2013). The crosslinking data suggest 2S:2T:1A:1A' stoichiometry with 2T:1A:1A' forming a central core of the complex. Additionally, this data imply that two S-components in the complex may have different substrate specificities. This discrepancy may be explained by the tendency of purified membrane proteins to form non-specific aggregates. Therefore it is possible that the crosslinking studies picked up complexes of a non-physiological stoichiometry.

The 1:1:1:1 stoichiometry is also different from the stoichiometry proposed for a Group I ECF transporter for biotin (BioMNY from *Rhodobacter capsulatus*). The difference comes from the fact that BioY dimer was found to be sufficient for biotin transport based on *in vivo* FRET lifetime experiments (Finkenwirth et al., 2010), *in vivo* uptake assay (Hebbeln et al., 2007) and *in vivo* studies on BioY mutants (Kirsch et al., 2012). This observation lead to the hypothesis that the BioY homodimer is the central core of the transporter. Additionally, the crosslinking analysis of the membrane fraction of the cells overexpressing BioMNY indicated 2S:2T:2A or 2S:1T:2A stoichiometry as the most probable (Neubauer et al., 2011). A possible explanation for the different results could be that ECF transporters in the membrane environment have a dynamic stoichiometry and may have one or more S-components associated with the ECF module. Alternatively, they could reflect genuine structural divergence between Group I and II ECF transporters.

Transport mechanism

Translocation pathway

On the basis of the structures of the solitary S-component two speculative models for the mechanism of substrate translocation through ECF transporters were presented. Based on the RibU structure, it was proposed that the substrate passes through the interior of the RibU molecule (Zhang et al., 2010b). For riboflavin (M_W 376 Da) to pass through the proposed channel, large conformational changes would be required involving a separation of the N- and C-terminal halves of the protein (helices 1-3 and 4-6 respectively) which are tightly packed in the crystal structure. The hypothesis that such a pathway would exist was based on the presence of moderately conserved amino acids that could line the path. In the ThiT structure, we did not find a potential translocation pathway lined with conserved amino acids (Erkens et al., 2011). In fact, many of the amino acids that were marked as conserved in the RibU structure turned out to be poorly conserved when a larger set of RibU homologues was used for the multiple sequence alignment. An alternative location for the translocation pathway could be on the interface between the S-component and the EcfT component. By rearranging the L1 loop, such a translocation pathway might become connected with the substrate binding site through a lateral gate. The translocation pathway at the interface of the TMDs is also common to all other ABC transporters (Davidson et al., 2008).

Surprisingly, the two recently published crystal structures of the complete ECF transporters revealed a remarkable feature of the S-components, which suggests a different and unprecedented mechanism of transport (Wang et al., 2013; Xu et al., 2013). In the ECF complex the S-component may be able to reorient in the lipid bilayer, which allows it to expose the binding site alternately to the both sides of the membrane. Thus, S-components can bind the substrates to a site that is close to the extracellular side of the membrane. Relatively small conformational changes in the

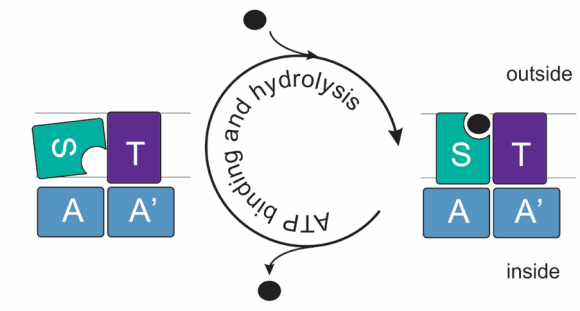

Figure 3: Schematic representation of the transport cycle of ECF transporter. Two conformations are depicted: The ECF complex with a substrate-free S-component in the inward facing conformation (left) or with a substrate-bound S-component in the outward facing conformation (right). ATP binding and hydrolysis allows for substrate translocation.

loop connecting membrane-spanning segments 1 and 2 open and close the access to the binding sites (Majsnerowska et al., 2013 and **Chapter 3**). Then -probably assisted by the ECF module- the loaded S-component topples over and brings its binding site together with the substrate to the cytoplasm. Toppling of the S-component rearranges the binding site to lower the affinity for the substrate enabling its release (Xu et al., 2013) (figure 3).

Coupling of the transport to ATP hydrolysis

ATP-dependence of ECF transporters was already observed in the 1970s, long before ABC transporters were discovered (Henderson et al., 1979a), and confirmed recently using purified transporters, reconstituted in lipid bilayers (ter Beek et al., 2011; Xu et al., 2013; Karpowich and Wang, 2013). How could ATP hydrolysis by the NBDs be coupled to substrate translocation? There is a wealth of structural and biochemical data available on the function of the NBDs in ABC transporters (Davidson et al., 2008; Rees et al., 2009). NBDs in ABC transporters form a dimeric arrangement with two active sites for ATP binding and hydrolysis that are formed with contributions from both monomers (Oldham et al., 2008). Large conformational changes take place during the ATP hydrolysis cycle (Chen et al., 2003) and these conformational changes are transmitted to the TMDs through a structurally conserved element named 'the coupling helix' (Hollenstein et al., 2007; Locher, 2002). The coupling helix is an α-helical segment with a length of 8-12 amino acids that is located in a cytoplasmic loop of the TMD. There is little sequence conservation between coupling helices from different ABC transporters, making their location in the amino acids sequences of TMDs hard to predict. The coupling helices of the two TMDs fit into two grooves of the NBD dimer (one in each NBD). During the ATP hydrolysis cycle, the conformational changes in the NBDs are transmitted to the coupling helices and consequently lead to a structural rearrangement in the TMDs. The TMDs thus alternate between outward and inward-facing conformations, allowing substrate translocation to take place (Jardetzky, 1966).

As noted above, EcfA and EcfA' have all the conserved structural motives important for ATP binding and hydrolysis. Thus, it is reasonable to assume that conformational changes of the ATPase dimer induced by ATP binding and hydrolysis are propagated to the transmembrane part of the transporter. The S-components do not make contact directly with the EcfA/EcfA' subunits, but instead the interactions are mediated by two X-shaped α-helices which are part of the EcfT. As in the other ABC transporters, these helices are most likely involved in the transmission of the conformational changes in the ATPases to the transmembrane part of the transporter.

However, it is unclear which translocation steps are coupled to the specific steps of ATP hydrolysis. A possible coupled step could be the toppling of the S-component, either to bring the bound substrate from the extracellular side of the membrane to the cytoplasm, or to reorient the empty binding site from the inward-facing state observed in the crystal structure to the outward facing state, ready to pick up another substrate molecule. ATP binding to the EcfA/EcfA' dimer will bring the two ATPase subunits close together, simultaneously pushing the anchoring ends of the X-shaped helices of EcfT towards each other. This movement could alter the interaction interface with the S-component, and may force the toppled S-component back up to an upright orientation in which the binding site is exposed to the extracellular side. Another possibility is that conformational changes in the X-shaped helices squeeze the S-component out of the complexes. The dissociated S-component might then spontaneously reorient to expose the binding site to the outside. Dissociation of S-components during the translocation cycle could explain a previous observation that competition of different S-components for the same ECF module depends on the presence of the transported substrates (Henderson et al., 1979b and **Chapter 4**). More detailed discussion about possible mechanisms of transport of the Group II ECF transporters can be found in the **Chapter 5** of this thesis.

The modular interaction platform of S-components

In ECF transporters of Group II, several sequence-unrelated S-components interact with the same ECF module to form an active ECF transporter. Therefore, different S-components must provide a structurally conserved interface that is recognized by the ECF module. A comparison between the structures of ThiT , BioY and RibU revealed that a conserved alanine motif (AxxxA) is present on the outer surface of helix 1. Mutation of either of the alanines in ThiT into tryptophan resulted in a complete loss of transport activity caused by an inability of this S-component to form a complex with the ECF module (Erkens et al., 2011 and **Chapter 4**). This alanine motif is present at the same position (transmembrane helix 1) in all eight S-components from *L. lactis* that interact with the same ECF module and is conserved in many orthologs (figure 2).

The structures of ECF-FolT and ECF-HmpT revealed that interactions between EcfT and the S-component take place largely in the bilayer but also residues from the X-shaped coupling helices are involved in the formation of this interface. The interactions are mostly hydrophobic and the only conserved sequence motif is the AxxxA motif of S-components which interacts with the coupling helices. Interestingly, the alanine motif is not completely conserved among S-components. In

FolT from *L. brevis* the second alanine from the motif is replaced by valine. Therefore the question remains how different S-components can interact specifically with the same ECF module. Given the differences in sequence between the S-components (within one organism usually less than 20 % identical) it is likely that they have different affinities, which may affect their ability to compete for the ECF module. The more specific interactions an S-component can form with EcfT, the stronger it can compete for the ECF module with other S-components.

Concluding remarks

With the discovery of ECF transporters, a new type has been added to the versatile family of ABC transporters. Although united by the utilization of the NBD 'motor domain', ECF and ABC transporters display some striking differences. In particular the substrate binding by integral membrane proteins (S-components), which may reorient in the membrane to translocate the substrate sets ECF transporters apart from other ABC transporters. Intriguingly in many ECF transporters multiple S-components can make use of the same ECF module. Further structural and functional analysis will be required to elucidate the transport mechanism of ECF transporters.

Outline of this thesis

The aim of this thesis is to investigate a mechanism of vitamin transport via ECF transporters. Therefore ECF transporters from *Lactoccocus lactis* specific for niacin, thiamin and biotin were studied with various biochemical and biophysical techniques.

Chapter 2 provides a structural and biochemical characterization of BioY, the S-component specific for biotin. The high resolution structure of BioY from *L. lactis* is compared to the previously solved structures of two other S-components - RibU (riboflavin specific) from *S. aureus* and ThiT (thiamin specific) from *L. lactis*. The binding affinity of two purified BioY proteins (from *L. lactis* and *R. capsulatus* - $BioY_{Ll}$ and $BioY_{Rc}$) was determined. The activity of the solitary $BioY_{Ll}$ and $BioY_{Rc}$ reconstituted in liposomes was assayed. It was concluded that the solitary BioY proteins can bind, but not transport biotin.

In **chapter 3** the high-affinity thiamin binding to the S-component ThiT from *L. lactis* was studied. EPR spectroscopy and molecular dynamics simulations revealed the structural rearrangements that take place in the S-component upon substrate

binding. The kinetic parameters of thiamin binding were determined by stopped-flow fluorescence measurements. It was concluded that only small conformational changes take place upon substrate binding, consistent with the function of S-components as binding proteins rather than transporters.

Henderson and colleagues showed in the late 1970s that vitamin transport in *L. casei* depends on the presence of the common "energizing module" (ECF module) and substrate binding proteins (S-components). Different S-components, specific for different vitamins competed for the ECF module, and the presence of the transported substrates enhanced the competitiveness of the S-component to interact with the ECF module (Henderson et al., 1979b). **Chapter 4** describes studies on ECF transporters for thiamin and niacin (ECF-ThiT and ECF-NiaX) heterologously expressed in *E. coli*. The dependency on the ECF module in the translocation process was tested in the whole cell uptake assay. The ability of the S-components NiaX and ThiT to compete for the same ECF module was shown in the cells where ECF module was coexpressed with NiaX and ThiT, the amounts of the two S-components were modulated, and the concentrations of the substrates niacin and thiamin was varied.

In **chapter 5** an effort was made to characterize the mechanism of action for ECF transporters *in vitro* upon reconstitution of purified ECF-NiaX into liposomes. A speculative model of transport is presented.

Chapter 2

Structural divergence of paralogous S-components from ECF-type ABC transporters

Ronnie P-A Berntsson*
Josy ter Beek*
Maria Majsnerowska*
Ria H. Duurkens
Pranav Puri
Bert Poolman
and Dirk Jan Slotboom

This chapter is published in: *Proc. Natl. Acad. Sci.* U.S.A. (2012) *109*, 13990–13995.

* Authors contributed equally to this work.

ABSTRACT

Energy Coupling Factor (ECF) proteins are ATP Binding Cassette (ABC) transporters involved in the import of micronutrients in prokaryotes. They consist of two nucleotide-binding subunits and the integral membrane subunit EcfT, which together form the ECF-module, and a second integral membrane subunit that captures the substrate (the S-component). Different S-components, unrelated in sequence and specific for different ligands, can interact with the same ECF module. Here, we present a high-resolution crystal structure at 2.1 Å of the biotin-specific S-component BioY from *Lactococcus lactis*. BioY shares only 16% sequence identity with the thiamin-specific S-component ThiT from the same organism, of which we recently solved a crystal structure. Consistent with the lack of sequence similarity, BioY and ThiT display large structural differences (RMSD = 5.1 Å), but the divergence is not equally distributed over the molecules: The S-components contain a structurally conserved N-terminal domain that is involved in the interaction with the ECF module, and a highly divergent C-terminal domain that binds the substrate. The domain structure explains how the S-components with large overall structural differences can interact with the same ECF module, while at the same time specifically bind very different substrates with subnanomolar affinity. Solitary BioY (in the absence of the ECF module) is monomeric in detergent solution, binds D-biotin with a high affinity, but does not transport the substrate across the membrane.

INTRODUCTION

Energy Coupling Factor (ECF) proteins are an abundant class of ATP Binding Cassette (ABC) transporters, involved in the import of vitamins and transition metal ions in prokaryotes (Erkens et al., 2012; Hebbeln et al., 2007; Rodionov et al., 2009; 2006). Like all ABC transporters, ECF transporters consist of two cytosolic nucleotide-binding domains (NBDs), which are associated with integral membrane subunits that form the translocation pore. In ECF transporters the two NBDs (EcfA and EcfA' which may be identical or homologous) and a single membrane subunit (EcfT) form a so-called energizing or ECF module. A second integral membrane protein (the S-component) binds the substrate and forms a complex with the ECF module to create a functional transporter. This organization is typical for ECF transporters (ter Beek et al., 2011; Erkens et al., 2012; Rodionov et al., 2009), since other ABC importers utilize a soluble substrate-binding protein to capture ligands (Berntsson et al., 2010; Higgins, 1992). In many ECF transporters multiple S-components (specific for different substrates) can interact with the same energizing module (Rodionov et al., 2009; ter Beek et al., 2011). Strikingly, S-components from a single organism, which interact with the same ECF module, are generally not homologous at the sequence level.

To gain insight in the characteristic modularity of ECF transporters, one needs to compare crystal structures of different S-components that interact with the same ECF module, *i.e.* S-components from a single organism. Crystal structures of the S-components ThiT from *Lactococcus lactis* (thiamin-specific) and RibU from *Staphylococcus aureus* (riboflavin-specific) have recently been determined (Erkens et al., 2011; Zhang et al., 2010). We now present the crystal structure at 2.1 Å of the S-component BioY from *Lactococcus lactis.* BioY and ThiT form complexes with the same ECF module (ter Beek et al., 2011) and share only 16 % sequence identity. We show that BioY from *L. lactis* and the well-studied homologue from *Rhodobacter capsulatus* bind biotin with different kinetics, but neither of the proteins can transport the substrate in the absence of the ECF module.

MATERIALS AND METHODS

Protein expression

Selenomethionine-substituted BioY containing a N-terminal decahistidine tag was expressed in *Lactococcus lactis* strain NZ9000 (de Ruyter et al., 1996), as previously described (Berntsson et al., 2009). Briefly, the cells were grown semi-anaerobically in chemically defined medium (CDM) to an OD_{600} of 1.5. At this point, the cells were spun down and resuspended in CDM with selenomethionine instead of methionine.

After 20 minutes, *bioY* expression was induced by the addition of 0.1% (v/v) of culture supernatant from the nisin A-producing strain NZ9700 (de Ruyter et al., 1996). The cells were grown to an OD_{600} of 4, and then harvested by centrifugation and subsequently resuspended in buffer A (50 mM Na-Hepes pH 7.5 supplemented with 300 mM NaCl and 10% (v/v) glycerol).

Cell lysis was performed by passing the cells twice trough a cell disruptor (Constant Systems Ltd) at a pressure of 39 kPsi, 4 °C. Prior to the disruption, $MgSO_4$ (5 mM) and DNase (100 μg/mL) were added. Unbroken cells were removed by centrifugation at 6000x*g*, 15 min, 4 °C. Membrane vesicles were collected by a subsequent centrifugation at 267,000x*g* for 80 min at 4 °C, resuspended and homogenized in buffer A to a protein concentration of 40 mg/mL, flash frozen in liquid nitrogen and stored at -80 °C.

Protein purification

Membrane vesicles (100 mg total protein) were thawed, and diluted in buffer A to approximately 5 mg/mL total protein. Solubilization was done by the addition of 1% (w/v) of dodecyl-β-D-maltoside and incubation at 4 °C for 1h (under gentle rotation). Unsolubilized material was spun down at 267,000x*g*, 4 °C for 20 min. 0.5 mL Ni-Sepharose plus 15 mM imidazole pH 7.8 were added to the supernatant, and the mixture was incubated at 4 °C for 1h (under gentle rotation). The suspension was poured into a 10 mL disposable column (Bio-Rad), and the flow-through was discarded. The column was washed with 20 column volumes of buffer B (50 mM Na-Hepes pH 7.5 supplemented with 300 mM NaCl, 50 mM imidazole pH 7.8 and 0.35% (w/v) *n*-nonyl-β-D-glucopyranoside (NG, Anatrace)). The protein was eluted from the column in 2 fractions (0.35 and 0.75 mL, respectively) with buffer B supplemented with 500 mM imidazole pH 7.8. The second elution fraction was loaded onto a Superdex 200 10/300 GL gel filtration column (GE Healthcare), equilibrated with buffer C (20 mM Na-Hepes pH 7.5 supplemented with 150 mM NaCl, 0.35% (w/v) NG). Peak fractions were concentrated to 7 mg/mL, using a Vivaspin 30 kDa molecular weight cutoff concentrator (VVR International), and immediately used for crystallization trials or other biochemical assays.

For biochemical characterization of BioY, the protein was purified from cells grown in CDM without biotin (for the isolation of substrate-free protein). The purification protocol was slightly modified: solubilization was done in a buffer containing 50 mM potassium-phosphate pH 7.5 supplemented with 300 mM NaCl, 10% glycerol and 1% maltose-neopentyl glycol 3 (MNG-3) (Chae et al., 2010). The nickel-sepharose column was washed with 20 column volumes of 50 mM potassium phosphate pH 7.5, supplemented with 300 mM NaCl, 10% glycerol, 50 mM imidazol

and 0.03% MNG-3, and eluted with the same buffer supplemented with 500 mM imidazol. Size-exclusion chromatography was done in 50 mM potassium phosphate pH 7.5 supplemented with 150 mM NaCl and 0.03% MNG-3.

Crystallization

Initial crystal hits of BioY were found in several conditions, all containing high concentrations of PEG and pH values between 7 and 9. Optimization of the conditions yielded diffraction-quality crystals with a size of ca 100x50x50 μm. The best crystals were grown at 5 °C with the reservoir solution containing 0.1 M Tris pH 8.0, 0.05-0.2 mM $CaCl_2$ plus 45-50% PEG400. Due to the high PEG400 concentration, no further cryo-protectant was needed, and the crystals were directly fished from the drop and flash frozen in liquid nitrogen.

Structure determination

Diffraction data was collected at the PX1 beam-line at the Swiss Light Source. Single-wavelength Anomalous Dispersion (SAD) data on SeMet-BioY was collected to 2.1 Å, at 100 K with a wavelength of 12.657 keV. Data processing and reduction were carried out, using XDS (Kabsch, 1993) and programs from the CCP4 suite (Collaborative Computational Project, 1994). Relevant statistics can be found in Table 1. Initial phase information was found using autoSharp (Vonrhein et al., 2007), and an initial model containing 95% of the residues could be built using ARP/warp (Langer et al., 2008). 15 selenium sites were found within the asymmetric unit, corresponding to all 5 of the possible sites per BioY molecule. A few cycles of refinement using Refmac5 (Murshudov et al., 1997), and non-crystallographic symmetry with loose restraints, interspersed with manual model building in Coot (Emsley and Cowtan, 2004), were necessary to finish the model. Water molecules were automatically placed in F_O-F_C Fourier difference maps at 3σ cutoff levels and validated to ensure correct positioning, using Coot. The final protein model contains residues 1-188 for all 3 molecules in the asymmetric unit. Electron density that could correspond to acyl chains (without visible density for headgroups) was not modeled. R_{work} and R_{free} of the final model after refinement were 18.6% and 20.6%, respectively. All structure figures were prepared using PyMOL.

Fluorescence titration

Tryptophan fluorescence was measured in a stirred quartz cuvette on a SPEX Fluorolog 322 fluorescence spectrophometer (Jobin Yvon) at 25°C. Purified biotin-free BioY was diluted in size-exclusion chromatography buffer to the indicated

concentration (final volume 1000 μL). D-biotin was added in 0.5 μL steps. The excitation and emission wavelengths were 280 nm and 360 nm, respectively. The data was analyzed as described in Erkens *et al* (Erkens and Slotboom, 2010). Because of the high-affinity binding by BioY, the protein was diluted to ~10 nM for titrations with biotin. For BioY from *R. capsulatus,* the fluorescence measurements were done in the same way, except that the emission wavelength was 349 nm and that the protein concentration was ~50 nM.

Light scattering

The oligomeric state of BioY was determined via size-exclusion chromatography coupled to multi-angle laser light scattering (SEC-MALLS) as described before (ter Beek et al., 2011; Erkens and Slotboom, 2010). We used BioY isolated from cells grown on rich medium (with biotin) that was purified in the same way as the biotin-free protein.

Uptakes by proteoliposomes containing BioY

Substrate-free BioY (in a buffer of 50 mM potassium phosphate pH 7.5 supplemented with 150 mM NaCl and 0.03% MNG-3) was reconstituted into proteoliposomes at a protein:lipid ratio of 1:100 (w/w), essentially as described in before (Geertsma et al., 2008; ter Beek et al., 2011). Proteoliposomes were subjected to three cycles of freeze-thawing using liquid nitrogen, extruded through a 400 nm pore size polycarbonate filter (Avestin), centrifuged (267,000 rcf, 4°C, 40 min, Beckman TLA 100.4 rotor) and resuspended in 50 mM potassium phosphate, pH 7.5 to 80 μg/μL lipid concentration. For transport assays, 2 μL of proteoliposomes were diluted into 200 μL of buffers containing 20 nM [^{3}H]biotin and 150 nM unlabeled biotin. Different buffer compositions were used depending on whether membrane gradients were required: (i) 57 mM sodium phosphate pH 6.5 containing 1 μM valinomycin (diluted from a 3 mM stock in ethanol) to obtain gradients for protons and sodium ions in combination with membrane potential; (ii) 50 mM potassium phosphate pH 7.5 (no gradients). Buffers were pre-warmed to 25°C and the suspension was briefly vortexed after addition of proteoliposomes. At the indicated times 2 mL of ice-cold 50 mM potassium phosphate pH 7.5 was added followed by rapid filtration over 0.45 μm pore-size cellulose nitrate filter (Whatman Maidstone UK). The filters were washed once with 2 mL ice-cold 50 mM potassium phosphate pH 7.5. Background signal was determined by using liposomes without BioY. Radioactivity trapped on the filters was measured by addition of 2 mL of emulsifier plus scintillation liquid, and subsequent counting in a Perkin Elmer 1600CA scintillation counter.

RESULTS

Selenomethionine (SeMet)-substituted BioY was produced in the expression strain *L. lactis* NZ9000 (Kunji et al., 2003) and purified using the detergent *n*-nonyl-β-D-glucopyranoside, which was also used for the crystallization of RibU and ThiT (Erkens et al., 2011; Zhang et al., 2010). SeMet-BioY crystals of space group C2 diffracted to 2.1 Å and were used to solve the structure using multi-wavelength anomalous dispersion (MAD) phasing (Table 1).

Table 1: Data collection and refinement statistics

Data collection	SeMet-BioY
Space group	C2
Cell dimensions	
a, b, c (Å)	89.8, 57.4, 166.9
α, β, γ (°)	90.0, 91.1, 90.0
Resolution (Å)	48.3 – 2.1
R_{sym} (%)	6.5 (50.4)
I/σ (I)	15.3 (2.5)
Completeness (%)	98.4 (90.7)
Redundancy	10,8
Refinement	
Resolution	48.3 – 2.1
No. unique reflections	47255
R_{work}/R_{free}	18.5/20.5
No. atoms	
Protein	4335
Biotin	48
Water	123
B-factors	
Protein	33
Biotin	38
Water	52
R.m.s. deviations	
Bond lengths (Å)	0,015
Bond angles (°)	1,51

Values in parenthesis are for highest-resolution shell.

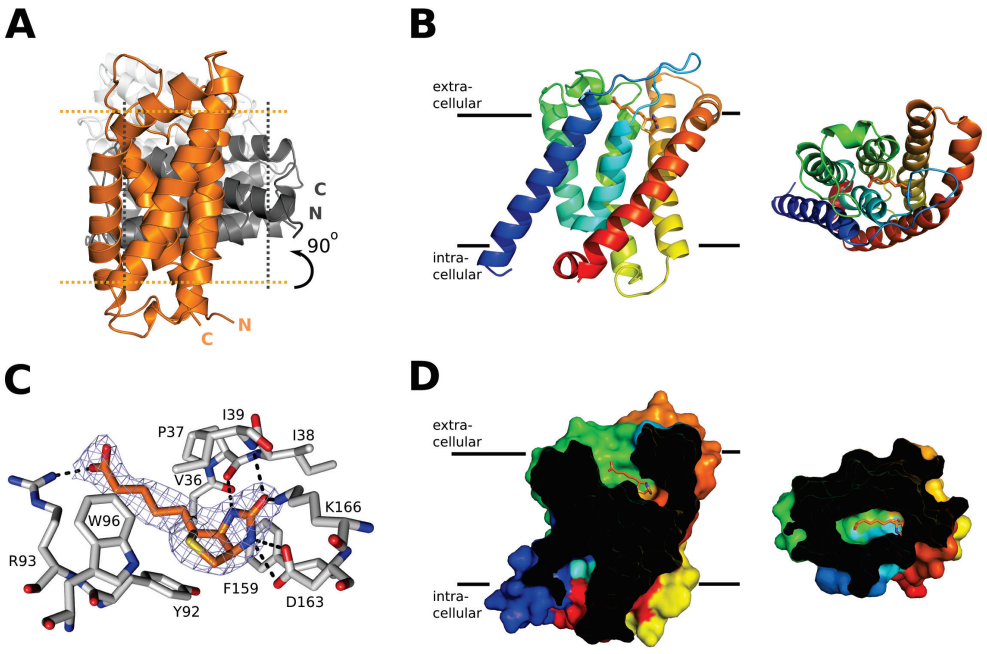

Figure 1: (A) Secondary structure cartoon showing the relative orientation of the three molecules of BioY in the asymmetric unit of the BioY crystals. The three molecules are colored differently (orange, dark grey and light grey) and the approximate membrane boundaries are indicated with dotted lines for the orange and dark grey molecules. The trimeric arrangement is incompatible with a membrane-embedded oligomer. (B) A monomer of BioY in secondary structure cartoon representation colored from blue (N-terminus) to red (C-terminus). The bound biotin molecule is shown in stick representation with carbon atoms in orange. The left and right views are from the plain of the membrane and along the membrane normal (from the outside), respectively. (C) Binding site of biotin. The biotin molecule is shown in orange and the interacting residues from BioY in gray. Electron density for biotin ($2F_O$-F_C map contoured at 1.5σ) in blue mesh. (D) Sliced surface representation of BioY showing the binding cavity, with the bound biotin shown in orange. Coloring and viewpoints as in panel B.

The electron density was of high quality and allowed for modeling of the entire amino acid sequence of BioY, except for the N-terminal tag (MHHHHHHHHA), which was used for metal-affinity purification. After refinement well-defined residual density was observed inside the protein, which could be assigned unambiguously to a D-biotin molecule. In addition, five complete detergent molecules were modeled into densities around the protein. The asymmetric unit contained three copies of BioY that were virtually identical (r.m.s. deviation <0.2 Å), with molecule A rotated ~90° with respect to B, and molecule C rotated ~160° with respect to B (figure 1A). The relative orientation of the three proteins in the asymmetric unit is incompatible with a membrane environment, and the observed crystallographic trimer is very

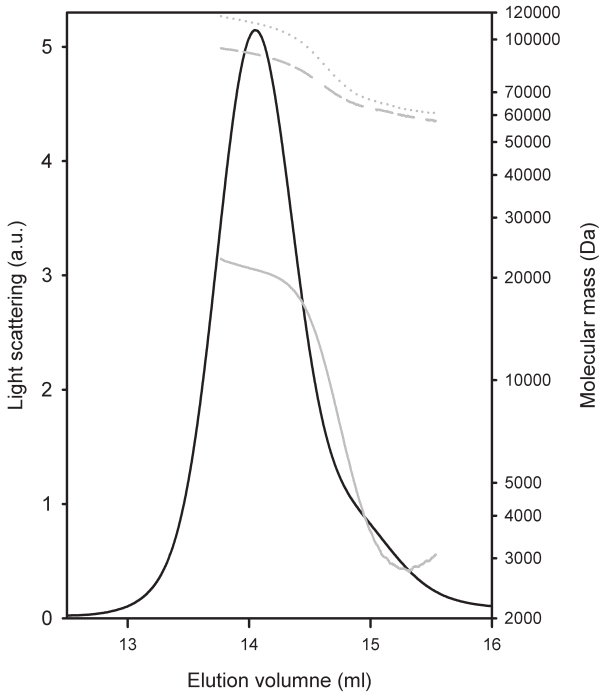

Figure 2: SEC-MALLS analysis of BioY. The chromatogram of a size exclusion experiment (black line) and calculated masses of the protein (solid gray line), detergent micelle (dashed gray line) and the protein-detergent complex (dotted gray line) are shown. His-tagged BioY has a calculated mass of 21,778.1 Da.

likely only due to crystal contacts. Indeed, light-scattering experiments (SEC-MALLS) confirmed that BioY is monomeric in detergent solution (figure 2).

BioY has six membrane-spanning α-helices (figure 1A-B). The fold of BioY resembles the folds of RibU and ThiT, but superimposition of all backbone atoms of BioY and either ThiT or RibU revealed large structural differences with root mean square deviations of 5.1 and 4.4 Å, respectively. The structural divergence is not equally distributed over the whole length of the proteins. BioY, ThiT and RibU have a structurally very similar N-terminal domain (Helices 1-3) and a highly variable C-terminal domain (Helices 4-6) (figure 3A). The long membrane-embedded loop between helices 1 and 2 reaches over from the N-terminal to the C-terminal domain and likely has an important functional role (see below).

The structural conservation of the N-terminal halves of S-components likely explains their shared use of the ECF module. The N-terminal domains of the S-components contain a conserved motif (AxxxA, with x mostly hydrophobic amino acids) in helix 1. For ThiT we have shown that the motif is essential for the interaction with the ECF module (Erkens et al., 2011). The alanines of the motif in BioY and ThiT are located at very similar positions on the lipid-exposed face of helix 1.

The variable domain contains the substrate-binding site. BioY was crystallized with a biotin molecule bound to a site near the extracellular face of BioY (figure 1C).

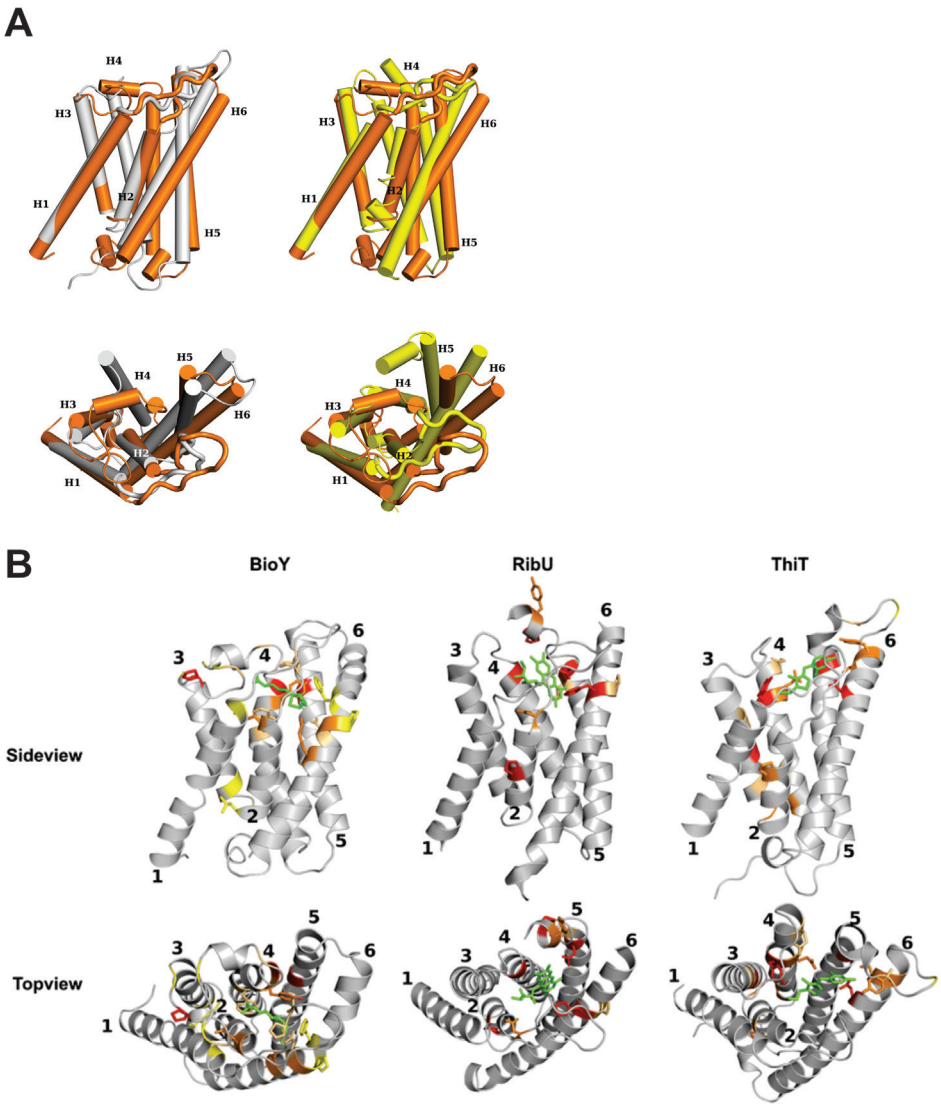

Figure 3: Comparison of structures of BioY, ThiT and RibU. (A) Superimposed structures of BioY (orange), ThiT (gray) and RibU (yellow), viewed from the plane of the membrane (top part) and from the outside of the cell (bottom part, direction of view perpendicular to the membrane plane). The structures have been superimposed on helices 1 & 3 in order to highlight the structural similarities of helices 1-3 and the differences of helices 4-6. Loops 1 are indicated in thick lines. The N- and C-terminus are marked with N and C, respectively (left panel). Helices 1-6 are marked with H1-H6. (B) Secondary structure cartoon representations of BioY, RibU and ThiT with the conserved residues highlighted. Gray, not conserved; yellow to red, low to high conservation. Most conserved residues are involved in the binding of ligand (green stick representation). The remaining conserved residues are involved in the tight helical packing; most often glycines located in turns and places where the helices face each other. Notably, the interface between the N- and C-terminal domains (helices 1-3 and 4-6, respectively) is not conserved.

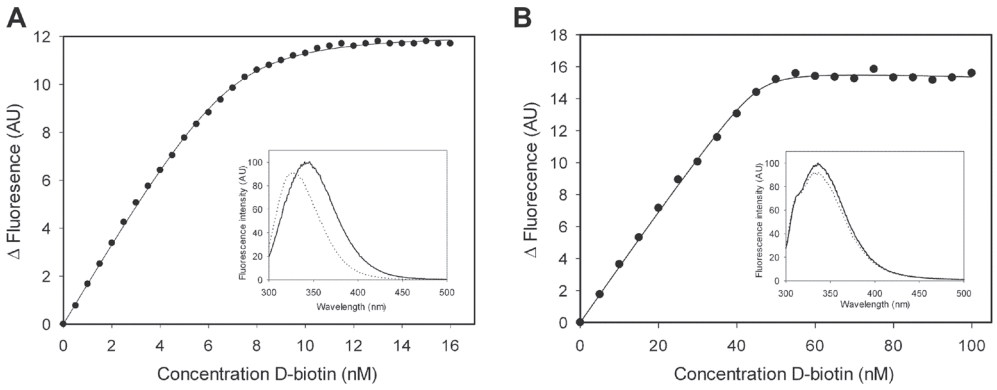

Figure 4: Biotin binding to BioY. (A) Titration of 10 nM BioY with D-biotin. The intrinsic protein fluorescence was measured (excitation wavelength 280 nm, emission wavelength 360 nm). Inset: fluorescence spectrum of 300 nM BioY in the absence of biotin (solid line) and in the presence of a saturating amount of biotin (1 mM, dotted line) (B) Biotin binding to $BioY_{RC}$. Titration of 50 nM BioY from *Rhodobacter capsulatus* with D-biotin. The intrinsic protein fluorescence was measured (excitation wavelength 280 nm, emission wavelength 349 nm). Inset: fluorescence spectrum of BioY in the absence of biotin (solid line) and in the presence of a saturating amount of biotin (100 nM, dotted line).

The ligand is mostly occluded, except for the carboxylate tail that has access to the solvent via a narrow tunnel (figure 1D). The tunnel is too small to allow passage of the biotin molecule. Biotin interacts with helices 4, 5 and 6, and the loop between helix 3 and 4 in the variable domain (figure 1C). In addition, the loop between helices 1 and 2 from the N-terminal domain directly binds the ligand. The residues involved in biotin binding are conserved among BioY homologues (figure 3B). The side-chains of Asp163 and Lys166, as well as the backbone carbonyl of Pro37 and the backbone NH of Ile39 interact with the imidazole ring. The sidechains of Phe159 and Tyr92 stack with the imidazole and thiophene rings of biotin, respectively, and Arg93 interacts with the carboxylate of the pentanoic acid group.

Biotin had not been present during the purification or crystallization procedure, yet the substrate was bound to BioY in the crystals. Apparently, biotin originating from the growth medium remained associated with the protein, indicating slow off-rates and high-affinity binding. To produce biotin-free BioY, the expressing cells were cultivated in defined growth medium in the absence of biotin. Biotin binding to the purified *apo*-protein was measured using the intrinsic protein fluorescence titrations. These measurements revealed a protein:biotin binding stoichiometry of 1:1 and a dissociation constant K_d of 0.3 nM (figure 4A).

We reconstituted purified *apo*-BioY into proteoliposomes to determine if BioY could mediate transport of biotin in addition to binding. The reconstituted protein

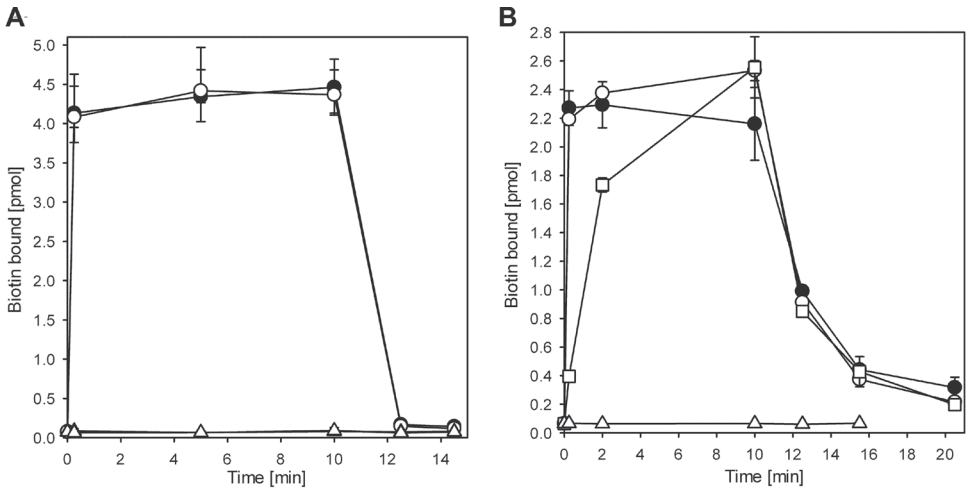

Figure 5: Biotin binding to liposomes containing purified and reconstituted BioY from *L. lactis* (A) and $BioY_{Rc}$ from *R. capsulatus* (B), respectively. Biotin binding was measured in the presence (black circles) or absence (white circles) of membrane gradients of proton gradient, sodium ions and a membrane potential (-120 mV). Black and white triangles represent the same experiment using liposomes without BioY. After 10.5 minutes an excess (1 mM) of unlabeled biotin was added. 160 μg lipids (~1.6 μg of BioY) was used per time-point. Squares in panel (B): counterflow experiment. Proteoliposomes were loaded with 15 μM unlabeled biotin before 100-fold dilution into buffer containing 20 nM labeled biotin to start the experiment. All experiments were performed in duplicate or triplicate, and the error bars represent the spread in the data. The amounts of biotin bound to the liposomes in (B) is lower than in (A) because the $BioY_{Rc}$ is less stable in detergent solution (prone to aggregation) causing lower reconstitution efficiencies of functional protein.

mediated rapid binding of radiolabeled biotin to the proteoliposomes, but the substrate did not accumulate inside the liposomes regardless of whether membrane gradients of protons and sodium ions and a membrane potential of -120 mV were present (figure 5A). After chasing of the bound radiolabeled biotin with an excess of unlabeled biotin, the radioactivity was rapidly released from the proteoliposomes, again indicative of bound rather than transported biotin.

BioY from *L. lactis* is homologous with BioY from *Rhodobacter capsulatus* ($BioY_{Rc}$, 35% sequence identity) (Hebbeln et al., 2007). Transport assays using *E. coli* cells expressing $BioY_{Rc}$ have indicated that the protein may transport biotin in the absence of the ECF module (Hebbeln et al., 2007). To test whether the transport capabilities of $BioY_{Rc}$ are indeed different than those of BioY from *L. lactis*, we also purified and membrane-reconstituted $BioY_{Rc}$. Biotin bound rapidly to the proteoliposomes containing *apo*-$BioY_{Rc}$, just like it did to BioY from *L. lactis*, and again no accumulation was observed, neither in the presence nor in the absence of membrane gradients

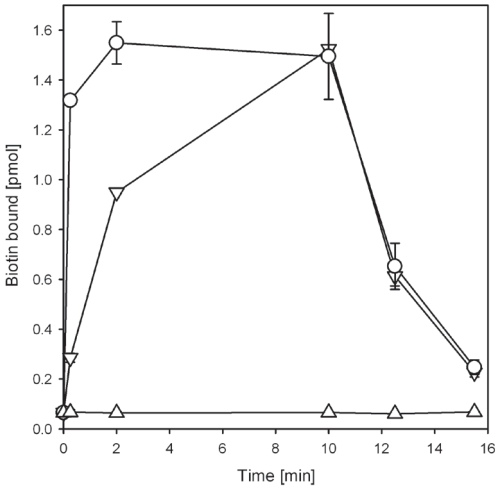

Figure 6: Binding of biotin to liposomes containing purified and reconstituted $BioY_{Rc}$. Biotin association with the liposomes was measured in the absence of transmembrane ion gradients. Circles: proteoliposomes containing *apo*-protein, inverted triangles: the same proteoliposomes in which the protein was saturated with unlabeled biotin (by preincubation for 2 minutes with 150 nM unlabeled biotin), before 20 nM of labeled biotin was added to start the experiment; Triangles: liposomes without $BioY_{Rc}$. After 10.5 minutes an excess (1 mM) of unlabeled biotin was added in all cases. ~1.6 μg of BioY was used per time-point, assuming that the reconstitution was quantitative. However, $BioY_{Rc}$ was not very stable in detergent solution giving rise to batch-to-batch variation in the absolute amounts of functionally reconstituted protein (cf. the amounts of biotin bound to the liposomes in figure 5).

for protons and sodium ions, and a membrane potential (figure 5B). However, the kinetics of the subsequent chase of radiolabeled biotin from the proteoliposomes with an excess of unlabeled biotin was much slower than in the case of the lactococcal protein. The fast association of radiolabeled biotin with the proteoliposomes and the slow chase are indicative of biotin binding with fast on-rates and slow off-rates compared to *L. lactis* BioY. To test whether substrate release indeed was slow, we repeated the binding experiment using proteoliposomes in which $BioY_{Rc}$ was saturated with unlabeled biotin at the start of the experiment, instead of using *apo*-$BioY_{Rc}$ (figure 6). In this case, the apparent binding rates of radiolabeled biotin were slow, and similar in magnitude to the release rates of the chase experiment, indicating that indeed the off rates were limiting in the experiment, and showing that $BioY_{Rc}$ alone is a binding protein rather than a transporter. To further confirm that $BioY_{Rc}$ does not mediate transport of biotin we performed a counterflow experiment (figure 5B). If exchange of biotin between the luminal pool of unlabeled biotin (15 μM) and the external radiolabeled pool (150 nM) were to occur, an apparent accumulation of the radiolabel should become visible. However, the same amount of radiolabel

associated with the proteoliposomes as in the case where unloaded liposomes were used, again showing that binding but not transport took place.

The low k_{off} rate of biotin from $BioY_{Rc}$ is indicative of very high affinity binding. Indeed, fluorescence titrations showed that biotin binds with high affinity to $BioY_{Rc}$ (figure 4B), but it was impossible to accurately determine the K_d, because the change in fluorescence upon biotin binding was small. Therefore, high protein concentrations were needed in assay to obtain good signal-to-noise ratios, which is incompatible with accurate determination of low K_d values.

DISCUSSION

The ECF module from *L. lactis* can interact with eight different S-components, six of which share less than 20% sequence identity with any of the other S-components in the organism (ter Beek et al., 2011). For two of the S-components from *L. lactis*, BioY and ThiT, we now have determined crystal structures at high-resolution. There is large structural variation between BioY and ThiT, with the two proteins displaying an RMSD of 5.1 Å. The structural differences are in line with the lack of sequence conservation (16% identity between BioY and ThiT). Most variation is in the C-terminal domain (helix 4-6), which is involved in substrate binding. The substrates thiamin and biotin are chemically very different explaining the large structural variation in the binding domains. Similarly, the C-terminal domain of the riboflavin-binding S-component RibU from *S. aureus*, for which a crystal structure of moderate resolution is available, is structurally divergent. The N-terminal domains (consisting of helices 1-3) are more similar in all structures and -at a the same position in helix 1- contain the AxxxA motif that was found to be essential for thiamin transport by the ECF module-ThiT complex (Erkens et al., 2011). Although BioY, ThiT from *L. lactis* and RibU from *S. aureus* are structurally very different, there are also similarities. In all three proteins, not only residues from the non-conserved C-terminal domain interact with the substrate, but also residues from the loop between helices 1 and 2 in the N-terminal domain (residues 36-39 in BioY). Loop 1-2 forms a direct link between the substrate-binding site and the N-terminal domain that interacts with the ECF module. The loop therefore may mediate coupling between conformational changes in the ECF module induced by ATP binding/hydrolysis, and substrate binding/release in the S-component (figure 3). In response to ATP binding/hydrolysis in the ATPase domains, the loop may rearrange and thereby perturb the substrate-binding site while at the same time opening up the pathway for substrate translocation. Because loop 1-2 is located on the external face of the S-components, whereas the nucleotide-binding domains are cytoplasmic, the ATP-dependent conformational

changes will have to be communicated/transduced via a transmembrane protein, *e.g.* the EcfT subunit.

BioY from *L. lactis* and BioY from *Rhodobacter capsulatus* ($BioY_{Rc}$) share 35% sequence identity. The latter protein is the archetypical member of the S-component superfamily (Hebbeln et al., 2007). Based on the characterization of $BioY_{Rc}$ expressed in *E. coli* cells it has been suggested that the BioY-family of S-components may be different from other S-components both in terms of oligomeric structure, and in terms of transport mechanism. Nonetheless, our biochemical and structural characterization of BioY suggest a unifying structure and mechanism.

First, the stable structural unit of BioY in detergent solution is a monomer. Analysis of the crystal packing showed that adjacent BioY molecules in the crystals do not represent physiological oligomers, because their relative orientations are incompatible with embedding in a membrane environment. In addition, static light scattering experiments (SEC-MALLS) confirmed that BioY is monomeric, just like other S-components such as ThiT (Erkens and Slotboom, 2010) and RibU (Zhang et al., 2010). Similarly, we found that $BioY_{Rc}$ from *Rhodobacter capsulatus* is monomeric in detergent solution (Finkenwirth et al., 2010). Therefore, from a structural point of view the BioY-family is not different from other S-components. In contrast, *in vivo* fluorescence lifetime measurements have indicated that $BioY_{Rc}$ forms oligomers when heterologously overproduced in *E. coli*. We cannot exclude that the oligomeric state of S-components is different in membranes, but none of the available structures (BioY, ThiT and RibU) show possibilities for extensive interfaces, which would be required for stable oligomer formation. Therefore the structure in membranes must be different for oligomerization to occur.

Second, D-biotin binds to BioY with a high affinity (K_d of 0.3 nM). The affinity measured *in vitro* compares well to the K_d of 0.15 nM that was found in the 1970s for biotin binding to whole cells of *L. casei* (Henderson et al., 1985), which was likely mediated by a BioY orthologue. Fluorescence titrations showed the presence of a single binding site per BioY molecule, which is consistent with the crystal structure. Subnanomolar K_d values and 1:1 binding stoichiometry are conserved features of S-components (Erkens and Slotboom, 2010; Henderson et al., 1985; Duurkens et al., 2007; Eudes et al., 2008; Henderson and Zevely, 1978) and these properties are also conserved in $BioY_{Rc}$ from *R. capsulatus* (figure 4).

Third, in the absence of the ECF module, $BioY_{Rc}$ from *R. capsulatus* was reported to be a low affinity, high capacity transporter when overexpressed heterologously in *E. coli* cells (Hebbeln et al., 2007). Such transport kinetics combined with the high affinity binding that we find for BioY and $BioY_{Rc}$ would require input of free energy. However, regardless of the presence of membrane gradients for protons and sodium

ions, and a membrane potential, we could not detect transport of biotin by BioY from *L. lactis* or $BioY_{Rc}$ reconstituted in proteoliposomes. The reconstituted proteins supported binding of radiolabeled biotin only. Therefore, we conclude that, in the absence of the ECF module, BioY from *L. lactis* and $BioY_{Rc}$ act as a high-affinity substrate-binding protein, and that they cannot transport biotin on their own.

How then can we explain the apparent biotin transport reported for $BioY_{Rc}$ expressed in *E. coli* cells? Our data show that the release of bound biotin from solitary $BioY_{Rc}$ is very slow (low off-rate, figure 5B and figure 6). In the paper where solitary $BioY_{Rc}$ was reported to transport biotin (Hebbeln et al., 2007) the protein most likely was biotin-saturated rather than *apo* at the onset of the experiment. We hypothesize that these experiments showed slow exchange of the bound, unlabeled biotin for radiolabeled substrate rather than transport.

The lack of transport activity by solitary BioY is consistent with the absence of an obvious translocation path through BioY. Most of the conserved residues in BioY are involved in either ligand binding (near the extracellular face of the protein), tight packing of the helices (many glycines, figure 3B) or interaction with the ECF module (AxxxA motif). In contrast, a speculative pathway for the transport of riboflavin through solitary RibU was proposed based on the presence of conserved residues in the RibU family (Zhang et al., 2010). We re-evaluated the residue conservation in RibU and found that the proposed pathway-lining residues are not conserved when a larger set of sequences was used (Erkens *et al* (Erkens et al., 2011) and figure 3B). Therefore, we believe that there is no evidence for a translocation path through the protein, which is consistent with the experimental observation that RibU alone does not support uptake of riboflavin in cells (Zhang et al., 2010). Similarly, ThiT does not support transport of thiamin, and the structure does not show a translocation pathway. Also the S-components for folate and pantothenate cannot transport their substrates without the ECF module (Rodionov et al., 2009; Neubauer et al., 2009). We conclude that S-components in the absence of additional components are binding proteins rather than transporters (Erkens et al., 2011). Together with the ECF module, they form a substrate translocation path across the membrane.

Chapter 3

Substrate-induced conformational changes in the S-component ThiT from an Energy Coupling Factor transporter

Maria Majsnerowska[*1]
Inga Hänelt[*2]
Dorith Wunnicke[*2]
Lars V. Schäfer[3]
Heinz-Jürgen Steinhoff[2]
and Dirk Jan Slotboom[1]

This chapter is published in:
Structure (2013) *21*, 861–867

*Authors contributed equally to this work.

[1]Department of Biochemistry, Groningen Biomolecular Sciences and Biotechnology Institute, Netherlands Proteomics Centre and Zernike Institute for Advanced Materials, University of Groningen, Nijenborgh 4, 9747 AG Groningen, The Netherlands
[2]Department of Physics, University of Osnabrueck, Barbarastrasse 7, 49076 Osnabrueck, Germany
[3]Institute of Physical and Theoretical Chemistry, Goethe-University Frankfurt, Max-von-Laue-Str. 7, D-60438 Frankfurt am Main, Germany 4These authors contributed equally to this work

ABSTRACT

Energy Coupling Factor (ECF) transporters are a recently discovered class of ABC transporters that mediate vitamin uptake in prokaryotes. Characteristic for ECF-type ABC transporters are small integral membrane proteins (S-components) that bind the transported substrates with high affinity. S-components associate with a second membrane protein (EcfT) and two peripheral ATPases to form a complete ATP-dependent transporter. Here, we have used EPR spectroscopy, stopped-flow fluorescence spectroscopy and molecular dynamics simulations to determine the structural rearrangements that take place in the S-component ThiT from *Lactococcus lactis* upon binding of thiamin. Thiamin-induced conformational changes were confined to the long and partially membrane-embedded loop between transmembrane helices 1 and 2 that acts as a lid to occlude the binding site. The results indicate that solitary ThiT functions as a *bona fide* high-affinity substrate binding protein, which lacks a translocation pathway within the protein.

INTRODUCTION

Energy Coupling Factor (ECF) proteins are ATP-binding cassette (ABC) transporters that mediate uptake of vitamins and trace elements in prokaryotes (Rodionov et al., 2009; Erkens et al., 2012). They consist of two identical or homologous nucleotide-binding or ATPase subunits (EcfA), which are characteristic for the ABC transporter superfamily. The peripheral ATPase subunits form a complex, the ECF module, with the integral membrane protein EcfT. A second integral membrane protein (the S-component) is responsible for substrate binding and associates with the ECF module to form a functional ATP-dependent transporter. ECF transporters do not make use of soluble substrate binding proteins/domains (SBP or SBD), which are usually part of bacterial ABC importers (Duurkens et al., 2007; Erkens and Slotboom, 2010; Erkens et al., 2011; Davidson et al., 2008).

Multiple S-components, specific for different substrates, can make use of the same ECF module (ter Beek et al., 2011; Rodionov et al., 2009). These different S-components usually share too little sequence similarity to establish homology. Nonetheless, the crystal structures of three S-components have revealed a similar fold: RibU (PDB:3P5B) from *Staphylococcus aureus* (riboflavin-specific, (Zhang et al., 2010), ThiT (for thiamin, PDB:3RLB (Erkens et al., 2011) and BioY (for biotin, PDB:4DVE, (Berntsson et al., 2012), both from *Lactococcus lactis*, all have 6 transmembrane segments with cytoplasmic N- and C-termini. S-components bind their substrates with high affinity (dissociation constants below 1 nM) (Duurkens et al., 2007; Berntsson et al., 2012; Erkens and Slotboom, 2010). In the crystal structures of ThiT, BioY and RibU a substrate molecule (thiamin, biotin and riboflavin, respectively) was found in an occluded site near the extracellular surface (Erkens et al., 2011; Berntsson et al., 2012; Zhang et al., 2010)

In vitro experiments have shown that solitary S-components, in the absence of the ECF module, can bind substrates but cannot translocate them across the membrane (Erkens et al., 2011; Zhang et al., 2010). In contrast, *in vivo* experiments on BioY from *Rhodobacter capsulatus* have suggested that the protein can also translocate biotin across the membrane (Hebbeln et al., 2007), although the data might alternatively be interpreted as ligand binding rather than transport (Berntsson et al., 2012). The structural basis for the potential translocation pathway was proposed based on the crystal structure of RibU (Zhang et al., 2010). Large structural rearrangements were postulated which could open a pathway that runs from the extracellular binding site (observed in all available crystal structures) to the cytoplasm in the presence of ECF module. The rearrangements include substantial shifts in the relative positions of transmembrane helices. Here we have tested whether such large conformational

changes take place in the absence of ECF module that would facilitate substrate translocation by solitary S-components. We have used the S-component ThiT rather than RibU, because of the crystal structure of ThiT is of higher resolution. We find that binding of thiamin to ThiT only requires opening of lid-like loop 1-2 that occludes the binding site while the transmembrane helices form a rigid scaffold. A translocation path for thiamin transport is absent in solitary ThiT.

MATERIALS AND METHODS

Plasmids construction.

Plasmids containing mutations in the gene encoding ThiT were generated from plasmid pREnHis-ThiT (Erkens and Slotboom, 2010) by PCR using the QuikChange method (Stratagene). The pREnHis-ThiT mutants were converted into expression vectors for *L. lactis* (pNZ plasmids) using the vector backbone exchange (VBEx) protocol (Geertsma and Poolman, 2007). All plasmids were verified by DNA sequencing (Seqlab, Germany).

Overexpression, purification and spin labeling of ThiT mutants.

L. lactis strain NZ9000 containing pNZnHis-ThiT variants were grown semi-anaerobically in 1 L bottles at 30 °C using either chemically defined medium (Berntsson et al., 2009) without thiamin, to obtain substrate-free protein (Erkens and Slotboom, 2010), or M17 broth (Difco), to obtain liganded protein. Both growth media were supplemented with 1.5 % (w/v) glucose and 5 μg/mL chloramphenicol. Expression was induced at an OD_{600} of 1.0 by the addition of 0.1 % (v/v) of the culture supernatant from the Nisin A producing strain NZ9700 (Kuipers et al., 1998). The cells were allowed to continue growing for 2 hours and harvested at a final OD_{600} of 2.5-3.5. Cells were broken and membrane vesicles were prepared as described (Erkens and Slotboom, 2010). The previously described purification protocol (Erkens et al., 2011) was modified as follows: 50 mM potassium phosphate (KP_i) buffer pH 7.0 supplemented with 150 mM KCl was used throughout the purification. Membrane vesicles were solubilized in 1 % (w/v) n-dodecyl-β-d-maltopyranoside (DDM, Anatrace), but in all subsequent steps 0.15 % n-decyl-β-d-maltopyranoside (DM, Anatrace) was used. Two washing steps were performed when the protein was bound to the Ni-Sepharose column: The first with 20 column volumes (CV) of washing buffer containing 5mM β-mercaptoethanol (to reduce all sulfhydryl groups) and the second with 20 CV degassed washing buffer (to remove reducing agent). The ThiT variants were spin-labeled during purification on the Nickel-Sepharose. The protein was incubated overnight at 4 °C with 1mM spin label

(1-oxyl-2,2,5,5-tetramethlpyrroline-3-methyl)- methanethiosulfonate (TRC, Toronto, Canada) dissolved in washing buffer. Free spin label was washed away with 20 CV of washing buffer.

The peak fractions after size exclusion chromatography were concentrated on a Vivaspin 30-kDa molecular weight cutoff concentrator (GE Healthcare) to 2-3 mg/ml. During concentration the SEC buffer (50 mM KPi pH 7.0, 150 mM KCl, 0,15 % DM) was exchanged for SEC buffer with D_2O instead of H_2O. Concentrated ThiT variants were used for EPR measurements and supplemented with 20 % D_2-glycerol and 100 μM thiamin if indicated.

Reconstitution into liposomes

Purified and spin-labeled ThiT was reconstituted into liposomes prepared from a 3:1:1 molar ratio of 1,2-dioleoyl-*sn*-glycero-3-phosphoethanolamine (DOPE): 1,2-dioleoyl-*sn*-glycero-3-phosphocholine (DOPC): 1,2-dioleoyl-*sn*-glycero-3-phospho-(1'-*rac*-glycerol) (DOPG) (Avanti Polar Lipids, Inc.) at a protein:lipid ratio of 1:20 (w/w) according to the previously described protocol (Groeneveld and Slotboom, 2010). Proteoliposomes were resuspended in 50 mM KP_i buffer pH 7.0 (with D_2O) supplemented with 20 % D_2-glycerol to the final lipid concentration of 40 mg/ml.

Fluorescence measurements

Steady-state Trp fluorescence measurements were performed in SEC buffer with 50 nM protein concentration (Erkens and Slotboom, 2010).

Stopped flow measurements were performed at 25 °C on Applied Photophysics SX20 spectrometer using excitation wavelength of 280 nm and a 310 nm cutoff filter for emission. Measurements were done in SEC buffer with 20 nM final protein concentration. 7-9 traces were recorded (for each substrate concentration), averaged and fitted to a single exponential decay function of the form $F_t = \Delta F + A \cdot \exp(-k_{obs} \cdot t)$, where F_t denotes the fluorescence at time t; ΔF is the fluorescence quenching after completion of the binding reaction; A is the signal amplitude, and k_{obs} is the observed rate constant. Fitting was performed in Origin 7.0 (OriginLab) to obtain a value for k_{obs}.

EPR measurements

Low temperature (160 K) cw EPR spectra at X band were carried out using a homemade EPR spectrometer equipped with a Super High Sensitivity Probehead (Bruker) (microwave power: 0.2 mW, B-field modulation amplitude: 0.25 mT).

Temperature stabilization was achieved by a continuous flow helium cryostat (ESR 900, Oxford Instruments) in combination with a temperature controller (ITC 503S, Oxford Instruments). A RMN 2 B-field meter (Drusch) allowed measurement of the magnetic field. Sample volumes of 30-40 µl were loaded into EPR quartz capillaries and frozen in liquid nitrogen before insertion into the resonator.

Pulse EPR measurements were performed at X-band frequencies using a Bruker Elexsys 580 spectrometer equipped with a 3-mm split ring resonator (ER 4118X-MS3, Bruker). A continuous flow cryostat (ESR900, Oxford Instruments) in combination with a temperature controller (ITC 503S, Oxford Instruments) was used for temperature stabilization. Sample volumes of 30-40 µl were loaded into EPR quartz capillaries and frozen in liquid nitrogen. The four-pulse DEER sequence $\pi/2(\nu_{obs}) - \tau_1 - \pi(\nu_{obs}) - \tau' - \pi(\nu_{pump}) - (\tau_1 + \tau_2 - t') - \pi(\nu_{obs}) - \tau_2 -$ echo was applied (Pannier et al., 2000). A two-step phase cycling (+‹x›, -‹x›) was realized on $\pi/2(\nu_{obs})$, while for all pulses at the observer frequency the ‹x› channels were applied. The pump frequency ν_{pump} was positioned at the center of the resonator dip corresponding to the maximum of the echo-detected nitroxide EPR absorption spectrum, whereas the observer frequency ν_{obs} was set to the low field local maximum of the absorption spectrum resulting in a 65 MHz offset. The pump pulse possessed a length of 12 ns and the observer pulses lengths of 16 ns for $\pi/2$ and 32 ns for π pulses. The dipolar evolution time was given by $t = t' - \tau_1$. Time t' was varied, whereas τ_1 and τ_2 were kept constant and data with $t > 0$ were analyzed. Deuterium modulation was averaged by adding traces at eight different τ_1 start values, starting at $\tau_{1,0} = 200$ ns and incrementing by $\Delta\tau_1 = 56$ ns.

Fitting of experimental cw EPR data

Simulated dipolar broadened EPR spectra were fitted to experimental low temperature cw EPR spectra using the program DipFit (Steinhoff et al., 1997). DipFit determines best-fit parameters for the interspin distance and distance distribution considering a Gaussian distribution of distances. During the fitting procedure the g tensor values, the A_{xx} and A_{yy} values of the hyperfine tensor and the Lorentzian and Gaussian line width parameters are fixed to $g_{xx} = 2.0082$, $g_{yy} = 2.0063$, $g_{zz} = 2.0024$, $A_{xx} = 0.45$ mT, $A_{yy} = 0.46$ mT. EPR spectra are convoluted with a field-independent line shape function composed of a superposition of 52 % Lorentzian and 48 % Gaussian of 0.25 and 0.31 mT widths, respectively.

Analysis of pulse EPR data

For analyzing the pulse EPR data the experimental echo decay was background-corrected using a homogeneous 3.0 – 3.9- dimensional spin distribution. Interspin distance distributions were derived by fitting the background-corrected dipolar evolution function using Tikhonov regularization as implemented in DEERAnalysis2008 (Polyhach et al., 2011).

Simulations of distance distributions

Interspin distance distributions were simulated using an approach based on a rotamer library as implemented in the program MMM (Polyhach et al., 2011). The rotamer library contains 210 pre-calculated rotamers representing an ensemble of possible spin label side chain (R1) conformations. The orientation of the spin label side chain introduced at a specific residue with regard to the protein structure permits calculation of the energy for the R1-protein interaction in consideration of the Lennard Jones potential (Mackerell et al., 2004). An adjacent Boltzmann weighting and normalization by the partition function results in the probability for each rotamer. Multiplication of the probability for each rotamer with the probability of R1 to exhibit this conformation leads to the rotamer probability distribution for the specific residue. Interspin distance distributions are calculated as the histogram of all pairwise interspin distances weighted by the product of their respective probabilities.

Molecular Modeling

The starting structure for the unliganded ThiT model was the crystal structure of thiamin-bound ThiT (Erkens et al., 2011). The initial molecular structure was fixed except for loop 1-2 which was rearranged on the basis of the experimentally determined interspin distances using the program Yasara (Krieger et al., 2002). Finally the unliganded ThiT model was energy minimized using the minimization experiment provided by Yasara Dynamics.

Molecular dynamics simulations

Molecular dynamics (MD) simulations were carried out with the GROMACS program package, v4.5 (Hess et al., 2008). A ThiT monomer, taken from the crystal structure (PDB:3RLB) (Erkens et al., 2011), was simulated a fully solvated palmitoyloleoylphosphatidylcholine (POPC) lipid bilayer. For the simulations of *apo*-ThiT, thiamin was removed from the PDB structure. The periodic simulation

box contained 248 POPC lipids (124 in each leaflet), ~17660 TIP3P water (Jorgensen et al., 1983) molecules, and 55 Cl^- and 46 Na^+ ions (47 Na^+ in case of the *apo*-protein lacking the thiamin cation) to neutralize the simulation box. The box xyz-dimensions were about 9.2 * 8.8 * 10.6 nm. The AMBER99SB force field (Hornak et al., 2006) was used for the protein, together with the Berger lipid parameters (Berger et al., 1997), including the dihedral parameters by Bachar et al. (Bachar et al., 2004) for the torsion around the bond adjacent to the *cis* double bond in the POPC hydrocarbon tail; the lipid parameters were obtained from Cordomi and coworkers (Cordomi et al., 2012). For the Na^+ and Cl^- ions, the parameters of Joung and Cheatham (Joung and Cheatham, 2008) were applied. The thiamin parameters were obtained from the general AMBER force field (GAFF) (Wang et al., 2004), see below. Long-range electrostatic interactions were treated with the particle-mesh-Ewald (PME) method (Darden et al., 1993) with a grid-spacing of 0.12 nm. Short-range van der Waals interactions were described with a Lennard-Jones 6-12 potential that was cut-off at 1.0 nm. The non-bonded neighbor list was updated every 16 fs within this cut-off. Analytic corrections to the pressure and potential energy were applied to compensate for the truncation of the Lennard-Jones interactions (Allen and Tildesley, 1989). The SETTLE algorithm (Miyamoto and Kollman, 1992) was used to constrain the bonds and angles of the water molecules, and LINCS (Hess, 2008; Hess et al., 1997) was used to constrain all other bond lengths. The integration time step was 2 fs for the simulations with thiamin. For *apo*-ThiT, virtual interaction sites were used for the hydrogen atoms (Feenstra et al., 1999), allowing for an integration time step of 4 fs. The temperature was kept constant at 300 K by coupling to a velocity rescaling thermostat (Bussi et al., 2007) with coupling time constant 0.1 ps. For constant pressure, semi-isotropic coupling was applied by separately coupling the lateral (xy) and normal (z) directions to a pressure bath at 1 bar using a Berendsen barostat with a time constant of 0.5 ps and compressibility $4.5 * 10^{-5}$ bar^{-1}.

Thiamin GAFF parameters were obtained using the ANTECHAMBER program as part of the AMBER tools. The electrostatic potential (ESP) of thiamin in vacuo was calculated from a Hartree-Fock/6-31G(d) wavefunction with the Merz-Singh-Kollman scheme (Singh and Kollman, 1984) after geometry optimization at the B3LYP/6-31G(d) density functional level of theory using the GAUSSIAN09 software package. The final partial charges were determined with the RESP method (Bayly et al., 1993), as implemented in ANTECHAMBER. The AMBER topology was converted to GROMACS format with the amb2gmx.pl script (Mobley et al., 2006) downloaded from http://ffamber.cnsm.csulb.edu.

To determine the orientation and insertion of the protein in the lipid bilayer, the OPM (orientations of proteins in membranes) webserver (Lomize et al., 2012) was

used. The oriented protein was inserted into a pre-equilibrated POPC bilayer using the inflation / deflation protocol of Kandt *et al.* (Kandt et al., 2007). All crystallographic water molecules were kept during the preparation of the structure for MD simulations. The protein-bilayer system was solvated with water such that no water molecules were introduced in the hydrocarbon region of the bilayer, and Na^+ and Cl^- ions were added in the bulk water. The system was then energy minimized (1000 steps steepest descent). Subsequently, the system temperature was linearly raised from 60 to 300 K during 100 ps, followed by 6 ns equilibration at 300 K. During these simulations, harmonic position restraints with force constants 1000 kJ mol^{-1} nm^{-2} were applied to all protein heavy atoms. Finally, the position restraints were released during 9 subsequent 100-ps simulations by decreasing the force constants in steps of 100 kJ mol^{-1} nm^{-2}. Thus, the overall equilibration time prior to the production simulations was 7 ns. This relatively long equilibration time was chosen to allow the relaxation of the lipid and water molecules, and, for *apo*-ThiT, the wetting of the binding pocket. Both is the case, as evident from the time evolution of the simulation box vectors and potential energy of the system, and close visual inspection. For *apo*-ThiT, three statistically independent production MD simulations (of length 350 ns, 295 ns and 235 ns, respectively) were initiated by choosing different random seeds for the initial Maxwell velocity distribution at 300 K. Similarly, two independent 300-ns simulations were carried out for the thiamin-bound form. Thus, altogether, the overall simulation time is ~1.5 μs.

RESULTS

To determine the nature and extent of the structural changes upon thiamin binding to ThiT we used Electron Paramagnetic Resonance (EPR) spectroscopy. In the background of cysteine-less ThiT (C41A) we engineered pairs of cysteine residues, which were labeled with the methanethiosulfonate spin label (MTSSL) for EPR studies. We selected three positions for spin labeling in external loops (W34 in loop 1-2, A73 in loop 3-4, W138 in loop 5-6) and three in helices (I24, S79 and A145, in helix 1, 4 and 6, respectively), and combined them into seven pairs (figure 1). Position 34 in loop 1-2 was used in three pairs, in combination with positions 73, 79 and 145. Position 145 in helix 6 was combined with positions 24, 73, 79 and 138.

The distances between the spin labels in each of the purified ThiT variants were determined using continuous wave (cw) EPR spectroscopy (suitable for distances below 1.8 nm) and pulsed EPR methods (Double Electron Electron Resonance (DEER) spectroscopy, suitable for distances larger than 1.8 nm) (Joseph et al., 2011; Altenbach et al., 2008; Claxton et al., 2010; Mchaourab et al., 2011; Hellmich et al., 2012; Jeschke,

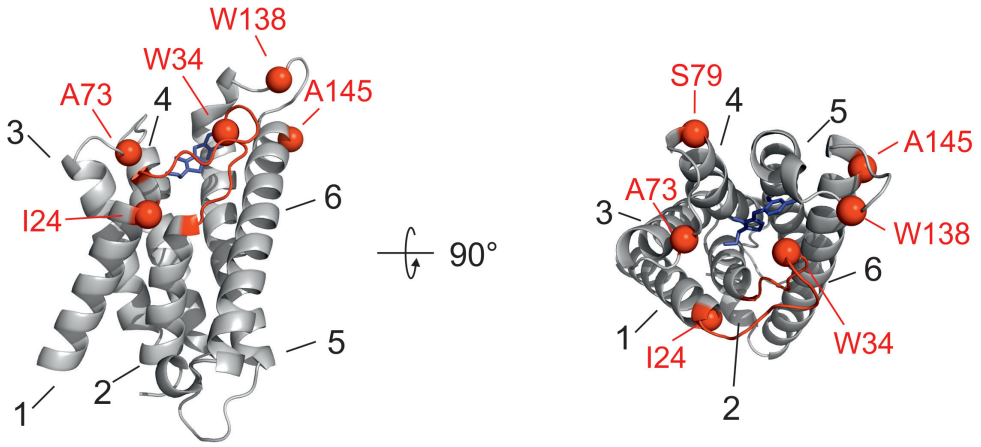

Figure 1: Crystal structure of ThiT with thiamin bound (PDB 3RLB) with the C_α atoms of the residues that were used for spin labeling shown as red spheres. The transmembrane helices are numbered 1-6 (black numbers). Thiamin is shown as blue sticks.

2012) at low temperatures (160 K and 50 K, respectively). The experiments were done both in the presence and absence of thiamin, with the proteins in the detergent-solubilized state. In addition, selected spin-labeled mutants were analyzed in a membrane environment after reconstitution in liposomes.

Table 1. Experimentally determined mean interspin distances between spin-labeled residues in the absence and in the presence of thiamin. Values for the reconstituted protein are shown in brackets.

Variant	Mean distance in ThiT without thiamin bound (nm)	Mean distance in ThiT with thiamin bound (nm)
A73R1 / A145R1	2.6 3.5	2.6 3.5
S79R1 / A145R1	3,4	3,2
W138R1 / A145R1	1.8 (1.5)	1.7 (1.6)
I24R1 / A145R1	3,6	3,6
W34R1 / A145R1	1,4	2,5
W34R1 / S79R1	3.4 (2.5)	2.4 (2.1)
W34R1 / A73R1	2.4 (2.8)	1.4 (1.4)

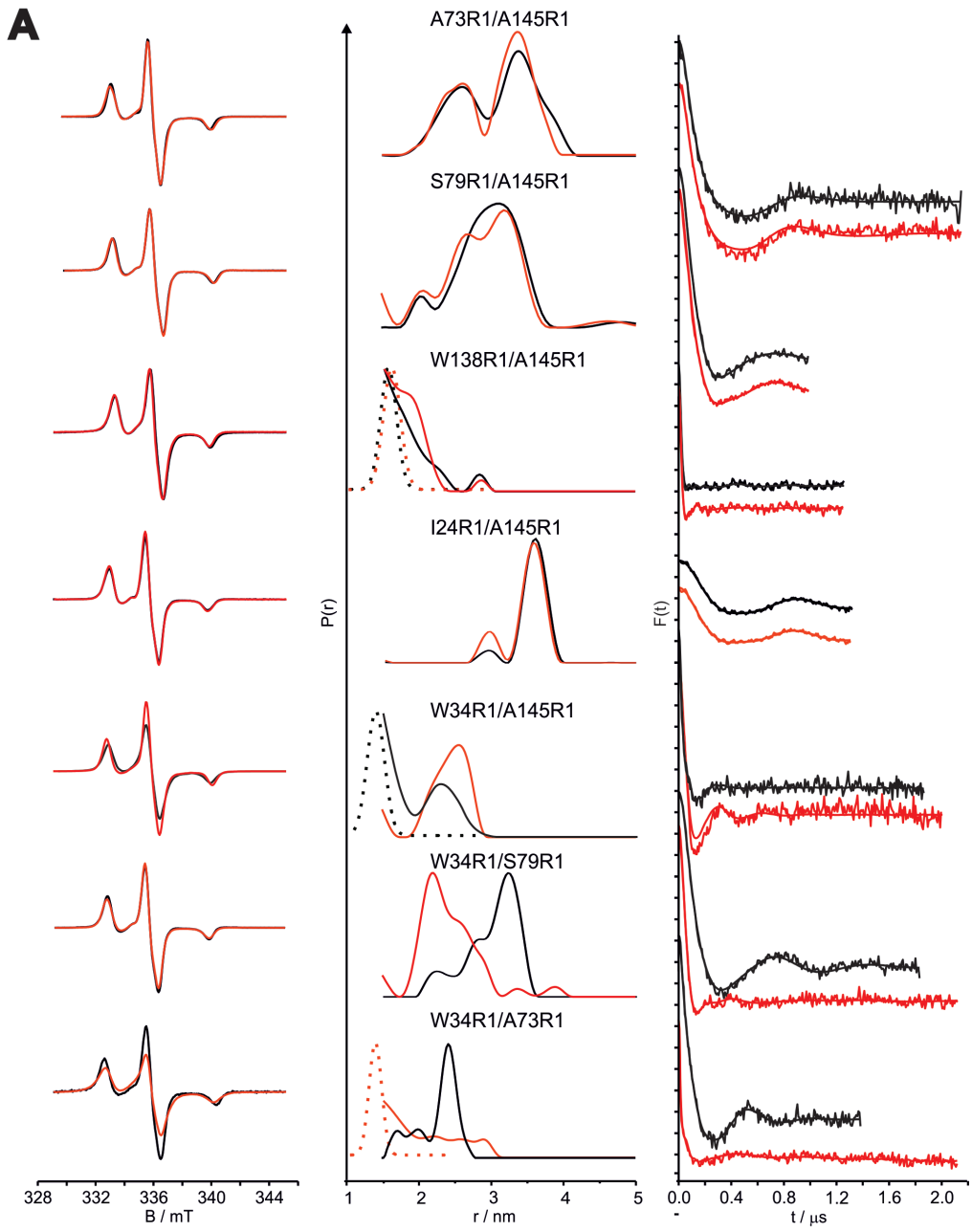
A
A73R1/A145R1
S79R1/A145R1
W138R1/A145R1
I24R1/A145R1
W34R1/A145R1
W34R1/S79R1
W34R1/A73R1
P(r)
F(t)
328
332
336
340
344
B / mT
1
2
3
4
5
r / nm
0.0
0.4
0.8
1.2
1.6
2.0
t / µs

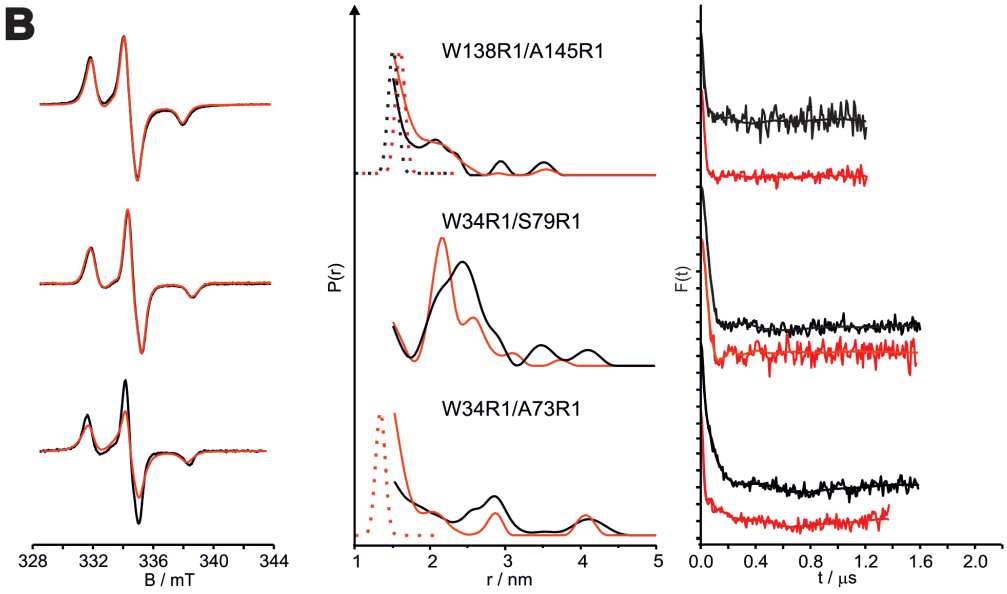

Figure 2: Interspin distance determination by cw and pulse EPR spectroscopy. EPR measurements were done in the absence (black line) or presence (red line) of thiamin. *left* Low temperature (160 K) spin normalized cw EPR spectra of doubly labeled ThiT variants. *center* Distance distributions obtained from cw and pulse EPR measurements. The Gaussian distance distributions from the cw EPR measurements obtained by DipFit are indicated as dotted lines (Steinhoff et al., 1997) only for interspin distances in the 1-1.8 nm range. DEER-derived distributions in the P(r) panel are indicated as solid lines (Steinhoff et al., 1997) for interspin distances above 1.8 nm. *right* Background-corrected dipolar evolution data F(t). Tick marks are separated by 0.05. (A) solubilized ThiT variants; (B) ThiT variants reconstituted in liposomes.

For four ThiT variants (with spin label pairs at positions 73/145, 79/145, 138/145 and 24/145) thiamin binding did not affect the interspin distance (figures 2A, S1 and Table 1). The experimentally determined distances were in agreement with the simulated distances of the labeled protein based on the crystal structure of thiamin-bound ThiT (Erkens et al., 2011) (figure S1A), although there were also differences (e.g. for the 24/145 pair). The latter indicates that the structure of the protein in solution is not identical to the crystal structure. Fluorescence titrations revealed that all spin-labeled variants were still capable of high-affinity thiamin binding (Table S1), which excludes the possibility that the lack of thiamin-induced distance changes was due to inactivation of ThiT, caused by the mutations or labeling.

Different results were obtained for variants with one of the spin labels located in extracellular loop 1-2. These variants all showed drastic changes in interspin distance upon substrate binding. The mean interspin distance between the labels at position

34 and 145 (located in loop 1-2 and helix 6, respectively) increased from 1.4 nm to 2.5 nm upon addition of thiamin, whereas the interspin distance for ThiT variants spin-labeled at positions 34/79 and 34/73 decreased upon thiamin addition (figures 2A and S1 and Table 1). These results show that loop 1-2 moves away from the thiamin binding site in the absence of thiamin. A structural model for the unliganded ThiT, in which we accounted for all the measured mean distances, is shown in figure 3.

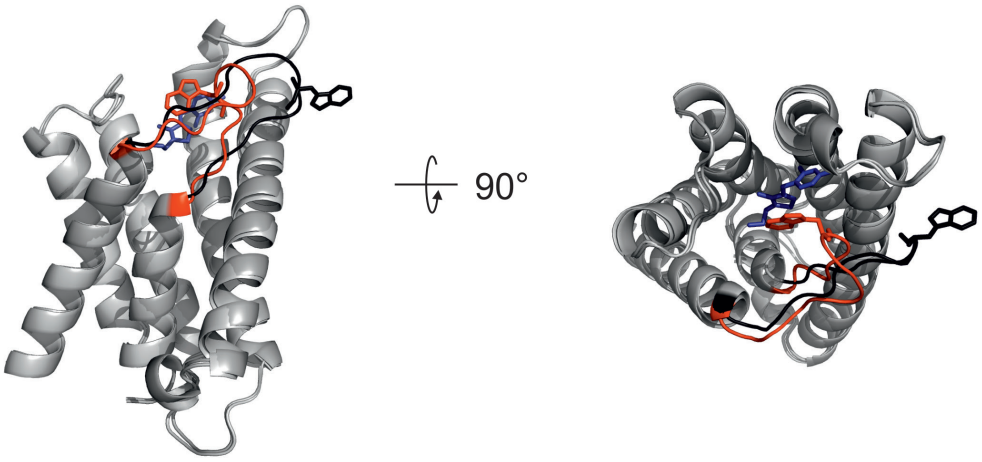

Figure 3: Overlay of ThiT with thiamin bound (crystal structure), and *apo*-ThiT using the distance constraints from the current study using detergent solubilized ThiT, illustrating the conformational changes of loop 1-2 upon thiamin binding. Loop 1-2 is colored red for liganded protein and black for thiamin-free protein. Tryptophan 34 is shown as sticks. Thiamin is shown as blue sticks.

We selected the ThiT variants with spin labels at positions 138/145, 34/79 and 34/73 to determine whether similar distance changes took place when the proteins were present in lipid bilayers after reconstitution in liposomes (figures 2B and S1 and Table 1). The distance between positions 138 and 145 was the same in the presence and absence of thiamin when the protein was reconstituted in liposomes, which is in agreement with the results of solubilized ThiT. The distances between the spin labels in the thiamin-bound variants 34/79 and 34/73 were smaller than in the thiamin-free protein, again consistent with the results obtained for the solubilized protein, and showing that loop 1-2 moved away from the thiamin binding site in the absence of substrate.

Although the direction of the distance change upon thiamin binding was the same in detergent solution and liposomes for the 34/79 and 34/73 variants, the

absolute distances in the thiamin-free state differed. For 34/79 and 34/73 the mean distances between the spin-labels measured in liposomes were 2.5 nm and 2.8 nm compared to 3.4 nm and 2.4 nm for the solubilized protein variants, respectively, showing that loop 1-2 adopts a slightly different conformation in the membrane environment than in the detergent micelle.

To further characterize the structure and dynamics of ThiT in the membrane we carried out all-atom molecular dynamics (MD) simulations of ThiT in a fully solvated POPC bilayer. The simulations provide an atomic-level picture of the changes of the protein structure in the presence and absence of thiamin, and help to interpret and validate the EPR data. The α-helices of ThiT form a stable and rigid scaffold, both in the thiamin-bound and -free forms, as evidenced by the low root-mean-square (rms) deviation of the C_α-atoms compared to the crystal structure and low rms fluctuations (figure 4, S2A, B). The most pronounced differences between the simulations of thiamin-bound and -unbound ThiT were observed for the conformation of loop 1-2 (figure 4): In the thiamin-bound structure, this loop seals off the binding pocket, with W34 being oriented inwards (i.e. toward the center of the protein) and in direct contact with thiamin (figure 4A, grey structure). In the absence of thiamin loop 1-2 moves toward helix 6 and the W34 side chain changes orientation, now forming contacts with Ala149 and Val150 in helix 6 (figure 4A). As a consequence, W34, which in the thiamin-bound conformation is buried in the structure and thus largely shielded from the lipid environment, establishes more contacts with POPC lipids in the surrounding bilayer (figure S2C). Similar structural rearrangements were observed in two additional, statistically independent MD simulations of *apo*-ThiT (of length 295 ns and 235 ns, respectively), whereas the protein conformation stayed close to the X-ray crystal structure during the two 300-ns MD simulations of the thiamin-bound form (figures 4C and S2). The movement of loop 1-2 is depicted in figure 4B and 4C, displaying the distance time-traces and distributions between residue pairs 34/79, 34/145, and 34/73, the same residue pairs that were used for spin labeling in the EPR studies. The distances between the other residue pairs (24/145, 73/145, 79/145, and 138/145) stayed very close to the respective distances in the crystal structure and did not depend on thiamin (figure S2D, E), in agreement with the EPR results.

In the *apo*-protein loops 3-4, 4-5 and 5-6 are equally flexible as loop 1-2 in terms of fluctuations (figures 4A and S2B). Thus, the observation that the distances between A145 (helix 6) and either W138, located in loop 5-6, or A73, located in loop 3-4, are about the same in the thiamin-bound and –free states does not imply that the loops are rigid, but rather that large-amplitude fluctuations yield structural ensembles with about the same mean distance. As loops 3-4 and 5-6 lack residues involved in

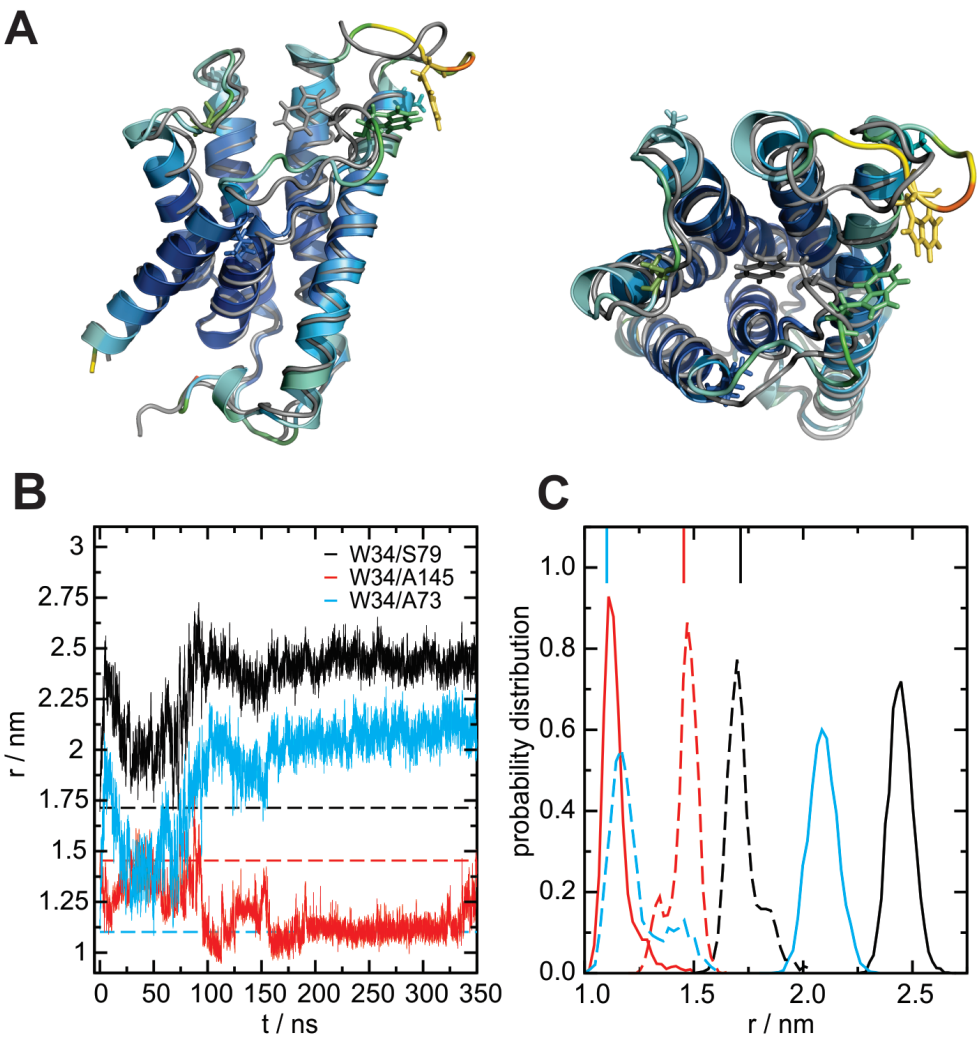

Figure 4: Molecular dynamics simulations. (A) Snapshot after 350 ns from MD simulation of *apo*-ThiT (no thiamin bound). The residues are colored according to their C_α-root-mean-square-fluctuation (rmsf), from small (blue) to large rmsf (red). Residues labeled for EPR spectroscopy (I24, W34, A73, S79, W138, A145) are shown as sticks. POPC, water, and ions are not shown for clarity. The crystal structure of ThiT (PDB 3RLB) is shown in grey. (B) Time-traces of the distances between the centers of mass of residue pairs W34/S79 (black), W34/A145 (red), and W34/A73 (cyan) during a representative simulation of *apo*-ThiT. (C) Distance distributions obtained from the last 100 ns of MD simulations in the absence (solid lines) and presence (dashed) of thiamin. The respective distances in the X-ray crystal structure are indicated by dashed lines in (B) and solid lines in (C), top.

substrate binding its motion does not contribute directly to the substrate binding kinetics.

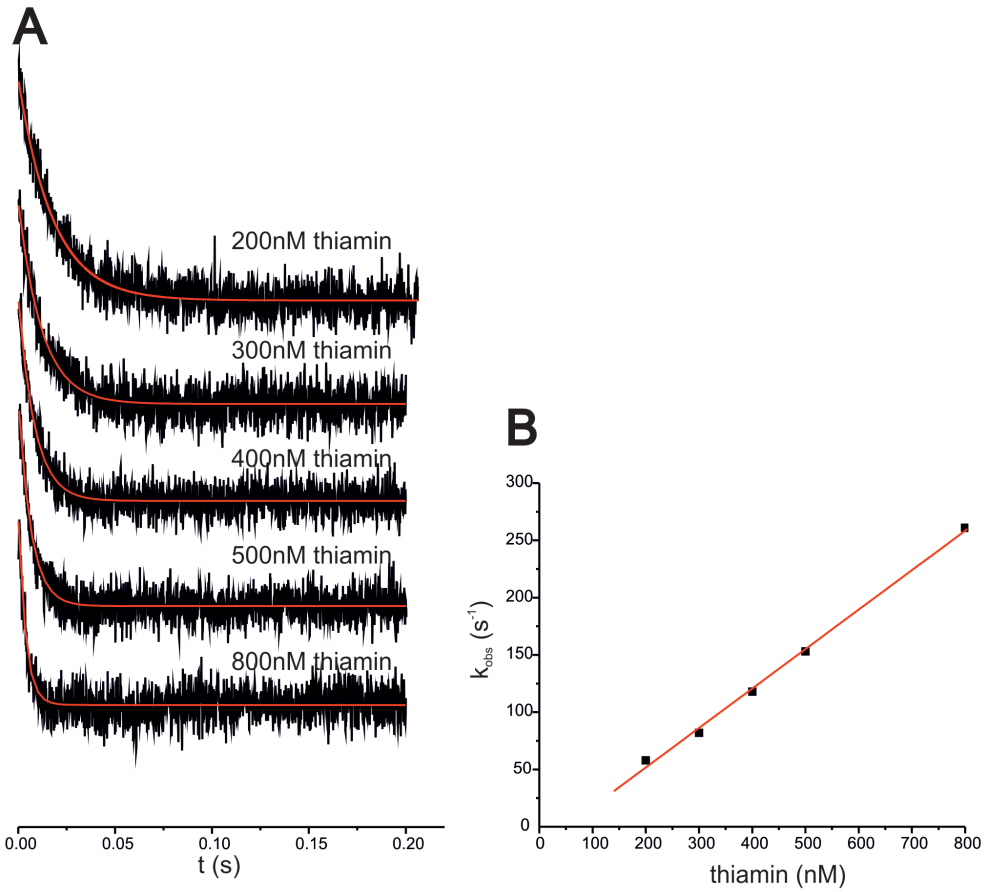

Figure 5: Rates of thiamin binding to WT ThiT. (A) Stopped flow tryptophan fluorescence measurements recorded after mixing of *apo*-ThiT with thiamin of indicated concentrations. Single-exponential fits are shown as red lines. (B) Concentration dependence of the apparent rates (k_{obs}) of thiamin binding. The linear fit is shown as solid red line.

The EPR distance measurements and MD simulations demonstrate that the conformational changes upon thiamin binding are restricted to loop 1-2 and do not lead to large structural rearrangements in the rest of the protein. To substantiate the localized nature of the structural changes, we determined the kinetic parameters of thiamin binding by stopped-flow fluorescence measurements. For these measurements we made use of the quenching of tryptophan fluorescence that takes place when thiamin binds to ThiT. Fluorescence quenching occurred at the millisecond time scale upon mixing of 20 nM ThiT and thiamin (200 - 800 nM) (figure 5A). Single exponential fits of the traces revealed the observed rate constants (k_{obs}). The k_{obs} values varied linearly with thiamin concentration (figure 5B), allowing

us to determine a k_{on} value of $3.4*10^8$ $M^{-1}s^{-1}$. The fast rate (near the diffusion limit) points to a small conformational rearrangement. The k_{on} is an order of magnitude faster than the k_{on} for sugar binding to periplasmic sugar binding proteins (Miller et al., 1983) or sialic acid binding protein (Müller et al., 2006) and two orders of magnitude faster than the k_{on} for peptide binding to OppA (Lanfermeijer et al., 1999). The latter proteins are unrelated to S-components and undergo more substantial conformational changes upon substrate binding, according to Venus flytrap model. The $k_{off,}$ value was so low that it could not be determined accurately from the linear regression, because the intercept with the abscissa was too close to zero. k_{off} instead was calculated from the equilibrium dissociation constant ($k_d = k_{off}/ k_{on}$,) and was found to be 0.04 s^{-1}.

DISCUSSION

The EPR spectroscopic data presented here show that the long and partially membrane-embedded extracytoplasmic loop 1-2 in ThiT undergoes a conformational change upon substrate binding. It is a lid on the binding site that –when open– allows access from the extracellular side of the membrane to the binding site, and –when closed– occludes the substrate. The MD simulations strongly support the conclusions of the EPR experiments and enable their interpretation at the atomic level. They show that indeed the transmembrane helices form a rigid scaffold that does not undergo large conformational changes upon thiamin binding whereas the loops are flexible. Loop 1-2 is directly involved in substrate binding.

Although the residue-to-residue centers of mass distances obtained from the MD simulations cannot be compared quantitatively to the EPR-derived distances between the NO-groups of the spin label side chains, both methods show the same trend. Both in the EPR measurements and in the MD simulations the distances between residue pairs 34/79 and 34/73 were larger in the *apo*-protein than in the thiamin-bound form, whereas the 34/145 distance was smaller. The simulations also predict the formation of more contacts between W34 and lipids in the *apo*-state than in the thiamin-bound state. Consistent with this observation the EPR distance measurements showed that loop 1-2 adopts a slightly different conformation in the membrane environment than in the detergent micelle (figure 2). These results highlight the importance to address the possible effect of the lipid environment on membrane protein structure and function.

All the results presented here strongly support the view that solitary ThiT functions as a binding protein, which captures its substrate with a rate close to the diffusion limit and extremely rarely allows its release. A low off-rate for biotin release

from BioY, had been indicated by binding assays in proteoliposomes (Berntsson et al., 2012) and is consistent with the k_{off} measured for ThiT here (0.04 s^{-1}). There are no indications that large structural rearrangements take place that would be required to open a translocation pathway within the S-component as was suggested for RibU. However, in complex with the ECF module we expect that additional conformational changes take place in the S-components, which allow for substrate translocation. Whether a pathway is then formed within the S-component, at the interface between the S-component and the ECF module, or within the ECF module remains to be determined.

SUPPLEMENTARY INFORMATION:

Table S1. Thiamin dissociation constants (k_d) of spin-labeled ThiT variants determined by fluorescence titration assays (Erkens and Slotboom, 2010).

Variant	k_d (nM)
WT	0,12
A73R1 / A145R1	1,85
S79R1 / A145R1	0,15
W138R1 / A145R1	0,15
W34R1 / S79R1	1.10[a]
W34R1 / A145R1	0,26
W34R1 / A73R1	5.45[a]
I24R1 / A145R1	0,15

[a] For the variants W34R1 / S79R1, A34R1 / A73R1 the dissociation constants were determined for the unlabeled mutants since no fluorescence changes could be detected in the labeled state. For EPR measurements of thiamin-bound ThiT these mutants were spin-labeled after thiamin binding. In all other cases the dissociation constants were determined for the spin-labeled mutants.

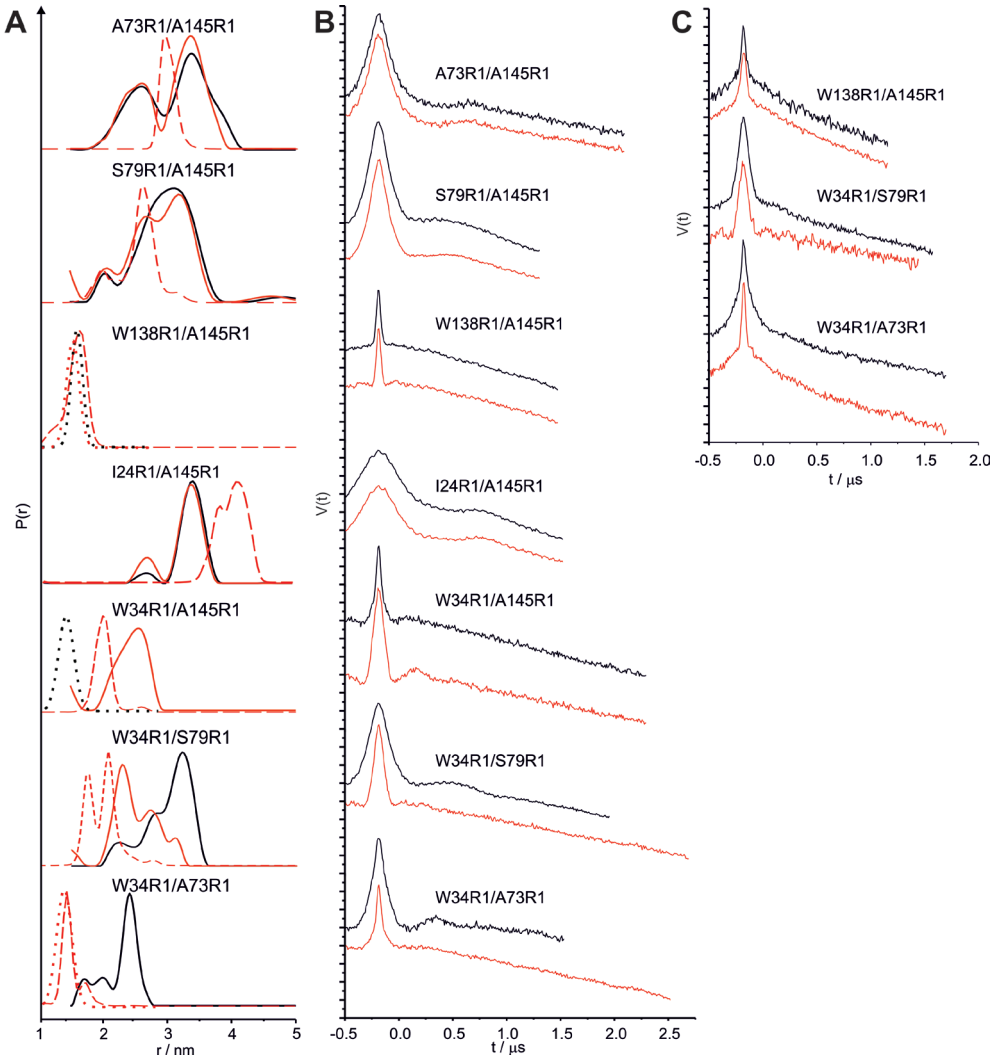

Figure S1 (related to figure 2)**: Experimental raw data and data analysis of cw and pulse EPR data.** (A) Interspin distance distributions obtained from DEER (P(r), solid lines) (Pannier et al., 2000) or cw EPR (dotted lines) measurements (Steinhoff et al., 1997) in the absence (black lines) and presence of thiamin (red lines) compared to simulated distance distributions obtained from the rotamer library approach (dashed red lines) (Polyhach et al., 2011). Experimentally determined distances were in good agreement with the simulated distances of the labeled protein based on chain A of the crystal structure of thiamin-bound ThiT by Erkens *et al.* (Erkens et al., 2011) except for the ThiT variant spin-labeled at positions 73 and 145. Here, the bimodal experimental distance distribution was not reproduced by the simulated distance distribution. The experimental result indicates either the presence of two conformers of the spin label side chain or of two ThiT conformations. Since a bimodal distance distribution was not observed for ThiT variants labeled at positions 34 and 73 or 138 and 145 it is likely that there were two conformers of the spin label side chain. (B) Experimental primary data of DEER experiments in the absence (black lines) and presence of thiamin (red lines) for ThiT

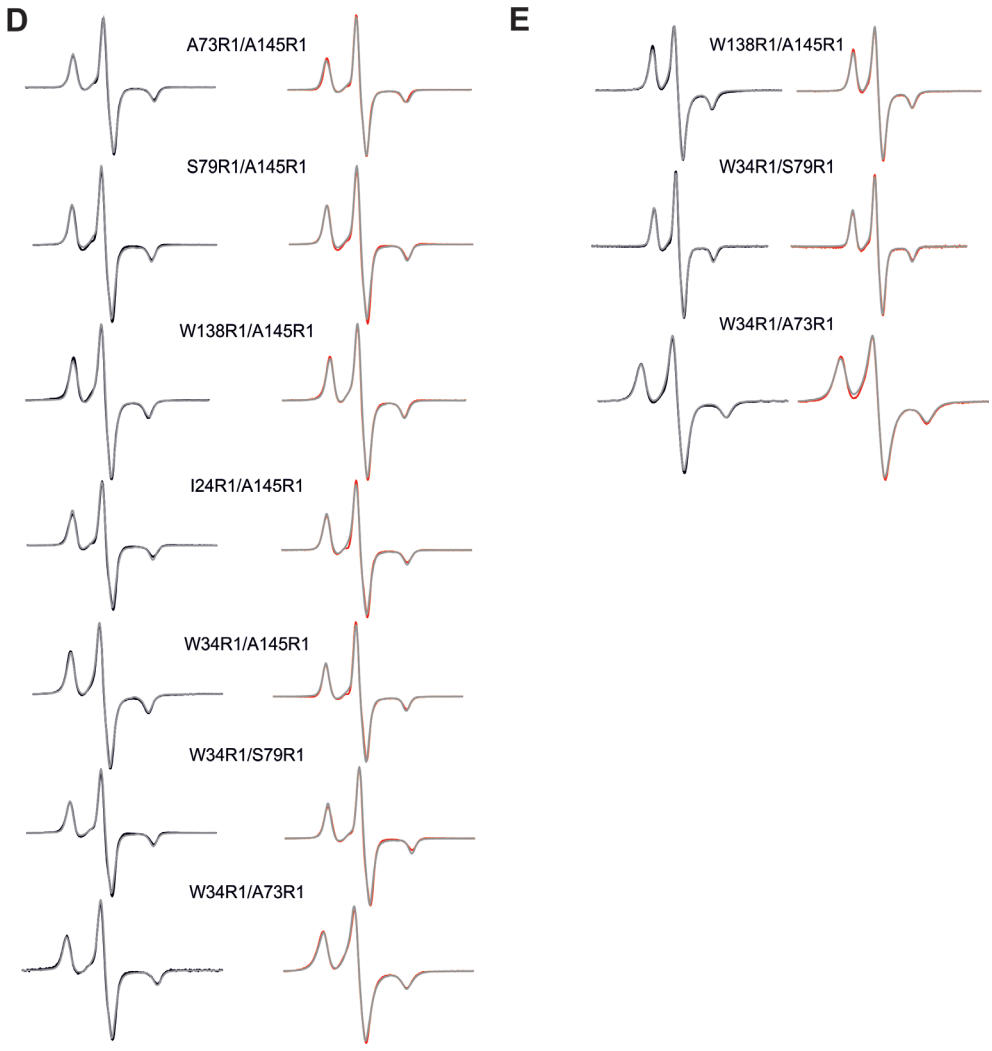

variants in detergent. (C) Experimental primary data of DEER experiments in the absence (black lines) and presence of thiamin (red lines) for ThiT variants reconstituted in liposomes. (D-E) Experimental low temperature cw EPR spectra in the absence (black lines) and presence of thiamin (red lines) and simulated EPR spectra (grey lines) using the program DipFit (Steinhoff et al., 1997) in detergent (D) and reconstituted in liposomes (E).

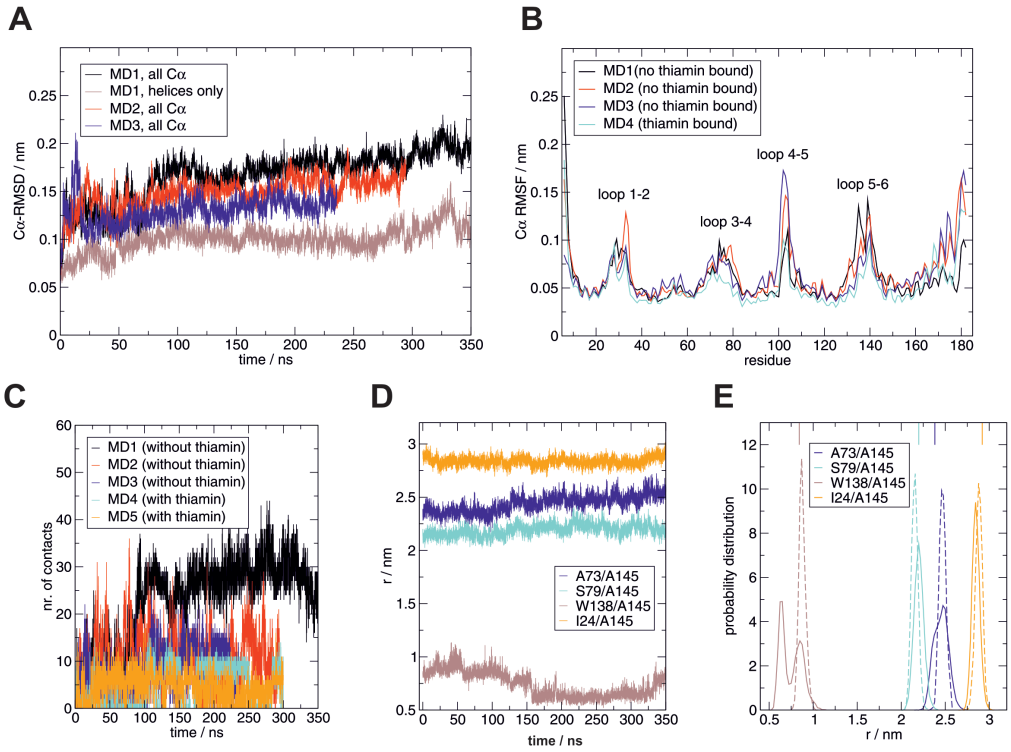

Figure S2 (related to figure 4)**: (A) RMS deviation of C_α-atoms with respect to the starting structure.** The rms deviations during the three MD simulations of *apo*-ThiT, MD1, MD2, and MD3 are shown in black, red, and blue, respectively. For MD1, the curves are shown for the entire protein (black) and for the α-helical scaffold only (brown). Similar curves were obtained from the two simulations of the thiamin-bound form, i.e., **C_α-rmsd plateauing at ca. 0.15 nm after 300 ns (not shown for clarity). (B) RMS fluctuations of C_α-atoms, averaged over the last 100 ns of the respective MD simulations. (C) Time evolution of the number of contacts between W34 and POPC molecules.** A contact was counted if the distance between the backbone N-atom of W34 and any POPC atom was smaller than 0.8 nm. Although W34 establishes more contacts with POPC during simulation MD1 (black curve) as compared to MD2 (red) and MD3 (blue), the number of W34-POPC contacts is significantly higher in all three simulations of *apo*-ThiT than for simulations MD4 and MD5 of thiamin-bound ThiT (cyan and orange, respectively). The average number of W34-POPC contacts is 22.6, 10.5, and 8.0 in MD1, MD2, and MD3, respectively, as compared to 4.4 and 4.5 in MD4 and MD5, respectively. (D-E) Time-traces of the distances between the centers of mass (D) and distributions (E) of residue pairs A73/A145 (black), S79/A145 (cyan), W138/A145 (brown), and I24/A145 (orange). Distance distributions represented by solid lines were obtained from MD simulations of the *apo*-ThiT, whereas the dashed curves show the distributions for the thiamin-bound.

Chapter 4

Interactions between components forming functional ECF transporters

ABSTRACT

The mechanism of transport by ECF transporters from *Lactococcus lactis* that share the ECF module for different S-components (Group II ECF transporters) was studied *in vivo*. The shared ECF module was expressed in *Escherichia coli* together with the S-components specific for thiamin (ThiT) and/or niacin (NiaX), and uptake of the radiolabeled substrates was assayed. As previously established for thiamin, we show that uptake of the niacin is dependent on the presence of the S-component and active ECF module. No thiamin and niacin uptake was observed with an mutated ECF module, which is deficient in ATP hydrolysis. The mutants at the end of the Walker B motif of each ATPase - E166Q in EcfA and E170Q in EcfA' - were used. Subsequently, we investigated whether the conserved AxxxA motif located in the first α helix of the *L. lactis* S-components has a generic role in the interaction with the ECF module. Systematic mutagenesis of the AxxxA motif in ThiT, where each of the alanines (at position 15 and 19) was mutated separately to 15 different amino acids revealed that many aminoacids were tolerated at both positions but position 15 was more sensitive to mutations than position 19. Only two substitutions (to tryptophan and phenylalanine) caused complete loss of function when introduced at either of the two positions. Similarly, niacin transport was severely effected by the single alanine to tryptophan mutations in AxxxA motif of NiaX (A39W and A43W). However only mutation at position 43 completely inhibited niacin transport, while some residual activity was found in case of A39W mutation. We conclude that the differences between NiaX and ThiT may indicate different affinities of the S-components for the ECF module. Finally, we questioned whether different S-components can compete for the ECF module. Uptake of radiolabeled niacin or thiamin was measured in cells where along with the ECF module NiaX and ThiT were expressed at different levels. We show that thiamin uptake by ECF-ThiT was diminished when NiaX was highly overexpressed and even further reduced in the presence of non-labeled niacin. Conversely, niacin uptake was also affected by co-expression of ThiT in the presence of thiamin. The data allow us to conclude that S-components can compete for the ECF module in the substrate dependent manner and that NiaX may have a higher affinity for the ECF module than ThiT.

INTRODUCTION

Vitamin uptake in lactic acid bacteria has been studied since late 1970's but detailed biochemical characterization of the transporters involved in this process is still missing. Initial functional data was obtained by Gary Henderson *et al*. over 30 years ago. In a series of publications the folate, thiamin and biotin transport systems from *Lactobacillus casei* were described. Experiments on *L. casei* cells induced for expression of different vitamin transport systems revealed the existence of specific binding proteins for each of the mentioned vitamins. These proteins were small integral membrane proteins showing high affinity for their substrates (Henderson and Zevely, 1978; Henderson et al., 1976; 1977a; 1977b). They also showed that transport of one vitamin was inhibited by the presence of another one (Henderson et al., 1979b). To explain this observation, a model was proposed in which individual vitamin binding proteins were competing for a common partner that would provide energy for substrate translocation. The shared component was named Energy Coupling Factor and was shown to use ATP hydrolysis as a energy source for folate transport in *L. casei* (Henderson et al., 1979a). However, the genes coding for proteins involved in vitamin uptake could not be determined at that time.

Recently, the molecular identity of the vitamin transporters was discovered. They turned out to be a new type of ABC importers, specific for vitamins and trace elements, and were named ECF transporters. They consist of two ATPases (EcfA and EcfA'), homologues to the classical ABC transporter ATPases or NBDs and two transmembrane proteins, one of which is responsible for substrate binding (S-components). The second transmembrane protein (EcfT) together with two ATPases forms the ECF module (Hebbeln et al., 2007; Rodionov et al., 2009; 2006). An extensive bioinformatics analysis of 365 bacterial and archaeal genomes revealed two groups of ECF transporters. In over 300 of the analyzed genomes genes for putative S-components were found in operons together with *AA'T* genes. The encoded transporters were named Group I ECF transporters (Rodionov et al., 2009). About 100 genomes harbored gene cassettes encoding the ATPases, together with EcfT (*ecfAA'T* operons). These operons did not contain S-component genes. Instead genes for the S-components were found elsewhere in the genome. It was postulated that in this case various S-components share a common, constitutively expressed ECF module as it was proposed by Henderson *et al.* These were named Group II ECF transporters. ECF transporters with shared ECF modules are very abundant in *Firmicutes*, and have been studied extensively over the past 7 years. The two binding proteins studied by *Henderson et al.* specific for folate (FolT) and thiamin (ThiT) from *L. casei* have been purified and their substrate specificity and binding affinity were

determined (Eudes et al., 2008). The shared use of ECF module was shown for FolT (Neubauer et al., 2009; Rodionov et al., 2009), PanT (Neubauer et al., 2009), RibU (Rodionov et al., 2009; Zhang et al., 2010; Karpowich and Wang, 2013; ter Beek et al., 2011) and ThiT (Rodionov et al., 2009; Erkens et al., 2011) from *L. mesonteroides, L. casei, B. subtilis*, *L. lactis, S. aureus* and *S. thermophilus.* It has also been shown that the ECF module is indispensable for transport by the *Firmicutes* proteins. However, the biotin specific S-components from *Rhodobacter capsulatus* ($BioY_{RC}$) and a few other organisms have been reported to transport biotin in the absence of the S-component (Hebbeln et al., 2007; Finkenwirth et al., 2013).

Here, we investigated whether the ECF-module is required for the transport of thiamin and niacin by ThiT and NiaX S-components from *L. lactis,* respectively. The ability to transport substrates was tested (i) in the absence of ECF module, (ii) in the presence of ECF module with non-functional ATPases or (iii) when interaction between ECF-T and S-component was disrupted. Furthermore, we looked into mechanism of competition for ECF module between the two S-components.

MATERIALS AND METHODS

Plasmids construction.

For the transport assays in whole *E. coli* cells with EcfAA'T-S-component complexes, p2BAD and pLEMO vectors were used. The p2BAD vector contains two arabinose-inducible promoters (P_{BAD}) and ampicillin resistance marker (Birkner et al., 2012). The pACYS derived vector called pLEMO contains a rhamnose-inducible promoter and chloramphenicol resistance marker (Wagner et al., 2008). In a first step the gene for the S-component with a C-terminal STREPII-tag (WSHPQFEK) was placed behind the second promoter of the p2BAD vector, via *Xba*I and *Eco*RI or *Xho*I restriction sites. The resulting plasmid was named p2BAD:-*,s-component*. Then, the *ecfAA'T* genes were placed behind the first promoter. This was done by replacing part of the p2BAD:-*,s-component* plasmid with *ecfAA'T* from the pBAD:*ecfAA'T* plasmid that was constructed via ligation independent cloning (LIC) (Geertsma and Poolman, 2007). The restriction enzymes *Bsp*E1 and *Hind*III or *Bgl*II were used to obtain correct DNA fragments for ligation. When the *ecfAA'T* was cloned into the pBAD vector via LIC, the *ecfT* gene was extended with a sequence coding for a TEV cleavage site and a C-terminal 10-His tag and this is therefore also the case in the p2BAD vector (ter Beek et al., 2011).

Additionally, genes encoding for *ecfAA'T* and *niaX* were cloned in pACYS (Wagner et al., 2008). First, the *ecfAA'T* operon with a TEV cleavage site and 10-His tag sequences at the C-terminus were placed behind rhamnose promoter via

*Sal*I and *Bam*HI restriction sites. Downstream of the ECF module operon the *niaX-strepII-tag* gene preceded by artificial linker sequence was cloned via BamHI and NdeI restriction sites. The specific linker sequence was: *GGATCC*ATTAT**AGGAGG** CACTCACCATG (in italics the used *Bam*HI restriction site, in bold the RBS and underlined the start codon of the *niaX* gene).

The genes coding for NiaX with STREPII sequence at a C-terminus or the EcfAA'T module with 10-His tag sequence at a C-terminus were also cloned separately in the pACYS vector, between *Sal*I and *Bam*HI sites right behind rhamnose promoter.

Point mutations were made by introducing one mutation at the time in the *ecfAA'T* operon in the pBAD:*ecfAA'T* plasmid, via the megaprimer approach (Kammann et al., 1989; Ray and Nickoloff, 1992). In the first PCR round, the megaprimer was obtained. It was purified from agarose gel, before it was used in a second round of PCR to obtain the whole *ecfAA'T* operon. This was then cloned into the pBAD vector via the LIC method (Geertsma and Poolman, 2007). To get the double mutation in the *ecfAA'T* operon, one of the single mutants was taken as the starting plasmid.

The obtained mutated pBAD:*ecfAA'T* plasmids were sequenced and subsequently cloned into the vector with the S-component as described above. The ATPases were

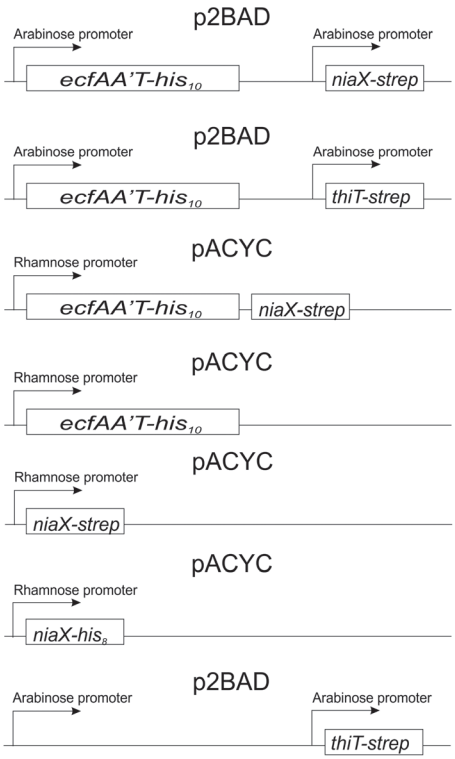

Figure 1: Schematic representation of the plasmid system used in this study. From the top to the bottom: The p2BAD vector with the *ecfAA'T* operon under control of the first arabinose promoter and the gene for niacin specific S-component *niaX* under control of the second arabinose promoter; the p2BAD vector with *ecfAA'T* operon under control of the first arabinose promoter and the gene for thiamin specific S-component *thiT* under control of the second arabinose promoter; the pACYS vector with the *ecfAA'T* operon and *niaX* gene in the constructed operon under control of the rhamnose promoter; the pACYS vector with the *ecfAA'T* operon under control of the rhamnose promoter; the pACYS vector with the *niaX* gene under control of the rhamnose promoter; the pACYS vector with the *thiT* gene under control of the rhamnose promoter; the p2BAD vector with the first multicloning site empty and the gene for thiamin specific S-component *thiT* under control of the second arabinose promoter;

mutated by replacing the glutamate at the end of the walker B motif for a glutamine (E166Q in EcfA and E170Q with EcfA').

Plasmids for the uptakes with the mutated S-components were generated from p2BAD plasmids with S-components cloned behind the second promoter (p2BAD:-,*s-component*) by PCR using Qiukchange method (Stratagene). Subsequently, *ecfAA'T* operon was cloned using *Bsp*EI and *Hind*III or *Bgl*II restriction sites.

For competition assays the gene coding for a S-component was cloned with a C-terminal His_8-tag in a pACYS via *Sal*I and *Bam*HI restriction sites (NiaX) or p2BAD vector with a C-terminally streptagged S-component (ThiT) behind second arabinose promoter.

In this way a collection of p2BAD and pACYS vectors was constructed to be later individually transformed or co-transformed to *E. coli* (figure 1).

Growth, expression and transport assays.

E. coli MC1061 cells containing the two vectors were grown in Luria Broth medium supplemented with 30 μg/mL chloramphenicol and 100 μg/mL ampicillin at 37 °C and with continuous shaking at 200 rpm. Cells with only the p2BAD vector were grown with ampicillin and with a pACYS only with chloramphenicol. For transport assays, cells were grown until OD_{600nm} ~ 1.0 then the temperature was lowered to 25 °C and the indicated amount of L-arabinose and rhamnose were added to induce expression from the p2BAD vector or the pACYS vector, respectively. After 2 hours the cells were spun down, washed and resuspended in ice-cold buffer (50 mM potassium phosphate, pH 7.5) to a final OD_{600nm} of 5 and kept on ice. For the transport assays, the cells were energized with 10 mM glucose for 1 min at 30 °C. Subsequently, [^{3}H]thiamin (American Radiolabeled Chemicals) was added to a final concentration of 25 nM for thiamin uptake assays or 25 nM [^{3}H]niacin diluted with 100nM unlabeled niacin (American Radiolabeled Chemicals) for niacin uptake assays. At the indicated time points, 200 μL samples were taken and mixed with 2 mL stop buffer (ice-cold 50 mM potassium phosphate, pH 7.5). The suspension was rapidly filtered over a BA-85 nitrocellulose filter, which was subsequently washed once with 2 mL stop buffer. For time point zero, 200 μL of cell suspension was added to 2 mL stop buffer containing the radioactive substrate, and this mixture was directly filtered. Filters were dried for 1 hour at 80 °C. 5 mL of Filter Count scintillation liquid (PerkinElmer) was added and the samples were vortexed. The levels of radioactivity were determined with a PerkinElmer Tri-Carb 2800 TR isotope counter.

Western blotting analysis. The membrane fraction form 5 mL cell culture used in transport assay (OD_{600} 5) was isolated as described by Marreddy et al (Marreddy et

al., 2011) and resuspended in 60 μL 1x loading buffer for SDS-PAGE (120 mM Tris-HCl pH 6.8, 50% glycerol, 100 mM DTT, 2% (w/v) SDS, and 0,1% (w/v) bromophenol blue). Samples of 20 μL were resolved on a 4-20% Tris-Glycine precast gels (Thermo Scientific) and transferred using Fast Semi-Dry Transfer Buffer (Thermo Scientific) to a PVDF membrane or 0.45 μm pore sized nitrocellulose membrane for further detection of proteins with primary antibody against STREPII-tag (Qiagen) or HisProbe-HRP (Thermo Scientific), respectively. Transfer was done for 40 minutes at 400 mA in a Trans-Blot® SD Semi-Dry Transfer Cell (Bio-Rad). Chemiluminescence detection was done by using the Western light kit (Tropix, Inc.) or HisProbe-HRP kit (Thermo Scientific) for Strep-tagged and His-fagged proteins, respectively. Imaging was done with the LAS-3000 imaging system (Fujifilm).

Purification of ECF-ThiT complex after overexpression in E.coli. The ECF-ThiT complex was overexpressed in *E.coli* and purified as described by ter Beek *et al* (ter Beek et al., 2011) with following modification. To reduce amount of free phosphate which interferes with ATPase assays, potassium phosphate buffer was replaced by ammonium acetate buffer during wash step on the Nickel-Sepharose column and this buffer was subsequently used in all following steps.

ATPase activity assay. ATPase activity was measured via the malachite green phosphate assay kit (POMG-25H, BioAssay Systems) and protocol for a 96 well plate was followed. Absorbance was measured at 620 nm in a plate reader (BioTek PowerWave 340)

RESULTS

Transport of niacin by ECF-NiaX assayed in the intact *E. coli* cells

To study the interaction of S-components with the ECF module, and the competition between different S-components for the same ECF module, we expressed the ECF module from *L. lactis* in *E. coli* cells, and co-expressed either ThiT (the S-components specific for thiamin) or NiaX, (the S-component specific for niacin) or both. The reason we chose *E. coli* for expression is that the organism lacks indigenous ECF transport systems. The reason why we chose ThiT and NiaX is that uptake via these transport systems can be assayed well in *E. coli.* This has been show before for ThiT (Erkens et al., 2011), and here we also show niacin uptake by ECF-NiaX (figure 2, black circles). Whether S-components can support transport of substrates in the absence of the ECF module is still under debate. For the thiamin specific S-component ThiT from *L. lactis,* it was shown that it cannot support thiamin transport in the absence of ECF module, when expressed in *E. coli* (Erkens et al., 2011). To look further into this controversy, similar transport assays were performed for niacin specific NiaX. When

NiaX was co-expressed together with ECF module in *E. coli*, efficient transport of radiolabeled niacin could be observed, whereas in the absence of either ECF or NiaX transport activity could not be detected (figure 2), indicating that the ECF module is required for niacin transport.

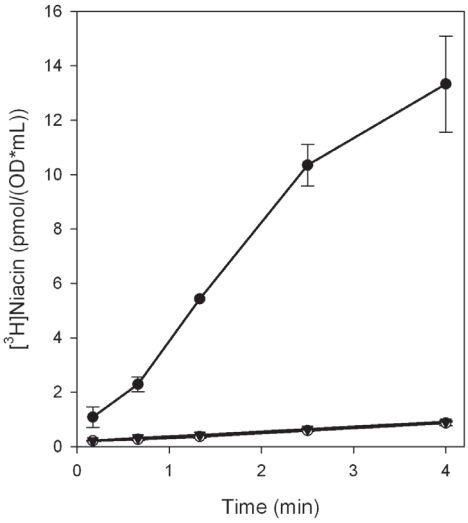

Figure 2: Niacin transport by *E. coli* cells overexpressing ECF-NiaX (black circles), only ECF (white circles) and only NiaX (black inverted triangles). Error bars indicate the range of values from two measurements.

The requirement of the active ATPases for transport

To investigate further the role of the energizing module in the substrate translocation we introduced point mutation in the ATPases and co-expressed ThiT or NiaX with the mutated ECF modules. The introduced mutations are substitutions of the glutamates at the end of the Walker B motif by glutamines (EcfA: E166Q, EcfA': E170Q). These mutations are expected to inactivate the ATPase domains, as in the case of many other ABC transporters (Davidson et al., 2008; Geourjon et al., 2001; Moody et al., 2002; Orelle, 2003). Single mutations of E166Q in EcfA or E170Q in EcfA' alongside with a double mutant were made. We expressed the mutant proteins in *E.coli* and assayed transport of radiolabeled substrates using intact cells. Transport of niacin by ECF-NiaX and thiamin by ECF ThiT was strongly inhibited by the mutations in the ECF module (figure 3A,B). The E166Q mutation decreased transport activity of niacin and thiamin by 85% and 65%, respectively. The E170Q mutant and the double mutant had even stronger effects on transport activity inhibiting it by 90% and 75%, respectively. To confirm the observations made in the whole-cell uptake assay, we performed ATPase activity assays on the purified ECF-ThiT complexes (figure 3C).

Single mutations in each of the individual ATPase had a large effect on the ATPase activity of the transporter, both inhibiting the activity by over 65%, whereas the double mutant showed no activity above the background level.

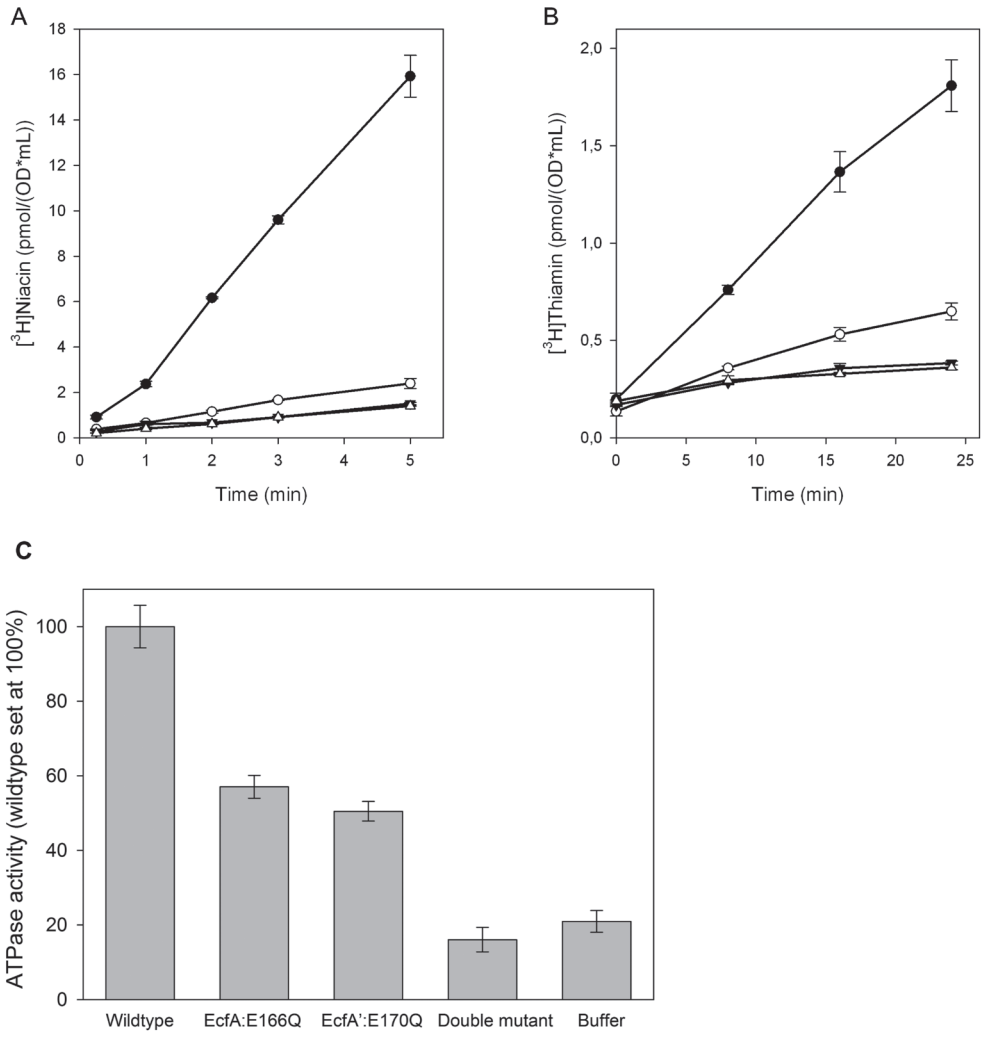

Figure 3: Niacin (A) and thiamin (B) uptake by *E. coli* cells overexpressing ECF-NiaX and ECF-ThiT, respectively; wildtype (black circles), EcfA: E166Q (white circles), EcfA': E170Q (black inverted triangles), double mutants EcfA: E166Q, EcfA':E170Q (white triangles). (**C**) ATPase activity of ECF-ThiT wildtype, mutated EcfA (EcfA: E166Q), mutated EcfA' (EcfA': E170Q) or with both ATPases mutated (EcfA: E166Q, EcfA': E170Q). As the control background level of the phosphate in the buffer was measured. Wildtype activity was set to 100%. Error bars represents range of two measurements.

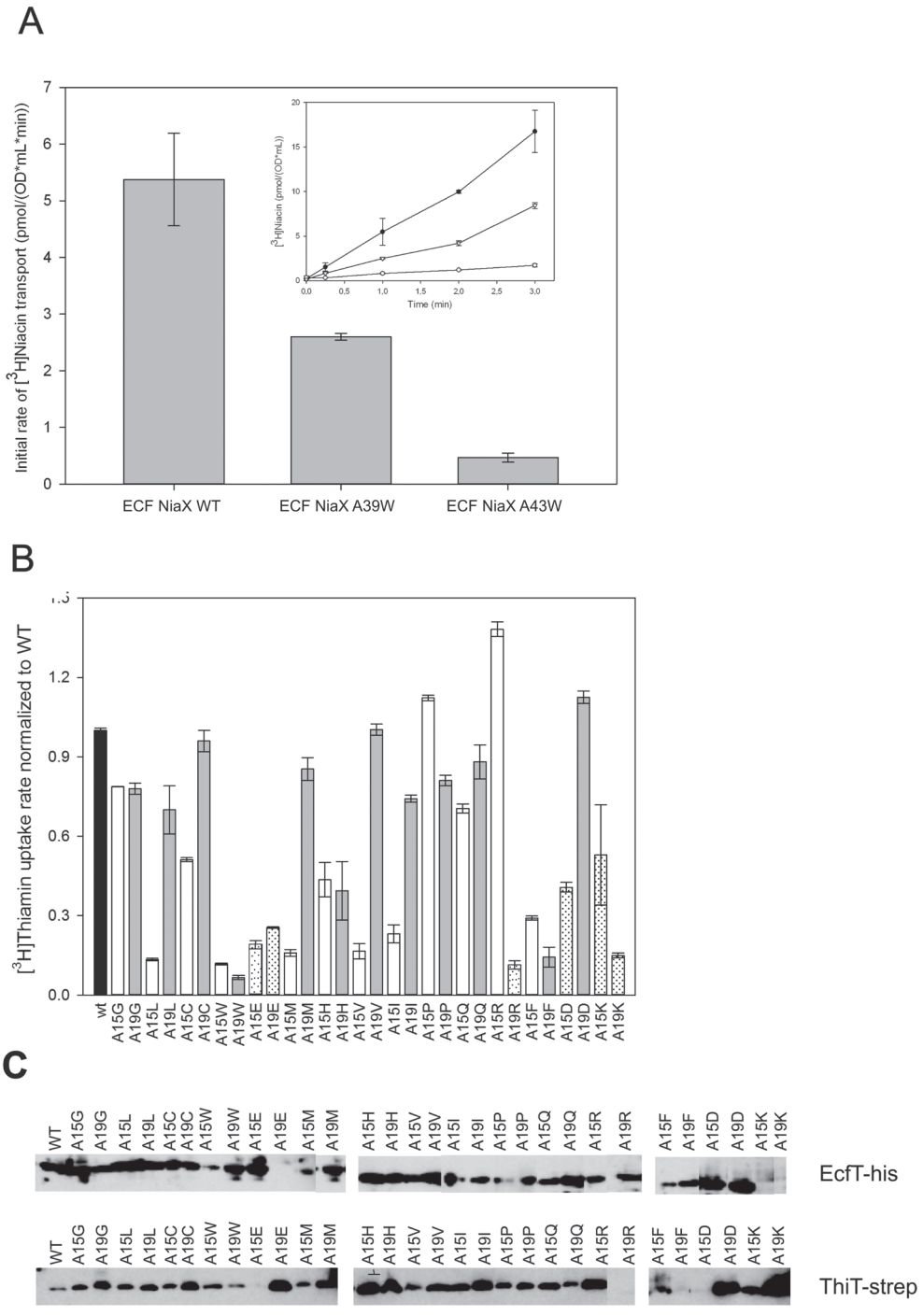
A
Initial rate of [3H]Niacin transport (pmol/(OD*mL*min))
ECF NiaX WT
ECF NiaX A39W
ECF NiaX A43W
[3H]Niacin (pmol/(OD*mL))
Time (min)
B
[3H]Thiamin uptake rate normalized to WT
wt
A15G
A19G
A15L
A19L
A15C
A19C
A15W
A19W
A15E
A19E
A15M
A19M
A15H
A19H
A15V
A19V
A15I
A19I
A15P
A19P
A15Q
A19Q
A15R
A19R
A15F
A19F
A15D
A19D
A15K
A19K
C
WT
EcfT-his
ThiT-strep

The role of the AxxxA motif in the S-components

S-components contain one reasonably well conserved sequence motif: AxxxA, located in the first α helix. The alanine residues of the motif play an important role in the interaction between ECF module and ThiT from *L. lactis* (Erkens et al., 2011). A single substitution of either of the alanines to tryptophan resulted in a complete abolition of thiamin uptake (Erkens et al., 2011; 2012). Accordingly, the two crystal structures of complete ECF transporters (ECF-FolT and ECF-HmpT from *L. brevis*) have shown that the conserved motifs located in the first α helix, AxxxA (in HmpT) and VxxxA (in FolT), are involved in the formation of the interaction surface with the ECF module (Wang et al., 2013; Xu et al., 2013).

To investigate the generic role of the AxxxA motif we also mutated the alanines in NiaX the S-component for niacin from *L. lactis*. The alanines are found at positions 39 and 43 in first predicted α helical segment of NiaX. Mutagenesis of alanine 43 to tryptophan led to a complete inhibition of niacin transport, while some residual activity was found in case of ECF-NiaX A39W (figure 4A). This result suggests that the second alanine in the motif is more crucial than the first for NiaX interacting with ECF module.

To study the role of two alanines in more detail, systematic mutagenesis of the AxxxA motif in ThiT was performed. Each of the two alanines, at position 15 and 19 in ThiT was mutated separately to 15 different amino acids. In this way 30 mutants were constructed and analyzed using whole-cell uptake assays (figure 4B). Surprisingly, many amino acids were tolerated at both positions but position 15 was more sensitive to substitutions than position 19. Notable exceptions were Arg substitution. To exclude that lower uptake activity was caused by different expression levels of the proteins Western blot analysis of the membrane fraction of the cells used in the uptake assay was performed. The C-terminally strep-tagged

Figure 4: Niacin and thiamin transport by *E. coli* cells overexpressing ECF-NiaX and ECF-ThiT respectively, with alanines in AxxxA motif mutated. (A) Initial rates of niacin transport mediated by ECF-NiaX wildtype, ECF-NiaX A43W and ECF-NiaX A39W. Original uptake curves are shown in the inset; ECF-NiaX wildtype (black circles), ECF-NiaX A39W (white inverted triangles), ECF-NiaX A43W (white circles). Error bars represent the range of values obtained in two measurements. (B) Initial thiamin transport rates of the mutants normalized to the initial transport rate of the wild-type averaged form 12 measurements for mutants at position 15 (white bars) and 19 (grey bars). Dotted bars represent the mutants for which the expression could not be detected. The results for each mutants are the average from two measurements. (C) Western blot analyses of membranes from the cells used in (B) showing the expression levels of His-tagged EcfT (using probe directed against the His-tag) and Strep-tagged ThiT (using antibodies against the Strep-tag).

ThiT was detected with anti-strep antibody and expression of the ECF module was checked with probe against the C-terminal His_{10}-tag of EcfT. Expression of both components could be shown for most of the mutants (figure 4C). For six mutants the expression detection was problematic (A15E, A19E, A19R, A15D, A15K and A19K), and the activity results in the figure 4B are shown as dotted bars.

Competition of different S-components for the same ECF module

Experiments performed over 30 years ago by Henderson *et. al* on vitamin transport by *L. casei,* indicated that competition between vitamin binding proteins (S-components) for the common energizing module (ECF module) depended on the presence of a corresponding substrate. Here we tested whether competition between S-components indeed takes place by using the ECF transport system from *L. lactis* heterologously expressed in *E. coli.* We expressed the ECF module together with two different S-components. We chose ThiT and NiaX because we could readily measure ECF dependent transport of thiamin and niacin, respectively, in *E.coli* (figure 2 and (Erkens et al., 2011). We tested if thiamin uptake by the ECF-ThiT complex was affected by co-expression of NiaX and the presence of niacin and vice-versa. To modulate the levels of the S-components and the ECF module we used two different expression vectors. In order to detect competition between two different S-components it was important that the amount of ECF module was limiting. Additionally, the ability to independently vary the S-component expression levels was necessary because NiaX and ThiT appeared to have different affinities for the ECF module. In the cells where ECF-ThiT complex was expressed from the arabinose promoter and NiaX was expressed from the rhamnose promoter [^{3}H]thiamin transport was measured (figure 5). Cells where NiaX expression was induced showed a lower [^{3}H]thiamin uptake rate than cells where NiaX expression was not induced. It is possible that the reduced rate is due to binding of substrate-free NiaX to the ECF module, but it is also possible that co-expression of multiple membrane proteins causes stress to the cells which affected the thiamin uptake. Addition of an excess of unlabeled niacin (100 μM) had little effect on thiamin uptake by the cells which were not induced for NiaX production, but significantly reduced [^{3}H]thiamin uptake activity in cells with expressed NiaX. These results indicate that substrate-bound NiaX competes more effectively for the ECF module than substrate-free NiaX. As a control, we also assayed the uptake of niacin by uninduced cells and cells induced for NiaX expression (figure 5 inset). Induced cells showed much higher transport rates than uninduced cells, but even in the uninduced cells uptake was detectable. This result

shows that a low level of NiaX expression occurs also in the absence of rhamnose, revealing leakiness of the rhamnose promoter.

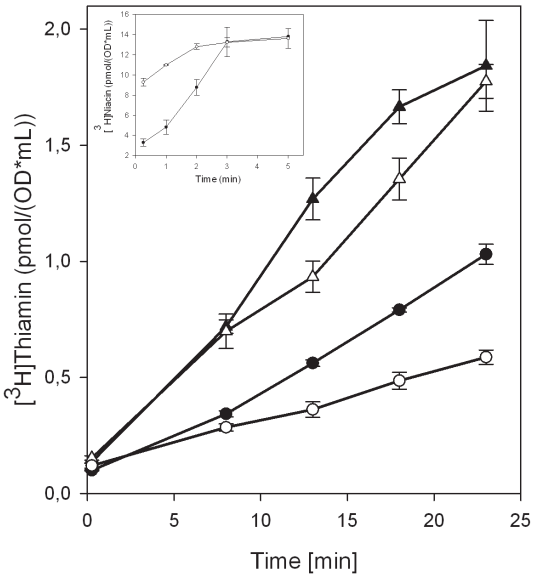

Figure 5: Effect of NiaX and niacin on thiamin uptake via ECF-ThiT. Expression of ECF-ThiT was induced with 10^{-3}% arabinose, while NiaX expression was varied: no rhamnose added (triangles) and 250 μM rhamnose added (circles). Black symbols represent cells were no niacin was added, while white symbols represent the same cells were 100 μM niacin was added during transport assay. The inset shows niacin uptake by the same cells where NiaX expression was not induced (black circles) or induced with 250 μM rhamnose (white circles).

In the reciprocal experiment the transport of radiolabeled niacin by the ECF-NiaX complex in the presence of ThiT and unlabeled thiamin was assayed. In the presence of unlabeled thiamin [^{3}H]niacin uptake significantly decreased (figure 6). The effect of thiamin on niacin uptake was smaller than the effect of niacin on thiamin uptake (figure 5). To confirm that ThiT was indeed produced the ability of the same cells to support [^{3}H]thiamin uptake was shown (figure 6 inset).

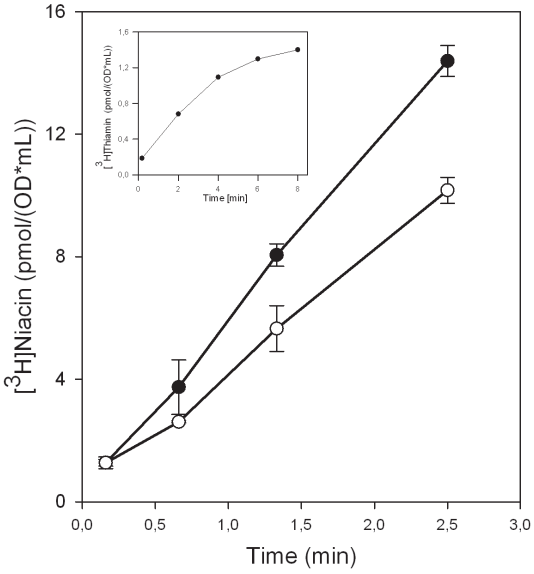

Figure 6: Effect of ThiT and thiamin on niacin uptake via ECF-NiaX. The ECF-NiaX complex was expressed from the leaky rhamnose promoter and ThiT was expressed from arabinose promoter induced with 10^{-3}% arabinose. Black circles represent cells were no thiamin was added, while white circles represent the same cells were 100 µM thiamin was added during transport assay. The inset shows thiamin uptake by the same cells.

DISCUSSION

Here, we show that the niacin specific S-component NiaX depends on the presence of an active energizing module (ECF) for transport when expressed in *E.coli*. We previously already showed that the ECF module is obligatory for thiamin uptake, when ThiT was heterologously expressed in *E.coli* (Erkens et al., 2011). The same has been shown using various assays for many more ECF transporters from different organisms. The dependence on the ECF module for transport of pantothenate, folate and riboflavin transport mediated by PanT, FolT (from *L. mesenteroides*) and RibU (from *S. aureus*) has been shown in the growth assays using *E. coli* strains that were auxotrophic for the corresponding vitamin, and deficient in endogenous transport (Rodionov et al., 2009; Neubauer et al., 2009; Zhang et al., 2010). The ECF module was also indispensable for riboflavin transport by *B. subtilis,* as shown by *ribU*- and *ecfT*- knock-out strains. In addition, folate and thiamin uptake by *L. lactis* cells producing folate and thiamin transporter from *L. casei* (Rodionov et al., 2009) as well as riboflavin transport by *E.coli* cells expressing riboflavin transporter from *S. themophilus* (Karpowich and Wang, 2013) showed the need for the ECF module. The latter was supported by a lack of riboflavin transport activity in cells producing ECF mutants defective in ATPase activity(Karpowich and Wang, 2013). The results obtained here revealed the same dependence on ECF for niacin uptake. No transport activity could be detected in the *E.coli* whole cell uptake assay when only either NiaX or ECF was present.

All the above examples are from Group II ECF transporters. However, some biotin specific S-components which do not belong to Group II transporters have been attributed transport activity in the absence of the ECF module. First, transport was shown for BioY from *R. capsulatus* ($BioY_{Rc}$) on the basis of the whole cell biotin transport assay in *E. coli* as the special feature of the Group I ECF transporters (Hebbeln et al., 2007). The transport activity of the solitary $BioY_{Rc}$ could not be corroborated in *in vitro* uptake experiments performed of the purified protein reconstituted in the liposomes (Berntsson et al., 2012 and **Chapter 2**). Second, expression of BioYs from various proteobacteria lacking ECF module operons in the genome in a biotin-auxotrophic *E.coli* strain, deficient in the endogenous biotin transport system supported growth in the biotin limiting conditions (Finkenwirth et al., 2013). Thus transport by solitary S-components seems to be possible for some BioY proteins.

Single point mutations in the Walker B motif of the ATPases subunits abolish ATP hydrolysis activity in classical ABC transporters (Moody et al., 2002). These mutations also strongly inhibited the ATPase activity of the ECF transporters studied here (figure 3C). The loss of ability to hydrolyze ATP correlated well with decreased thiamin and niacin transport activity in the whole cell uptake assay. Some uptake activity (15%-35% of wildtype activity) could be detected when one of the ATP binding sites was mutated (E166Q mutant in EcfA). The ATPase activity of this single mutant was around 35% of wild-type activity. This correlation suggests that the activity detected in cells expressing the double mutant (E166Q in EcfA and E170Q in EcfA'), which doesn't show any ATPase activity in *in vitro* assay, may be interpreted as substrate binding to the inactive transporter, rather than transport. Surprisingly, the other single mutant (E170Q in EcfA') shows a similar transport activity as the double mutant, yet still maintains around 25% of the wildtype ATPase activity. This resembles ABC transporters with a degenerated single ATP binding site. In those ABC transporters the canonical site provides the free energy required for substrate translocation, whereas the degenerated site plays a structural role (Lubelski et al., 2006; Procko et al., 2009). This result may suggest that ATP binding site of EcfA' has a more important role in transport cycle and again strongly indicates the requirement of the ECF module in formation of the active transporter.

Niacin uptake via the ECF-NiaX complex showed a higher transport rate than thiamin uptake via ECF-ThiT. This may suggest a higher expression level of ECF-NiaX, than ECF-ThiT. Surprisingly, the higher transport rate is also observed when comparing cells that were not induced for ECF-NiaX production (leaky rhamnose promoter) with cells strongly induced for ECF-ThiT (via the arabinose promoter). Alternatively the differences could indicate that NiaX interacts with ECF module

more strongly than ThiT leading to higher transport rates of niacin. Comparison of the results obtained after substitution of the alanines in the AxxxA motifs in both ThiT and NiaX proteins into tryptophans, supports this hypothesis. Exchange of either of alanines in ThiT resulted in complete abolishment of thiamin transport whereas the A39W mutation in NiaX retained still approximately 50% of niacin transport activity.

The AxxxA motif was found in the first α-helical segment of eight different S-components from *L. lactis* but the motif is not completely conserved through all the species that make use of ECF transporters. In some S-components substitutions of the alanine by glycine, serine and valine can be found. In the ECF-ThiT complex from *L. lactis* alanine to tryptophan substitutions showed the importance of both alanines from the motif in the formation of the active transporter (Erkens et al., 2011). Nevertheless, it is unlikely that the two alanines form the only specific interaction with energizing module. Mutagenesis of each alanine to a tryptophan in NiaX led only in one case (A43W) to complete abolishment of niacin transport, whereas the protein with a mutation on the position 39 (A39W) retained residual transport activity. The recently published crystal structures of complete ECF-S-component complexes revealed that other residues are also involved in the interaction between S-component and EcfT proteins (Xu et al., 2013; Wang et al., 2013). This observation suggests that these residues may compensate for the loss of one interaction point in NiaX when alanine 39 is mutated to tryptophan, which is not possible in case of ThiT, possibly because the ECF-ThiT interaction is weaker than the interaction between the ECF and NiaX. However, complete loss of the transport activity in case of the second alanine mutation indicates that the two alanines are not of the equal importance in the contact formation. The extensive analysis of ThiT AxxxA motif mutants presented here additionally support this hypothesis. Although, many aminoacids were accepted on both positions, changes were better tolerated at position 19 than at position 15.

It was postulated that S-components involved in vitamin uptake in *L. casei* can compete for the same energizing module in a substrate-dependent manner (Henderson et al., 1979b). At that time the molecular identities of the proteins involved in vitamin transport were not known. Now we can test in a heterologous expression system whether such substrate-dependent competition indeed takes place. We expressed in *E. coli* the ECF module and different S-components (NiaX and ThiT) from *L. lactis* using a double plasmid system. This system allowed for separate control of the expression levels of the different proteins, which was crucial for the demonstration of competition between different S-components. One should realize

that only in conditions, where ECF module is limiting and one of the S-component is in excess, competition for the ECF module can be detected.

Our results show that ThiT and NiaX can compete for ECF module in the presence of their specific substrates. However niacin transport was not decreased as much by the co-expression of ThiT in the presence of thiamin as thiamin transport was decreased by NiaX and niacin. Similar differences in the effectiveness of competition were observed in the pioneering experiments in *L. casei*, where transport of folate was more severely inhibited in the presence of the thiamin binding protein and thiamin than thiamin uptake in the presence of folate binding protein and folate (about 45% and 25% reduction, respectively). Interestingly, biotin transport could be inhibited by both thiamin and folate whereas neither of them could be affected by biotin (Henderson et al., 1979b). This might again indicate that some S-components interact more tightly with the ECF module than others. Moreover it implies that S-components have higher affinity to the ECF-module in the substrate bound state, and that the ECF module can exchange one S-component for another.

The observed decrease in the thiamin transport rate upon overexpression of NiaX in the absence of niacin might suggest that cells are under stress caused by overall high overexpression of membrane proteins. Alternatively, it could indicate a (weak) interaction of the substrate-free S-component (NiaX) with the ECF module. The complex formation between ECF module and a substrate-free S-component is in the agreement with the recent crystal structures (Xu et al., 2013; Wang et al., 2013). However, those structures were obtained in nucleotide-free conditions, which are different from the conditions in a living cell, where this conformation may be very short-lived.

The data collected here shows that the interaction between ECF module and S-components is dynamic, and suggest that binding and release of the S-components is an important step in the transport cycle. This mechanism enables bacteria to make efficient use of the ECF module in the changing growth conditions. In the natural host cells S-components are under the control of substrate induced promoters or riboswitches. They are upregulated in the response to the substrate deficiency in the cytoplasm. In contrast no factors controlling gene expression were found for *ecfAA'T*, meaning that the ECF module is very likely to be expressed at the constant level (Rodionov et al., 2009). When expression of more than one S-component is induced, competition for limiting amount of ECF module comes into play. The observed effects on the uptake rates of one vitamin caused by the presence of another vitamin are the result of differences in the expression levels of the specific S-components as well as differences in the affinities of the substrate-loaded S-components for the ECF module.

Chapter 5

In vitro studies on niacin transport via ECF-NiaX

ABSTRACT

The mechanism of niacin transport by the ECF transporter ECF-NiaX was studied *in vitro*. The ECF module together with niacin (NiaX) specific S-components from *Lactococcus lactis* were expressed in *Escherichia coli*, purified, reconstituted in liposomes and uptake of the radiolabeled substrate was assayed. We show that the association of the radiolabeled niacin with the proteoliposomes depends on the presence of luminal Mg^{2+}-ATP and exhibits biphasic behavior (a rapid phase is followed by slower one). Addition of external Mg^{2+}-ATP to the liposomes after saturation of association of radiolabeled substrate leads to rapid but incomplete release of niacin, while Mg^{2+}-ADP and Mg^{2+}-AMP-PNP cause no release. Comparable results were obtained when proteoliposomes were preincubated with different nucleotides on the outside. Efflux of radiolabeled niacin encapsulated in the proteoliposomes without luminal nucleotides was stimulated by Mg^{2+}-ATP and also Mg^{2+}-AMP-PNP, but the kinetics of the release differ. These observations suggest that the purified ECF-NiaX complex is capable of niacin transport. The results can be explained only if one assumes both orientations of the reconstituted complexes in the liposomes (right side out and insight out). Based on the experimental data we propose a speculative model for vitamin transport by ECF transporters. However, the model does not explain all the observations, and therefore we make suggestions for additional experiments.

INTRODUCTION

Energy Coupling Factor (ECF) transporters are a subgroup of Mg^{2+}-ATP-binding cassette (ABC) transporters involved in the uptake of vitamins and micronutrients in prokaryotes. They show a similar subunit organization as classical ABC transporters with two identical or homologues cytosolic ATPase subunits (A- and A'-subunit), and two transmembrane subunits. In contrast to classical ABC transporters the transmembrane part of the ECF transporters consists of two unrelated proteins: a high-affinity substrate binding protein (S-component) and second transmembrane protein involved in conformational coupling of the ATPases with the S-component (T-component) (Rodionov et al., 2009). Recently two crystal structures of complete ECF transporters from *Lactobacilus brevis* revealed a 1S:1T:1A:1A' stoichiometry (Wang et al., 2013; Xu et al., 2013). The complexes were captured in the inward-facing, substrate- and nucleotide-free conformation, with S-component in a very unusual orientation. The α helical segments are lying almost parallel to the membrane plane, instead of spanning the membrane. Preliminary biochemical experiment showed that this conformation is more stable than the conformations induced by the presence of substrate and ATP (Xu et al., 2013). Recent *in vivo* studies using complete ECF transporters overexpressed in *E. coli* showed that ECF transporters support translocation of their specific substrates across the membrane (Erkens et al., 2011; Karpowich and Wang, 2013; Rodionov et al., 2009). Characterization of the purified and liposome-reconstituted ECF-S-component complexes have shown that transport activity is ATP dependent (ter Beek et al., 2011; Xu et al., 2013).

Over last couple of years the general mechanism of transport for the ECF transporters has been speculated on (Karpowich and Wang, 2013; Wang et al., 2013; Xu et al., 2013; Zhang et al., 2010). When the first crystal structure of a solitary S-component (RibU) was published, the authors suggested that there was a translocation pathway within the S-component, which in turn would require large conformational changes within this protein (Zhang et al., 2010). The elucidation of two other structures of the S-components (ThiT and BioY), and the superposition of these structures on RibU suggested that the translocation pathway might be located on the interface between the S- and T- subunits (Berntsson et al., 2012; Erkens et al., 2012 and **Chapter 2**). Studies of the conformational changes upon substrate binding by solitary thiamin specific S-component (ThiT), using Electron Paramagnetic Resonance, did not reveal the large conformational changes needed for a translocation pathway within the S-component. It showed that only small rearrangements of the long extracytoplasmic loop L1 are needed to occlude the substrate in the binding site (Majsnerowska et al., 2013 and **Chapter 3**). This conclusion, however, rose many

questions: whether the same small rearrangements take place in the context of the whole transporter, and how the substrate can be released from the high affinity binding site to the translocation pathway.

The available structural and biochemical data on the ECF transporters provide a good basis to study the mechanism of transport. One of the crucial questions is what is the role of the ATP binding and hydrolysis in the transport cycle. Here, we present *in vitro* work on the niacin ECF transporter from *Lactococcus lactis*. The collected data provides functional information necessary to develop a working model of the translocation cycle.

MATERIALS AND METHODS

Growth conditions for overexpression of ECF-NiaX complexes.

E. coli MC1061 cells transformed with p2BAD *ecfAA'T-10xHis, niaX-Streptag* plasmid (ter Beek et al., 2011) were cultivated using 2xTY medium in 10 L bioreactor .

Preparation of the membrane vesicles and protein purification and reconstitution.

Membrane vesicles were prepared as described previously (ter Beek et al., 2011). For protein purification membrane vesicles were solubilized at total protein concentration of 5 mg/mL in the 50 mM potassium phosphate buffer pH 7.5 supplemented with 10% glycerol, 300 mM NaCl, and 1% n-dodecyl-β-d-maltoside (DDM). The solution was incubated at 4 °C with rocking. Unsolubilized material was pelleted down by centrifugation at 286286 g, 4 °C for 30 minutes and supernatant was incubated for 1 hour at 4°C with 0.5 mL Nickel-Sepharose (GE Healthcare) equilibrated in solubilization buffer without DDM. Unbound material was allowed to flow through and column was washed with 20 column volumes (CV) of 50 mM ammonium acetate buffer, pH 7.5 supplemented with 10% glycerol, 300 mM NaCl, 50 mM imidazol and 0.03% DDM. The protein was eluted in three fractions of 300 μL, 600 μL and 500 μL with 50 mM ammonium acetate buffer, pH 7.5 supplemented with 300 mM NaCl, 500 mM imidazol and 0.03% DDM. Subsequently the second fraction (600 μL, containing most of the protein) was loaded on 23 mL Superdex 200 gel filtration column (GE Healthcare) equilibrated with 50 mM ammonium acetate buffer, pH 7.5 supplemented with 150 mM NaCl and 0.03% DDM. The peak fractions from after size-exclusion chromatography were used for reconstitution into liposomes, using a previously described method (Geertsma et al., 2008). The ECF-NiaX complex was reconstituted into liposomes composed of *E. coli* polar lipids and egg phosphatidylcholine (3:1, w/w) at protein to lipid ratio (w/w) 1:250.

Transport and efflux assay.

For transport assays proteoliposomes were loaded with 50 mM ammonium acetate buffer pH 7.0 supplemented with 2 mM ATP and 2 mM $MgSO_4$ or 2 mM ADP and 2 mM $MgSO_4$ by three steps of freezing in the liquid nitrogen and thawing. Subsequently, liposomes were extruded eleven times through a 400 nm pore size polycarbonate filter (Avestin), diluted about 10 times in 50 mM ammonium acetate buffer pH 7.0 and centrifuged at 286286 g, 4 °C for 45 minutes. The proteoliposomes were resuspended in 50 mM ammonium acetate buffer pH 7.0 to an estimated final protein concentration of 0,5 μg/μL. 200 μL aliquots of 50 mM ammonium acetate buffer pH 7.0 containing 100 nM [^{3}H]niacin were made, one for each time point, and the assay was started by addition of 2 μL of proteoliposomes. The experiment was done at 25 °C. At the indicated time points, 2 mL of ice-cold 50 mM ammonium acetate buffer pH 7.0 (stop buffer) was added and the solution was filtered over nitrocellulose filter. When indicated 2 μM niacin, 2 mM ATP and 2 mM $MgSO_4$, 2 mM ADP and 2 mM $MgSO_4$ or 2 mM AMP-PNP and 2 mM $MgSO_4$ was added to the uptake solution after 5 minutes of transport Alternatively, when indicated proteoliposomes were pre-incubated for 5 minutes with 2 mM ATP and 2 mM $MgSO_4$, 2 mM ADP and 2 mM $MgSO_4$ or 2 mM AMP-PNP and 2 mM $MgSO_4$ before reaction was started with addition of radiolabeled substrate (100 nM [^{3}H]niacin). The filters with trapped radioactivity were washed once with 2 mL of stop buffer, dried for 1 hour at 80°C and diluted in 5 mL of Counter Plus scintillation liquid (Perkin Elmer). Radioactivity was determined in the Perkin Elmer 1600CA counter.

For the efflux experiment the proteoliposomes were loaded with 5 μM [^{3}H]niacin as described above and resuspended in 50 mM ammonium acetate buffer pH 7.0 to the final protein concentration of 0,5 μg/μL. The assay was started by addition of 2 μL of proteoliposomes to 200 μL of 50 mM ammonium acetate buffer pH 7.0 supplemented with 10 mM ATP and 10 mM $MgSO_4$, 10 mM ADP and 10 mM $MgSO_4$ or 10 mM AMP-PNP and 10 mM $MgSO_4$. As a control the buffer without nucleotides was used.

RESULTS

The purified ECF-NiaX complex from *L. lactis* was reconstituted into liposomes to study niacin transport in the absence of any other proteins. The proteoliposome lumen was loaded either with Mg^{2+}-ATP to energize transport or with Mg^{2+}-ADP as control. The comparison of the [^{3}H]niacin uptake activity in the liposomes loaded with Mg^{2+}-ATP or Mg^{2+}-ADP showed that reconstituted ECF-NiaX supported ATP dependent association of the radiolabeled substrate with the proteoliposomes

(figure 1). The association showed a biphasic behavior. The first phase was very rapid (saturated within 10 seconds) whereas the second phase was much slower and and took place over the course of several minutes. It is possible that the fast phase represents binding of niacin to the ECF-NiaX complex (which is fast) and the second phase represents transport across the membrane. However, is difficult to conclusively distinguish in these experiments between ATP-dependent transport of the substrate into the liposome lumen and binding. One way to discriminate between these two possibilities is to calculate whether niacin was accumulated into the lumen, which would point at active transport of the substrate across the membrane. Approximately 2 pmol of niacin associated with the liposomes, which had a luminal volume of 0.225 μL (250 mg lipids, 400 nm diameter) (Geertsma et al., 2008). Thus the concentration of niacin would be approximately 9 μM, if all niacin was luminal. This concentration is 90 fold higher compared to the external concentration, and suggests accumulation of substrate in the lumen. A complication in this calculation is that there is ~ 8 pmol of ECF-NiaX complexes reconstituted in the same amount of liposomes, assuming that all of the purified protein was properly reconstituted into the liposomes, and no losses of the (active) protein had taken place. Therefore, the apparent accumulation of niacin to a level of 9 μM could alternatively be explained by binding to the ECF-NiaX proteins instead of transport across the membrane.

Chasing of radiolabeled niacin from the liposomes by unlabeled niacin or nucleotides.

To further study whether niacin was indeed transported, we added an excess of unlabeled niacin to the liposomes after ATP-dependent association of radiolabeled niacin with the liposomes had saturated (5 minutes). Complete and very fast release (within 15 seconds) of the associated radioactivity was observed upon addition of the unlabeled niacin. Such a fast chase of the label is usually indicative of an exchange of a radioactive molecule at the binding site with an unlabeled substrate (which is fast) rather than exchange of accumulated substrate via a transport step (which is generally slower). On the other hand, the slow association of niacin with the liposomes (after an initial fast phase, figure 1) is indicative of transport rather than binding. Thus it remains unclear whether the ECF-NiaX transports niacin across the membrane or is only capable of ATP dependent binding.

Another way to discriminate between transport and binding is supply the proteoliposomes with external Mg^{2+}-ATP to chase out the radio-labelled niacin. Reconstitution of purified membrane proteins in liposomes often leads to the insertion in two ways: right-side-out and wrong-side-out. The ratio between those

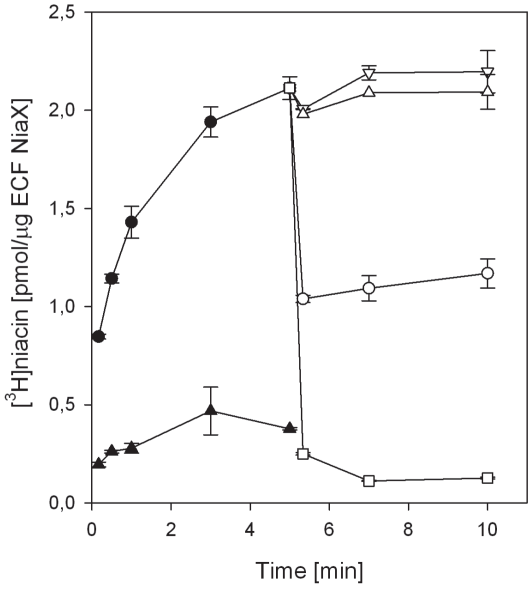

Figure 1: Transport of [^{3}H]niacin into proteoliposomes with reconstituted ECF-NiaX. The proteoliposomes were loaded with 50 mM ammonium acetate buffer (pH 7.0) supplemented with 2 mM ATP and 2 mM $MgSO_4$ (black circles) or 2 mM ADP and 2 mM $MgSO_4$ (black triangles). To the proteoliposomes loaded with 2 mM ATP and 2 mM $MgSO_4$ after 5 minutes time point 2 µM niacin (white squares), 2 mM ATP and 2 mM $MgSO_4$, (white circles) 2 mM ADP and 2 mM $MgSO_4$ (white triangles) or 2 mM AMP-PNP and 2 mM $MgSO_4$ (white inverted triangles) were added. Error bars represent range of two measurements.

two orientations differs from protein to protein (Geertsma et al., 2008). ATP is membrane impermeable, so in our experiments it can affect transport only if the nucleotide is located on the same side of the membrane as the ATP binding domains of the ECF transporters. Because association of the labeled niacin with the liposomes (figure 1) is stimulated by luminal ATP at least part of the proteins have a right-side-out orientation. The addition of the nucleotides on the outside would affect only the ATPases of the wrong-side-out oriented ECF-complexes. We added several different nucleotides to the liposomes after the association of radiolabeled niacin (by luminal ATP) had saturated (after 5 minutes, figure 1). The addition of Mg^{2+}-ATP caused very rapid release of approximately half of the associated radiolabeled niacin whereas the addition of Mg^{2+}-ADP or Mg^{2+}-AMP-PNP (a nonhydrolyzable analogue of ATP) did not cause release. This observation strongly suggest that the ECF-NiaX complex mediated ATP dependent transport activity: The radiolabeled niacin that was transported into the liposomes by the right-side-out reconstituted complexes was subsequently pumped out by the wrong-side-out oriented transporters upon addition of the Mg^{2+}-ATP on the exterior. The very fast kinetics of this process is unexpected for a transport step, but is reminiscent to the initial fast phase of niacin association with the liposomes with luminal Mg^{2+}-ATP present. The lack of the second slower phase is however surprising, but it is possible that a steady state is reached in the liposome set-up, with continuous uptake via the right-side-out complexes, and release via the wrong-side-out complexes.

ATP-stimulated efflux of niacin

To further support the notion that the reconstituted ECF-NiaX complex is able to transport niacin across the membrane, proteoliposomes were loaded with radiolabeled substrate (in the absence of luminal ATP), and an efflux assay was performed (figure 2). Upon dilution of the liposomes in the buffer without nucleotides, or buffer supplemented with Mg^{2+}-ADP, some efflux of the radiolabeled niacin took place. This could be caused by non-specific leakiness of the liposomes or uncoupled protein-mediated efflux, or both. The presence of external Mg^{2+}-ATP significantly increased the rate of efflux, showing that ECF-NiaX facilitates ATP dependent transport of niacin. Surprisingly, presence of Mg^{2+}-AMP-PNP also supported release of the incapsulated [^{3}H]niacin but the kinetics of the efflux were different - faster than in case of ADP but slower than caused by ATP. This experiment shows the that ADP and AMP-PNP influence the ECF transporter in different ways, which could not be detected in the uptake assay (figure 1).

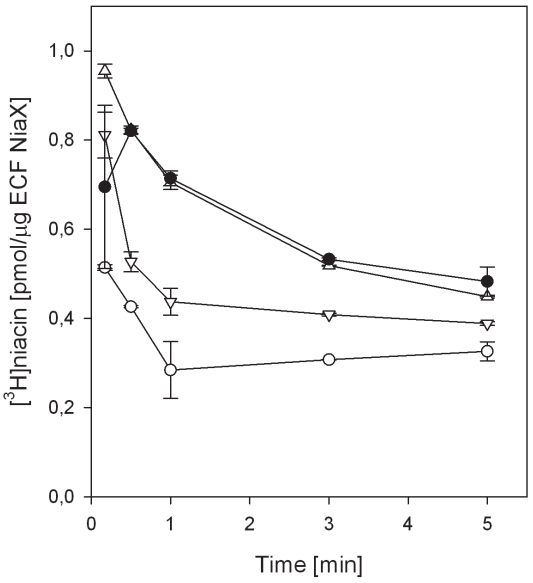

Figure 2: Efflux of [^{3}H]niacin from proteoliposomes with reconstituted ECF-NiaX. The proteoliposomes were loaded with 50 mM ammonium acetate buffer pH 7.0 supplemented with 5 µM [^{3}H]niacin. Samples were taken at indicated time points after diluting proteoliposomes in 50 mM ammonium acetate buffer pH 7.0 (black circles) supplemented with 10 mM ATP and 10 mM $MgSO_4$ (white circles), 10 mM ADP and 10 mM $MgSO_4$ (white triangles) or 10 mM AMP-PNP and 10 mM $MgSO_4$ (white inverted triangles) to determine the amount of radiolabeled niacin in the lumen. Error bars represent range of two measurements.

Liposomes preincubated with nucleotides show differences between ATP, ADP and AMP-PNP

In order to further investigate this difference, proteoliposomes loaded with Mg^{2+}-ATP were pre-incubated in the buffer with different nucleotides before radiolabeled substrate was added. The results were compared to the transport experiments using liposomes where Mg^{2+}-ATP was added to the reaction 5 minute after the addition of the [^{3}H]niacin (figure 3). The ATP pre-incubated liposomes rapidly reached the same final level of niacin accumulation as the liposomes to which ATP was added after 5 minutes. A clear difference could be observed between proteoliposomes pre-incubated with Mg^{2+}-ADP and Mg^{2+}-AMP-PNP. Liposomes preincubated with Mg^{2+}-ADP showed a higher transport rate than the Mg^{2+}-ATP-preincubated liposomes but a lower rate than control liposomes that had not been pre-incubated with nucleotides. Surprisingly, liposomes pre-incubated with AMP-PNP showed a higher transport rate and accumulation level than the control liposomes, which may suggest that AMP-PNP in these conditions prevented leakage of the radiolabeled substrate. This result contrasts with the efflux experiment, where external AMP-PNP induced substrate release in liposomes loaded with [^{3}H]niacin. More experiments are needed to reconcile these differences. For example, in order to study why there is a high basal efflux rate (in the absence of any nucleotides, figure 2) control experiments with protein-free liposomes or proteoliposomes containing ECF transporter of the different substrate specificity (e.g. ECF-RibU) should be performed.

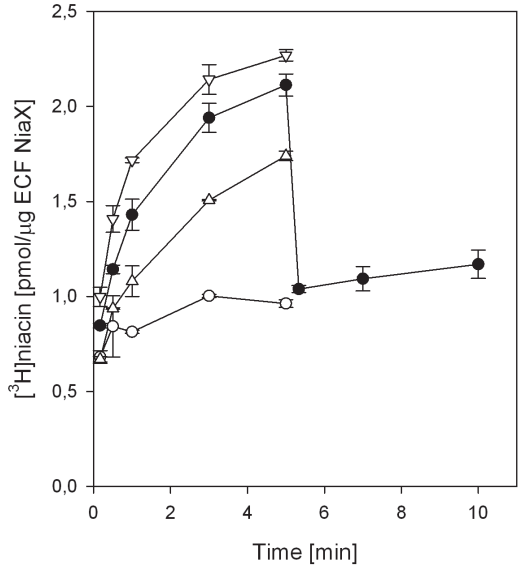

Figure 3: Transport of [^{3}H]niacin into proteoliposomes with reconstituted ECF-NiaX preincubated with nucleotides. The proteoliposomes were loaded with 50 mM ammonium acetate buffer (pH 7) supplemented with 2 mM ATP and 2 mM $MgSO_4$. Before radiolabeled substrate was added proteoliposomes were preincubated with 2 mM ATP and 2 mM $MgSO_4$ (white circles) 2 mM ADP and 2 mM $MgSO_4$ (white triangles) or 2 mM AMP-PNP and 2 mM $MgSO_4$ (white inverted triangles). As a control proteoliposomes were preincubated with buffer and after 5 minutes time point 2 mM ATP and 2 mM $MgSO_4$ were added (black circles). Error bars represent range of two measurements.

DISCUSSION

The recently published crystal structures of two whole ECF complexes revealed an unexpected property of the S-component: It can reorient in the membrane to expose the binding site to the interior of the cell and release the substrate. This "toppling over" appears to be connected with a reduction of the affinity for the substrate (Wang et al., 2013; Xu et al., 2013). Based on previous experiments (ter Beek et al., 2011; Rodionov et al., 2009), experiments presented in **Chapter 3** and new experiments presented here, we propose that the ability to topple over in the membrane is reserved for the substrate-bound S-components, which is the state that can associate more tightly with the ECF-module. We assume that ATP binding and hydrolysis are coupled to distinct changes in the conformation of the S-component. These changes could be toppling over (either in the substrate-loaded from, during uptake, or in the empty state, when the apo-carrier has to reorient its binding site to pick up a new substrate) or full dissociation of the S-component from the ECF module. Below we will discuss the possible model for transport based on the available data. Because the model cannot explain all experimental data, we will also suggest further experiments.

Model

The structural framework of the model is based on the crystal structures of nucleotide- and substrate-free ECF complexes (figure 4) (Wang et al., 2013; Xu et al., 2013), and structures of the individual S-components (Zhang et al., 2010; Erkens et al., 2011; Berntsson et al., 2012 and **Chapter 2**). In this model the substrate-bound S-component upon association with the ECF-module, reorients to the inward facing conformation, and subsequently releases the substrate. In both structures of the complete ECF complexes the two ATP-binding domains are in the open state, where A-components (EcfA and EcfA') are spatially separated from each other. ATP binding is likely to lead to the closure of the gap between the ATPases, just like in the classical ABC transporters. As a consequence the coupling helixes of EcfT are pinched together, causing dissociation of the empty S-component. Subsequent ATP hydrolysis resets the ECF-module to the conformation that is ready to accept another substrate-bound S-component. In the crystal structures the transporters are stuck in the ATP-free state.

Given that AMP-PNP can bind to the ATP binding sites of the EcfA/A', this model very well explains its effect in the uptake experiments (figures 1 and 3): Upon loading of the liposomes with Mg^{2+}-ATP all the transporters (both right-side-out and wrong-side-out) are in the state where the S-component is released form ECF module and has adopted un "upright" orientation with binding site ready to

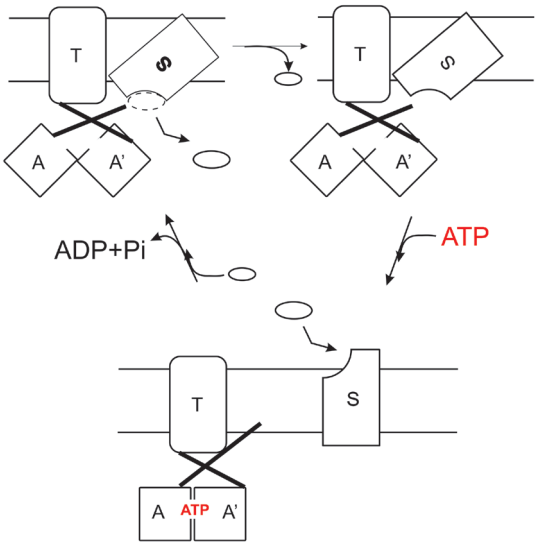

Figure 4: Model for substrate transport mechanism via ECF transporter. The substrate-bound S-component upon association with the ECF-module topples over and releases the substrate. ATP binding closes the gap between two ATPases which in consequence brings the coupling helixes of EcfT together, causing dissociation of the empty S-component. Empty S-components can bind another substrate molecule. ATP hydrolysis resets ECF-module to the conformation that is ready to accept another substrate-bound S-component.

accept the substrate. Addition of the radiolabeled substrate allows its translocation to the luminal side of the membrane, where it can subsequently be bound by the wrong-side-out oriented S-components. Upon association of these substrate-bound S-components with the wrong-side-out oriented ECF-module the substrate can be translocated back to the outside of the liposomes. Since there is no ATP on the external side of the membrane, the wrong-side-out inserted ECF transporters are not able to complete the transport cycle and stay trapped. Addition of the AMP-PNP allows for the dissociation of the empty S-component, which can bind another substrate accumulated in the lumen of the liposome. Since AMP-PNP cannot be hydrolyzed, the wrong-side-out oriented ECF module cannot reset to conformation that is ready to accept the substrate bound S-component, thus preventing substrate form being pumped out. Similarly in the experiment where ATP loaded liposomes where first preincubated with AMP-PNP, reverse translocation of the transported substrate (by the wrong-side-out transporters) appeared to be blocked.

In contrast, the substrate-bound, wrong-side-out, S-component can associate with the ECF-module and go through the whole cycle upon ATP binding and hydrolysis on the outside. That is the reason why addition of ATP causes partial release of the substrate (approximately 50% was released). However, the fast kinetics of ATP induced release cannot be explained easily. In the experiment where liposomes were preincubated with ATP, approximately half of the radiolabeled niacin, compared to the control non-preincubated liposomes, associates with liposomes. The observations that approximately 50% of the associated niacin is released upon addition of external

ATP (figure 1) may imply that half of the [^{3}H]niacin associated with the liposomes is not accessible to the wrong-side-out inserted transporters, possibly because the substrate is bound on the external side of the membrane by the right-side-out reconstituted complexes. Alternatively, the level of association can be interpret as a steady state reached by the system. This state can be considered as resultant of the rates of import and export and the ratio of the right-side-out and wrong-side-out oriented exporters.

It is very difficult to explain the effect of the addition of AMP-PNP in the efflux assay, where it triggers substrate release from the liposomes, which is unexpected because AMP-PNP cannot be hydrolyzed, and thus the complete transport cycle should not occur. In addition it is difficult to explain the effect of the addition of a 1000-fold excess of unlabeled niacin. This addition causes very rapid and complete release of all associated [^{3}H]niacin.

Membrane orientation

To better interpret the data it is necessary to determine the ratio between the two orientations of the ECF NiaX in the membrane. This can be done using fluorescent labeling of single cysteine mutants as it described for GltT and GltPh (Ryan et al., 2009; Slotboom et al., 2001). To perform this assay two single cysteine mutation should be introduced in the transporter: one on the extracellular side and the other on the intracellular location. Upon protein reconstitution the accessible cysteines can be protected using two different cysteine-reactive compounds: a membrane-impermeable and a membrane permeable one. This should be followed by solubilization of the liposomes and labeling of the unreacted cysteines with fluorescent dye. The extend of the fluorescent labeling can be visualize upon protein separation on the SDS-page gel. Comparison of the two samples with additional one, where cysteines stayed unprotected, will allow to estimate ratio between two orientations of the transporter in the membrane.

Does the binding affinity depend on the conformation?

Consistent with the postulated model, the initial fast phase of association of niacin with ATP-loaded liposomes as well the lower level of radioactivity associated with the liposomes loaded with ADP can be interpret as binding of substrate to the reconstituted transporters (figure 1). The difference in the relative amount of the bound [^{3}H]niacin can be explained by the fact that ECF-NiaX in each of the conditions adopts different conformation which differs in the binding affinity for the substrate. Loading of the proteoliposomes with ATP allows release of NiaX from the complex

(figure 4), whereas ADP treatment keeps complexes stuck in the inward-facing conformation. Substrate-free S-components that are released from the complex are characterized by a very high substrate binding affinity (Erkens and Slotboom, 2010; Berntsson et al., 2012 and **Chapter 2**), which is reflected in the rapid initial binding of the radiolabeled niacin. S-components associated with the ECF module in the ADP loaded liposomes most likely show much lower affinity for the substrate, as a result of the deformation of the binding site (Xu et al., 2013). Here, we propose an experiment, which may answer the question whether the ECF-NiaX complex indeed releases NiaX upon ATP binding. In the first step liposomes with reconstituted ECF-NiaX will be treated with Mg^{2+}-ATP which would allow for dissociation of the empty S-component from the complex. ATP will then be removed by centrifugation and washing steps and liposomes will be reloaded with Mg^{2+}-ADP. Subsequently, the results of the [^{3}H]niacin uptake assay will be compared with the experiments in figure 1.

What is the role of ATP binding and hydrolysis in the transport cycle?

The effects of AMP-PNP, the slowly-hydrolyzable analogue of ATP, shows inconsistencies between the uptake and efflux experiments (as discussed above). Therefore we propose an experiment that may reveal the effect of AMP-PNP on the transport cycle, thus helping in the understanding of the role ATP binding and hydrolysis in this process: An [^{3}H]niacin uptake experiment using AMP-PNP loaded liposomes. This experiment will answer the question if AMP-PNP binding to the ATPases can cause dissociation of the S-component from the ECF-complex. The reorientation of the S-component to the right-side up position in the membrane allows for high-affinity binding of radiolabeled substrate. According to the postulated model the AMP-PNP-bound ECF module cannot complete the cycle and stays trapped in the conformation which does not allow for accepting a substrate-bound S-component. This experiment should reveal the amount of high-affinity binding sites in the liposomes.

Summarizing, the model proposed here cannot fully explain all the observations made in the *in vitro* niacin uptake and efflux experiments. However, it composes a good base for further investigations into the mechanism of the vitamin transport by ECF transporters.

Chapter 6

Summary and future research

Samenvatting en voorstellen voor toekomstig onderzoek

Streszczenie w języku polskim dla osób niezajmujących się badaniami naukowymi

References

List of publications

Acknowledgements

The focus of the thesis is on the relationship between structure and mechanism in the ABC-type ECF transporters for vitamin uptake from *Lactococcus lactis*. Energy Coupling Factor (ECF) transporters are a subgroup of ATP-binding cassette (ABC) transporters involved in the uptake of vitamins and micronutrients in prokaryotes. They employ integral membrane proteins (S-components) for high affinity substrate binding. S-components form active translocation complexes with the ECF module, which energizes transport of the substrate from ATP hydrolysis. In many cases the ECF module can interact with several different S-components which are unrelated in sequence and bind diverse substrates. This feature enables the transport of chemically different substrates via a common route.

In the first two experimental chapters (chapters 2 and 3) two S-components from *L. lactis* specific for biotin (BioY) and thiamin (ThiT) were characterized.

In **chapter 2** we presented a high-resolution crystal structure (at 2.1 Å) of BioY which shows a very similar overall fold to the two previously solved structures of RibU (riboflavin specific S-component) from *Staphylococcus aureus* and ThiT from *L. lactis*. Comparison of those three structures revealed structural conservation in N-terminal part of proteins (transmembrane helices 1-3) that are involved in the interaction with the ECF module, and a high divergence in the C-terminal part (transmembrane helices 4-6) that binds the substrate. This observation very well explains how the S-components can interact with the same ECF module, while at the same time specifically bind chemically very different substrates with very high affinity. We performed biochemical analysis of two homologous, solitary BioY proteins (in the absence of the ECF module) from *L. lactis* and *Rhodobacter capsulatus*. Previous *in vivo* studies indicated that the latter can transport biotin in the absence of the ECF module. We found that both BioY proteins are monomeric in detergent solution, bind D-biotin with a high affinity, but do not transport the substrate across the membrane, when reconstituted in liposomes.

In **chapter 3** we used EPR spectroscopy, stopped-flow fluorescence spectroscopy and molecular dynamics simulations to determine the structural rearrangements that take place in ThiT upon binding of thiamin. Thiamin-induced conformational changes are confined to the long and partially membrane-embedded loop between transmembrane helices 1 and 2 that acts as a lid that opens to allow the substrate to enter binding site and closes to occlude it. The results indicated that solitary ThiT functions as a *bona fide* high-affinity substrate binding protein. Contrary to what was proposed for RibU, ThiT lacks a translocation pathway within the protein.

In chapter 4 and 5 the complete ECF transporters were investigated. In these two chapters *in vivo* and *in vitro* studies on ECF complexes from *L. lactis* are described.

In **chapter 4** the mechanism of niacin and thiamin transport by ECF transporters from *L. lactis* was studied *in vivo*. As previously established for thiamin, we show that uptake of the niacin is dependent on the presence of the S-component and active ECF module. Moreover transport of both vitamins is strongly inhibited or completely abolished in the presence of an ECF module in which one or two ATPases are inactivated by mutagenesis. Similarly, mutations in the AxxxA motif of both S-components lead to a drastic loss of transporting function when either of alanines was substituted with tryptophan. The reason for it is the deformation of interaction surface between S-components and T-component of ECF module. These results show that vitamin uptake via ECF transporters is ATP driven and depends on the presence of substrate specific S-component and fully active ECF module. Finally, we show that in Group II ECF transporters different S-components can compete for a shared ECF module. This competition is stimulated by the presence of the specific substrate.

In **chapter 5** the mechanism of niacin transport by ECF-NiaX was studied *in vitro* after reconstitution in liposomes. We show that the association of the niacin with the proteoliposomes is ATP dependent and exhibits biphasic behavior (rapid phase is followed by slower one). The uptake and efflux experiments presented in this chapter strongly indicate that the purified ECF-NiaX complex indeed is capable of transport when reconstituted in liposomes, and suggest a dual orientation of the reconstituted complexes in the liposomes. Based on the experimental data and available crystal structures of the whole ECF complexes as well as individual S-components we propose a model for vitamin transport by ECF transporters. In this model association of the substrate-bound S-component with ECF module allows substrate translocation. ATP binding and hydrolysis leads to release of the empty S-component and reset of ECF module to the conformation that is ready to accept another substrate-bound S-component, respectively.

The work presented here exemplifies how a combination of structural and biochemical data may bring an important contribution into understanding of biological systems. Although the results obtained in this study do not allow to fully characterize the mechanism of vitamin transport via ECF transporters, they constitute a fundament for a further research. There is a need for continuation of the biochemical and structural studies on this group of transporters. Results of the experiments proposed in chapter 5 may bring important insight into understanding of the substrate translocation cycle. Logical continuation of the work described in chapter 4 would be *in vitro* studies on the interactions between different components in the complete ECF transporters or between ECF module and S-components

specific for a different substrates. As it has been shown recently for glutamate transporter (Glt_{Ph}) the smFRET (Single molecule Fluorescence Resonance Energy Transfer) techniques are a very useful methods to study the functional mechanism of the membrane proteins in the native environment (liposomes) (Erkens et al., 2013). Moreover in chapter 3 we showed that EPR (Electron Paramagnetic Resonance) is a powerful tool to investigate membrane proteins. Both approaches can be used to study (complete) ECF transporters. In addition crystallographic attempts may lead to visualization of other conformational states which ECF transporters adopt in the transport cycle and may help to design mutants for EPR and single molecule studies.

Knowledge of the structure and mechanism of the ECF transporters could be used in the development of new antimicrobial agents. The ECF transporters are potential targets for antibiotics since they are found exclusively in procaryotes, many of each being human pathogens.

Dit proefschrift gaat over de relatie tussen de structuur en het mechanisme van ABC-type ECF transporters voor vitamines, uit de bacterie *Lactococcus lactis*. Energy-Coupling Factor (ECF) transporters vormen een subgroep van de ATP-binding cassette (ABC) transporters en zijn betrokken bij de opname van vitamines door prokaryoten. Ze maken hiervoor gebruik van membraaneiwitten (S - componenten) die hun substraten met een hoge affiniteit binden. S-componenten kunnen een complex vormen met de ECF-module zodat de substraten actief getransporteerd kunnen worden. De energie hiervoor wordt geleverd door hydrolyse van ATP. In veel gevallen kan de ECF module een complex vormen met verschillende S -componenten, die verschillende vitamines binden en ook een verschillende aminozuursequentie hebben. Op deze manier kunnen chemisch zeer diverse substraten via een vergelijkbare route in de cel worden opgenomen.

De eerste twee experimentele hoofdstukken (hoofdstuk 2 en 3) beschrijven de karakterisatie van twee verschillende S-componenten uit *L. lactis*; de S-componenten voor biotine (BioY) en thiamine (ThiT). In hoofdstuk 2 presenteerden we een hoge-resolutie kristalstructuur (resolutie 2,1 Å) van BioY die globaal gezien sterk overeenkomt met de eerder opgeloste structuren van RibU (de S-component voor riboflavine) uit *Staphylococcus aureus* en ThiT uit *L. lactis*. Een gedetailleerde vergelijking van deze structuren onthulde een geconserveerd structuurelement in the N-terminale deel van deze eiwitten (transmembraan helices 1-3) dat betrokken blijkt te zijn bij de interactie met de ECF module. Daarnaast blijkt er een structureel meer variabel deel te zijn (transmembraan helices 4-6) dat verantwoordelijk is voor het binden van substraat. Dankzij deze observatie werd het snel duidelijk hoe het mogelijk is dat verschillende S-componenten een interactie aan kunnen gaan met dezelfde ECF-module, maar toch chemisch zeer verschillende substraten met zeer hoge affiniteit kunnen binden. Vervolgens werden twee homologe BioY eiwitten (uit *L. lactis* en *Rhodobacter capsulatus*) in de afwezigheid van een ECF-module nader bestudeerd. Uit eerdere *in vivo* experimenten was gebleken dat BioY uit *R. capsulatus* in staat is biotine te transporteren zonder een ECF-module. Uit onze experimenten is gebleken dat beide BioY eiwitten wanneer ze in detergens gesolubiliseerd zijn monomeren vormen en D-biotine binden. Eenmaal gereconstitueerd in liposomen zijn ze echter niet in staat biotine te transporteren.

In hoofdstuk 3 hebben we gebruik gemaakt van EPR spectroscopie, *stopped-flow* fluorescentie spectroscopie en *molecular dynamics* simulaties om de structurele veranderingen die plaatsvinden in ThiT na de binding van thiamine te bepalen. De thiamine-geïnduceerde conformatieveranderingen zijn beperkt tot de lange en

gedeeltelijk in de membraan ingebedde lus tussen transmembraan helices 1 en 2 die fungeert als een deksel om de substraat-bindings site af te sluiten. De resultaten maakten duidelijk dat ThiT zonder de ECF-module functioneert als een *bona fide* hoog-affiniteit substraat-bindings eiwit. Anders dan geopperd voor RibU, mist ThiT een translocatie kanaal binnen in het eiwit.

In de hoofdstukken 4 en 5 worden de volledige ECF transporters uit *L. lactis* onderzocht met zowel *in vivo* als *in vitro* experimenten. In hoofdstuk 4 wordt het mechanisme van niacine en thiamine transport door ECF transporters uit *L. lactis in vivo* bestudeerd. Zoals ook eerder voor thiamine aangetoond, laten we zien dat transport van niacine alleen mogelijk is wanneer zowel de S-component als de ECF-module aanwezig zijn. Bovendien blijkt het transport van de vitamines sterk geremd te worden wanneer in de ECF-module mutaties worden geïntroduceerd die één of twee van de ATPases inactief maken. Ook wanneer in het geconserveerde AxxxA motief één van de alanines wordt vervangen door een tryptofaan zien we een zeer sterk gereduceerde transport activiteit. De reden hiervoor is dat het deel van de S-component dat verantwoordelijk is voor de interactie met de ECF-module vervormd is. Deze resultaten tonen aan dat transport van vitamines door ECF transporters gedreven wordt door ATP hydrolyse en afhankelijk is van de aanwezigheid van de specifieke S-component en een functionele ECF module. Tot slot laten we zien dat in type II ECF transporters verschillende S-componenten met elkaar kunnen wedijveren voor de gedeelde ECF module. Dit proces wordt gestimuleerd door de aanwezigheid van de specifieke substraten.

In hoofdstuk 5 wordt het transport mechanisme voor het ECF-NiaX complex *in vitro* bestudeerd met transporters die in liposomen gereconstitueerd zijn. We laten zien dat de associatie van niacine met de proteoliposomen ATP- afhankelijk is en bifasische gedrag vertoont (een snelle fase wordt gevolgd door een langzamere fase). De opname -en efflux experimenten in dit hoofdstuk leveren een sterke aanwijzing dat het gezuiverde ECF-NiaX complexen inderdaad in staat zijn tot actief transport wanneer ze gereconstitueerd zijn in proteoliposomen en suggereren een dubbele oriëntatie van de gereconstitueerde complexen in de liposomen. Op basis van deze resultaten en de beschikbare kristalstructuren van de volledige ECF-complexen en individuele S-componenten hebben wij een model opgesteld voor het mechanisme van vitamine transport door ECF-transporters. In dit model maakt de associatie van de substraat -gebonden S-componenten met ECF module substraat translocatie mogelijk. ATP binding en hydrolyse leiden tot het resetten van de lege

S-component en van de ECF module naar een toestand die het mogelijk maakt een nieuw substraat-gebonden S-component te accepteren.

Het hier gepresenteerde werk is een voorbeeld van hoe een combinatie van structurele- en biochemische gegevens kunnen bijdragen aan het begrip van biologische systemen. Hoewel deze resultaten niet het volledige mechanisme van vitamine transport via ECF transporters hebben blootgelegd, vormen zij een belangrijk fundament voor verder onderzoek. Er is daarom behoefte aan verdere voortzetting van de biochemische- en structurele studies van deze groep transporters. De in hoofdstuk 5 voorgestelde experimenten kunnen belangrijk inzichten geven de details van de transport cyclus. Een voor de hand liggende vervolgstap van de in hoofdstuk 4 beschreven experimenten zou een *in vitro* studie van de interactie tussen de verschillende componenten van de ECF-transporter of de onderlinge effecten van de interactie tussen S-componenten voor verschillende substraten en de ECF-module kunnen zijn. Zoals onlangs is aangetoond voor de glutamaattransporter Glt_{Ph} zijn smFRET (Single-molecule Fluorescence Resonance Energy Transfer) technieken zeer bruikbare methodes om het mechanisme van membraaneiwitten in hun natuurlijke omgeving (liposomen) te onderzoeken (Erkens et al., 2013). Bovendien is in hoofdstuk 3 aangetoond dat EPR (Electron-Paramagnetische Resonantie) een krachtige methode is om membraaneiwitten te bestuderen. Beide benaderingen kunnen toegepast worden op (volledige) ECF transporters. Daarnaast kunnen door middel van kristallografisch onderzoek tot zover onbekende conformaties van ECF-transporters tijden de transport-cyclus ontdekt worden. Deze informatie kan hepen om nieuwe mutanten te ontwerpen voor EPR en single-molecule experimenten. Kennis van de structuur en het mechanisme van de ECF transporters kunnen gebruikt worden voor de ontwikkeling van nieuwe antibiotica. De ECF transporters zijn potentiële doelwitten voor antibiotica omdat zij uitsluitend voorkomen in prokaryoten (waaronder veel voor mensen gevaarlijke ziekteverwekkers).

Książka ta zawiera wyniki badań, które wraz z kolegami prowadziłam podczas ostatnich prawie 5 lat spędzonych w Groningen (Holandia) na tamtejszym uniwersytecie w Zakładzie Enzymologii Błonowej. Zajmowaliśmy się tam badaniem systemów bakteryjnych odpowiedzialnych za wychwytywanie ze środowiska i transportowanie do wnętrza organizmu bakteryjnego witamin. Modelowym systemem w tych badaniach był system transportu u bakterii używanych często w przemyśle mleczarskim - *Lactoccocus lactis*.

Bakterie są organizmami jednokomórkowymi, co oznacza, że - w przeciwieństwie do organizmu ludzkiego, który zbudowany jest z wielu wyspecjalizowanych komórek - ich całe „ciało" składa się tylko z jednej komórki. Wnętrze każdej komórki odizolowane jest od otaczającego je środowiska błoną komórkową. Błona ta otacza całą komórkę i zbudowana jest z lipidów (tłuszczów - związków hydrofobowych, czyli „nielubiących" wody). Wnętrze komórki natomiast wypełnia cytoplazma - wodne środowisko, w którym jak w zupie pływają różne związki potrzebne komórce do życia. W związku z taką budową komórki potrzebują łączników między światem zewnętrznym a własnym wnętrzem. Rolę takich łączników pełnią białka błonowe - czyli makrocząsteczki zbudowane z aminokwasów - penetrujące błonę komórkową. Jest wiele rodzajów takich białek - receptory, enzymy i białka transportowe, które są przedmiotem tej rozprawy. Białka transportowe odpowiedzialne są za dostarczanie komórkom potrzebnych związków, w omawianym tu przypadku witamin, jak również wydalanie związków szkodliwych na zewnątrz.

Transport komórkowy, jak każdy transport, wymaga nakładów energii. Jednym ze źródeł energii często używanym przez komórki jest ATP - związek posiadający wysokoenergetyczne wiązanie, którego rozerwanie uwalnia energię potrzebną do przeprowadzenia procesów komórkowych. ATP można zatem porównać do wysokoenergetycznego paliwa komórkowego. Komórka wytwarza go w procesach dostarczających energię, np. w oddychaniu komórkowym. Białka opisane w tej dysertacji używają ATP jako źródła energii do transportu witamin.

Badane w tej pracy białka, a właściwie kompleksy białkowe, nazywają się ECF transportery (z ang. *Energy Coupling Factor transporters*). **Każdy transporter składa się z czterech białek, z których dwa są osadzone w błonie, a dwa pozostałe, zakotwiczone w nich, niemal identyczne białka, „wystają" do cytoplazmy** (zobacz ilustracja 1. - dolny panel - w rozdziale 1.). Jednym z białek błonowych jest tzw. **S-komponent** (z ang. *S-component*) - **białko wiążące substrat**, które jest odpowiedzialne za wychwytywanie witamin ze środowiska zewnętrznego. Drugie białko błonowe (T-komponent) oraz dwa białka cytoplazmatyczne tworzą tzw. **moduł energetyczny/moduł ECF** (z ang. *energizing module/ECF module*), czyli moduł

odpowiedzialny za pozyskiwanie energii chemicznej (z ATP) i przetwarzanie tej energii na energię mechaniczną umożliwiającą transport wychwyconego substratu.

Każda bakteria *Lactoccocus lactis* wytwarza osiem różnych S-komponentów - specyficznych dla siedmiu różnych witamin (wytwarza dwa białka wiążące biotynę) i posiada w swojej błonie komórkowej ograniczoną, stałą liczbę modułów energetycznych i zmienną liczbę S-komponentów. Produkcja S-komponentów jest ściśle regulowana i kontrolowana - produkcja danego białka wiążącego substrat wzrasta, gdy komórce zaczyna brakować wyłapywanej przez nie witaminy. Każdy z ośmiu S-komponentów po związaniu witaminy „szuka" w błonie modułu energetycznego, dzięki któremu będzie mógł przetransportować witaminę do środka komórki.

W pierwszych dwóch rozdziałach eksperymentalnych tej pracy (rozdziały 2. i 3.) opisane są badania nad dwoma S-komponentami (w izolacji od modułu energetycznego), specyficznie wiążącymi biotynę - witaminę B_7 (BioY) i tiaminę - witaminę B_1 (ThiT).

W rozdziale 2. zaprezentowana została struktura - o wysokiej rozdzielczości - białka BioY, dzięki czemu mogliśmy „zwizualizować" ten S-komponent. Na pierwszy rzut oka jego budowa jest bardzo podobna do dwóch innych S-komponentów - specyficznych dla tiaminy i ryboflawiny, których struktury zostały opisane wcześniej. Po dokładnym porównaniu tych trzech struktur, składających się z sześciu błonowych helis (zob. ilustracja 3A, rozdział 2.), okazało się, że tylko połowa helis się pokrywa (H1, H2, H3), podczas gdy druga jest dość różna (H4, H5, H6). Stąd wywnioskowaliśmy, że pierwsza połowa jest odpowiedzialna za oddziaływanie z modułem energetycznym, gdyż wszystkie S-komponenty muszą wejść z nim interakcję, aby przetransportować wychwycone witaminy. Druga zaś połowa zawiera miejsce wiązania substratu. Ponieważ poszczególne witaminy są chemicznie bardzo różne, ta część S-komponentów wykazuje wysokie zróżnicowanie strukturalne. Dodatkowo w rozdziale tym pokazaliśmy, że BioY ma bardzo wysokie powinowactwo do biotyny, co oznacza, że nawet przy bardzo niskim stężeniu tej witaminy w środowisku białko to potrafi ją bardzo wydajnie wyłapywać. Ponadto zademonstrowaliśmy, że białko to nie ma zdolności transportowania biotyny przez błonę bez udziału modułu energetycznego.

W rozdziale 3. zamieszczone zostały badania dotyczące tego, jaki jest mechanizm wiązania substratu przez ThiT. Innymi słowy - jakie zmiany w strukturze białka wywołuje wychwycenie tiaminy, a więc jak duża jest różnica w strukturze między białkiem „pustym" a białkiem ze związanym substratem. Aby to sprawdzić, użyliśmy spektroskopii EPR (z ang. *Electron Paramagnetic Resonance*). Pomiary wykazały, że białko to „wykonuje bardzo subtelny ruch" podczas wiązania tiaminy,

który ogranicza się tylko do jednej części białka, którą można by porównać do pokrywki zamykającej szkatułkę. W „pustym" białku jest ona otwarta, ale gdy tylko tiamina wpadnie do środka zamyka się, żeby uniemożliwić jej „ucieczkę".

W rozdziałach 4. i 5. badaliśmy kompletne transportery (moduł energetyczny + S-komponent) dla niacyny - witamina B_3 (ECF-NiaX) i tiaminy (ECF-ThiT).

Przeprowadzając badania opisane w rozdziale 4. pokazaliśmy, że transport niacyny i tiaminy, podobnie jak biotyny, nie może się odbyć przy braku moduły energetycznego. Ponadto dowiedliśmy eksperymentalnie, że jedna połowa S-komponentu, przewidziana w rozdziale 2., jest istotnie odpowiedzialna na oddziaływanie z modułem energetycznym. Udowodniliśmy to zarówno dla ThiT, jak i dla NiaX. Obecność w jednej komórce wielu S-komponentów, które do transportu witamin muszą utworzyć kompleks z ograniczoną liczbą modułów energetycznych, nasuwa pytanie, czy poszczególne S-komponenty rywalizują ze sobą o te moduły. Pokazaliśmy, że taka rywalizacja ma miejsce, ale tylko w określonych warunkach - przy znacznym nadmiarze jednego S-komponentu w stosunku do drugiego i w obecności specyficznego dla niego substratu. Obecność dużego nadmiaru NiaX i niacyny w stosunku do ThiT oraz modułu ECF powoduje spadek wydajności transportu tiaminy za pośrednictwem ECF-ThiT. Podobnie obecność dużego nadmiaru ThiT i tiaminy w stosunku do NiaX oraz modułu ECF powoduje spadek wydajności transportu niacyny przez ECF-NiaX.

W rozdziale 5. pokazaliśmy, że transport niacyny przez ECF-NiaX jest zależny od ATP oraz wyszliśmy z propozycją mechanizmu, według którego te transportery działają. Schemat zaproponowanego przez nas mechanizmu można znaleźć w rozdziale 5. (ilustracja 4.). Nasz model zakłada, że tylko S-komponent ze związanym substratem może wytworzyć stabilny kompleks z modułem ECF, a po jego utworzeniu „ślizga się" po powierzchni T-komponentu, aby ostatecznie „zanurkować" w błonie i uwolnić witaminę do cytoplazmy. Następnie wysokoenergetyczne wiązania w ATP jest rozrywane przez dwa białka cytoplazmatyczne, co wyzwala energię potrzebą do tego, aby fragment T-komponentu (na ilustracji w kształcie X), kontaktujący się z nimi, wypchnął S-komponent z powrotem do pierwotnej pozycji w błonie, jednocześnie umożliwiając jego odłączenie od modułu ECF.

W czasach, kiedy coraz więcej patogennych bakterii wykazuje oporność antybiotykową, wiedza na temat struktury i mechanizmu działania ECF transporterów może posłużyć w przyszłości do zaprojektowania bardzo specyficznych leków antybakteryjnych. ECF transportery są dobrym potencjalnym celem ataku takich leków, gdyż występują one powszechnie u bakterii będących patogenami dla ludzi i zwierząt.

REFERENCES:

Allen, M. P., and Tildesley, D. J. (1989). Computer simulation of liquids (Oxford University Press, USA).

Altenbach, C., Kusnetzow, A. K., Ernst, O. P., Hofmann, K. P., and Hubbell, W. L. (2008). High-resolution distance mapping in rhodopsin reveals the pattern of helix movement due to activation. Proc Natl Acad Sci USA *105*, 7439–7444.

Bachar, M., Brunelle, P., Tieleman, D., and Rauk, A. (2004). Molecular dynamics simulation of a polyunsaturated lipid bilayer susceptible to lipid peroxidation. J Phys Chem B *108*, 7170–7179.

Bayly, C. I., Cieplak, P., Cornell, W., and Kollman, P. A. (1993). A well-behaved electrostatic potential based method using charge restraints for deriving atomic charges: the RESP model. The Journal of Physical Chemistry *97*, 10269–10280.

Beek, ter, J., Duurkens, R. H., Erkens, G. B., and Slotboom, D. J. (2011). Quaternary structure and functional unit of energy coupling factor (ECF)-type transporters. Journal of Biological Chemistry *286*, 5471–5475.

Berger, O., Edholm, O., and Jähnig, F. (1997). Molecular dynamics simulations of a fluid bilayer of dipalmitoylphosphatidylcholine at full hydration, constant pressure, and constant temperature. Biophys J *72*, 2002–2013.

Berntsson, R. P.-A., Alia Oktaviani, N., Fusetti, F., Thunnissen, A.-M. W. H., Poolman, B., and Slotboom, D. J. (2009). Selenomethionine incorporation in proteins expressed in *Lactococcus lactis*. Protein Sci. *18*, 1121–1127.

Berntsson, R. P.-A., Beek, ter, J., Majsnerowska, M., Duurkens, R. H., Puri, P., Poolman, B., and Slotboom, D. J. (2012). Structural divergence of paralogous S components from ECF-type ABC transporters. Proc. Natl. Acad. Sci. U.S.A. *109*, 13990–13995.

Berntsson, R. P.-A., Smits, S. H. J., Schmitt, L., Slotboom, D. J., and Poolman, B. (2010). A structural classification of substrate-binding proteins. FEBS Letters *584*, 2606–2617.

Birkner, J. P., Poolman, B., and Koçer, A. (2012). Hydrophobic gating of mechanosensitive channel of large conductance evidenced by single-subunit resolution. Proc. Natl. Acad. Sci. U.S.A. *109*, 12944–12949.

Burgess, C. M., Slotboom, D. J., Geertsma, E. R., Duurkens, R. H., Poolman, B., and van Sinderen, D. (2006). The riboflavin transporter RibU in *Lactococcus lactis*:

molecular characterization of gene expression and the transport mechanism. J Bacteriol *188*, 2752–2760.

Bussi, G., Donadio, D., and Parrinello, M. (2007). Canonical sampling through velocity rescaling. J Chem Phys *126*, –.

Chae, P. S., Rasmussen, S. G. F., Rana, R. R., Gotfryd, K., Chandra, R., Goren, M. A., Kruse, A. C., Nurva, S., Loland, C. J., Pierre, Y., et al. (2010). Maltose–neopentyl glycol (MNG) amphiphiles for solubilization, stabilization and crystallization of membrane proteins. Nat. Methods *7*, 1003–1008.

Chen, J., Lu, G., Lin, J., Davidson, A. L., and Quiocho, F. A. (2003). A tweezers-like motion of the ATP-Binding Cassette dimer in an ABC transport cycle. Molecular Cell *12*, 651–661.

Claxton, D. P., Quick, M., Shi, L., De Carvalho, F. D., Weinstein, H., Javitch, J. A., and Mchaourab, H. S. (2010). Ion/substrate-dependent conformational dynamics of a bacterial homolog of neurotransmitter:sodium symporters. Nat Struct Mol Biol *17*, 822–829.

Collaborative Computational Project, N. 4. (1994). The CCP4 suite: programs for protein crystallography. Acta Cryst (1994). D50, 760-763 [doi:10.1107/S0907444994003112], 1–4.

Cordomi, A., Caltabiano, G., and Pardo, L. (2012). Membrane protein simulations using AMBER force field and Berger lipid parameters. J Chem Theory Comput *8*, 948–958.

Darden, T., York, D., and Pedersen, L. (1993). Particle mesh Ewald: An N·log(N) method for Ewald sums in large systems. J Chem Phys *98*, 10089.

Dassa, E., and Bouige, P. (2001). The \ABC\ of ABCs: a phylogenetic and functional classification of \ABC\ systems in living organisms. Res. Microbiol. *152*, 211–229.

Davidson, A. L., Dassa, E., Orelle, C., and Chen, J. (2008). Structure, function, and evolution of bacterial ATP-binding cassette systems. Microbiol. Mol. Biol. Rev. *72*, 317–64.

de Ruyter, P. G., Kuipers, O. P., and de Vos, W. M. (1996). Controlled gene expression systems for *Lactococcus lactis* with the food-grade inducer nisin. Appl. Environ. Microbiol. *62*, 3662–3667.

Duurkens, R. H., Tol, M. B., Geertsma, E. R., Permentier, H. P., and Slotboom, D. J. (2007). Flavin binding to the high affinity riboflavin transporter RibU. J Biol Chem *282*, 10380–10386.

Emsley, P., and Cowtan, K. (2004). \it Coot: model-building tools for molecular graphics. Acta Crystallographica Section D *60*, 2126–2132.

Erkens, G. B., and Slotboom, D. J. (2010). Biochemical Characterization of ThiT from *Lactococcus lactis*: A thiamin transporter with picomolar substrate binding affinity. Biochemistry *49*, 3203–3212.

Erkens, G. B., Berntsson, R. P.-A., Fulyani, F., Majsnerowska, M., Vujičić-Žagar, A., Beek, ter, J., Poolman, B., and Slotboom, D. J. (2011). The structural basis of modularity in ECF-type ABC transporters. Nat Struct Mol Biol *18*, 755–760.

Erkens, G. B., Hänelt, I., Goudsmits, J. M. H., Slotboom, D. J., and van Oijen, A. M. (2013). Unsynchronised subunit motion in single trimeric sodium-coupled aspartate transporters. Nature *502*, 119–123.

Erkens, G. B., Majsnerowska, M., Beek, ter, J., and Slotboom, D. J. (2012). Energy Coupling Factor-Type ABC Transporters for vitamin uptake in prokaryotes. Biochemistry *51*, 4390–4396.

Eudes, A., Erkens, G. B., Slotboom, D. J., Rodionov, D. A., Naponelli, V., and Hanson, A. D. (2008). Identification of genes encoding the folate- and thiamine-binding membrane proteins in Firmicutes. J Bacteriol *190*, 7591–7594.

Feenstra, K., Hess, B., and Berendsen, H. (1999). Improving efficiency of large time-scale molecular dynamics simulations of hydrogen-rich systems. J Comput Chem *20*, 786–798.

Finkenwirth, F., Kirsch, F., and Eitinger, T. (2013). Solitary BioY proteins mediate biotin transport into recombinant *Escherichia coli*. J Bacteriol *195*, 4105–4111.

Finkenwirth, F., Neubauer, O., Gunzenhäuser, J., Schoknecht, J., Scolari, S., Stöckl, M., Korte, T., Herrmann, A., and Eitinger, T. (2010). Subunit composition of an energy-coupling-factor-type biotin transporter analysed in living bacteria. Biochem J *431*, 373–380.

Geertsma, E. R., and Poolman, B. (2007). High-throughput cloning and expression in recalcitrant bacteria. Nat. Methods *4*, 705–707.

Geertsma, E. R., Nik Mahmood, N. A. B., Schuurman-Wolters, G. K., and Poolman, B. (2008). Membrane reconstitution of ABC transporters and assays of translocator function. Nat Protoc *3*, 256–266.

Geourjon, C., Orelle, C., Steinfels, E., Blanchet, C., Deléage, G., Di Pietro, A., and Jault, J.-M. (2001). A common mechanism for ATP hydrolysis in ABC transporter and helicase superfamilies. Trends Biochem Sci *26*, 539–544.

Groeneveld, M., and Slotboom, D. J. (2010). Na(+):aspartate coupling stoichiometry in the glutamate transporter homologue Glt(Ph). Biochemistry *49*, 3511–3513.

Hebbeln, P., Rodionov, D. A., Alfandega, A., and Eitinger, T. (2007). Biotin uptake in prokaryotes by solute transporters with an optional ATP-binding cassette-containing module. Proc Natl Acad Sci USA *104*, 2909–2914.

Hellmich, U. A., Lyubenova, S., Kaltenborn, E., Doshi, R., van Veen, H. W., Prisner, T. F., and Glaubitz, C. (2012). Probing the ATP hydrolysis cycle of the ABC multidrug transporter LmrA by pulsed EPR spectroscopy. J. Am. Chem. Soc. *134*, 5857–5862.

Henderson, G. B., and Potuznik, S. (1982). Cation-dependent binding of substrate to the folate transport protein of *Lactobacillus casei*. J Bacteriol *150*, 1098–1102.

Henderson, G. B., and Zevely, E. M. (1978). Binding and transport of thiamine by *Lactobacillus casei*. J Bacteriol *133*, 1190–1196.

Henderson, G. B., Kojima, J. M., and Kumar, H. P. (1985). Differential interaction of cations with the thiamine and biotin transport proteins of *Lactobacillus casei*. Biochim Biophys Acta *813*, 201–206.

Henderson, G. B., Zevely, E. M., and Huennekens, F. M. (1979a). Coupling of energy to folate transport in *Lactobacillus casei*. J Bacteriol *139*, 552–559.

Henderson, G. B., Zevely, E. M., and Huennekens, F. M. (1976). Folate transport in Lactobacillus casei: Solubilization and general properties of the binding protein. Biochemical and Biophysical Research Communications *68*, 712–717.

Henderson, G. B., Zevely, E. M., and Huennekens, F. M. (1979b). Mechanism of folate transport in *Lactobacillus casei*: evidence for a component shared with the thiamine and biotin transport systems. J Bacteriol *137*, 1308–1314.

Henderson, G. B., Zevely, E. M., and Huennekens, F. M. (1977a). Purification and properties of a membrane-associated, folate-binding protein from *Lactobacillus casei.* J Biol Chem *252*, 3760–3765.

Henderson, G. B., Zevely, E. M., Kadner, R. J., and Huennekens, F. M. (1977b). The folate and thiamine transport proteins of *Lactobacillus casei*. Journal of Supramolecular Structure *6*, 239–247.

Hess, B. (2008). P-LINCS: A parallel linear constraint solver for molecular simulation. J Chem Theory Comput *4*, 116–122.

Hess, B., Bekker, H., Berendsen, H., and Fraaije, J. (1997). LINCS: A linear constraint solver for molecular simulations. J Comput Chem *18*, 1463–1472.

Hess, B., Kutzner, C., van der Spoel, D., and Lindahl, E. (2008). GROMACS 4: Algorithms for highly efficient, load-balanced, and scalable molecular simulation. J Chem Theory Comput *4*, 435–447.

Higgins, C. F. (1992). ABC transporters: from microorganisms to man. Annu. Rev. Cell Biol. *8*, 67–113.

Hollenstein, K., Dawson, R. J., and Locher, K. P. (2007). Structure and mechanism of ABC transporter proteins. Current Opinion in Structural Biology *17*, 412–418.

Hornak, V., Abel, R., Okur, A., Strockbine, B., Roitberg, A., and Simmerling, C. (2006). Comparison of multiple Amber force fields and development of improved protein backbone parameters. Proteins *65*, 712–725.

Jardetzky, O. (1966). Simple Allosteric Model for Membrane Pumps. Nature *211*, 969–970.

Jeschke, G. (2012). DEER distance measurements on proteins. Annu Rev Phys Chem *63*, 419–446.

Jorgensen, W., Chandrasekhar, J., Madura, J., Impey, R., and Klein, M. (1983). Comparison of simple potential functions for simulating liquid water. J Chem Phys *79*, 926–935.

Joseph, B., Jeschke, G., Goetz, B. A., Locher, K. P., and Bordignon, E. (2011). Transmembrane gate movements in the type II ATP-binding cassette (ABC) importer BtuCD-F during nucleotide cycle. Journal of Biological Chemistry *286*, 41008–41017.

Joung, I. S., and Cheatham, T. E. (2008). Determination of alkali and halide monovalent ion parameters for use in explicitly solvated biomolecular simulations. J Phys Chem B *112*, 9020–9041.

Kabsch, W. (1993). Automatic processing of rotation diffraction data from crystals of initially unknown symmetry and cell constants. Journal of Applied Crystallography *26*, 795–800.

Kammann, M., Laufs, J., Schell, J., and Gronenbom, B. (1989). Rapid insertional mutagenesis of DNA by polymerase chain reaction (PCR). Nucleic Acids Res *17*, 5404–5404.

Kandt, C., Ash, W. L., and Tieleman, D. P. (2007). Setting up and running molecular dynamics simulations of membrane proteins. Methods *41*, 475–488.

Karpowich, N. K., and Wang, D.-N. (2013). Assembly and mechanism of a group II ECF transporter. Proc. Natl. Acad. Sci. U.S.A. *110*, 2534–2539.

Kirsch, F., Frielingsdorf, S., Pohlmann, A., Ziomkowska, J., Herrmann, A., and Eitinger, T. (2012). Essential amino acid residues of BioY reveal that dimers are the functional S unit of the *Rhodobacter capsulatus* biotin transporter. J Bacteriol *194*, 4505–4512.

Krieger, E., Koraimann, G., and Vriend, G. (2002). Increasing the precision of comparative models with YASARA NOVA--a self-parameterizing force field. Proteins *47*, 393–402.

Kuipers, O. P., de Ruyter, P. G. G. A., Kleerebezem, M., and de Vos, W. M. (1998). Quorum sensing-controlled gene expression in lactic acid bacteria. Journal of Biotechnology *64*, 15–21.

Kunji, E. R. S., Slotboom, D.-J., and Poolman, B. (2003). *Lactococcus lactis* as host for overproduction of functional membrane proteins. Biochim Biophys Acta *1610*, 97–108.

Lanfermeijer, F. C., Picon, A., Konings, W. N., and Poolman, B. (1999). Kinetics and consequences of binding of bona- and dodecapeptides to the oligopeptide binding protein (OppA) of *Lactococcus lactis*†. Biochemistry *38*, 14440–14450.

Langer, G., Cohen, S. X., Lamzin, V. S., and Perrakis, A. (2008). Automated macromolecular model building for X-ray crystallography using ARP/wARP version 7. Nat Protoc *3*, 1171–1179.

Locher, K. P. (2002). The *E. coli* BtuCD Structure: A framework for ABC transporter architecture and mechanism. Science *296*, 1091–1098.

Lomize, M. A., Pogozheva, I. D., Joo, H., Mosberg, H. I., and Lomize, A. L. (2012). OPM database and PPM web server: resources for positioning of proteins in membranes. Nucleic Acids Res *40*, D370–6.

Lubelski, J., van Merkerk, R., Konings, W. N., and Driessen, A. J. M. (2006). Nucleotide-binding sites of the heterodimeric LmrCD ABC-Multidrug Transporter of *Lactococcus lactis* are asymmetric. Biochemistry *45*, 648–656.

Mackerell, A. D., Feig, M., and Brooks, C. L. (2004). Extending the treatment of backbone energetics in protein force fields: limitations of gas-phase quantum mechanics in reproducing protein conformational distributions in molecular dynamics simulations. J Comput Chem *25*, 1400–1415.

Majsnerowska, M., Hänelt, I., Wunnicke, D., Schäfer, L. V., Steinhoff, H.-J., and Slotboom, D. J. (2013). Substrate-induced conformational changes in the S-component ThiT from an Energy Coupling Factor transporter. Structure/Folding and Design *21*, 861–867.

Marreddy, R. K. R., Pinto, J. P. C., Wolters, J. C., Geertsma, E. R., Fusetti, F., Permentier, H. P., Kuipers, O. P., Kok, J., and Poolman, B. (2011). The response of *Lactococcus lactis* to membrane protein production. PLoS ONE *6*, e24060.

Mchaourab, H. S., Steed, P. R., and Kazmier, K. (2011). Toward the fourth dimension of membrane protein structure: insight into dynamics from spin-labeling EPR spectroscopy. Structure *19*, 1549–1561.

Miller, D. M., Olson, J. S., Pflugrath, J. W., and Quiocho, F. A. (1983). Rates of ligand binding to periplasmic proteins involved in bacterial transport and chemotaxis. J Biol Chem *258*, 13665–13672.

Miyamoto, S., and Kollman, P. (1992). Settle - an analytical version of the Shake and Rattle Algorithm for rigid water models. J Comput Chem *13*, 952–962.

Mobley, D. L., Chodera, J. D., and Dill, K. A. (2006). On the use of orientational restraints and symmetry corrections in alchemical free energy calculations. J Chem Phys *125*, 084902

Moody, J. E., Millen, L., Binns, D., Hunt, J. F., and Thomas, P. J. (2002). Cooperative, ATP-dependent association of the nucleotide binding cassettes during the catalytic cycle of ATP-binding cassette transporters. J Biol Chem *277*, 21111–21114.

Murshudov, G. N., Vagin, A. A., and Dodson, E. J. (1997). Refinement of macromolecular structures by the maximum-likelihood method. Acta Crystallographica Section D *53*, 240–255.

Müller, A., Severi, E., Mulligan, C., Watts, A. G., Kelly, D. J., Wilson, K. S., Wilkinson, A. J., and Thomas, G. H. (2006). Conservation of structure and mechanism in primary and secondary transporters exemplified by SiaP, a sialic acid binding virulence factor from *Haemophilus influenzae*. J Biol Chem *281*, 22212–22222.

Neubauer, O., Alfandega, A., Schoknecht, J., Sternberg, U., Pohlmann, A., and Eitinger, T. (2009). Two essential arginine residues in the T components of energy-coupling factor transporters. J Bacteriol *191*, 6482–6488.

Neubauer, O., Reiffler, C., Behrendt, L., and Eitinger, T. (2011). Interactions among the A and T units of an ECF-type biotin transporter analyzed by site-specific crosslinking. PLoS ONE *6*, e29087.

Oldham, M. L., Davidson, A. L., and Chen, J. (2008). Structural insights into ABC transporter mechanism. Current Opinion in Structural Biology *18*, 726–733.

Orelle, C. (2003). The conserved glutamate residue adjacent to the Walker-B Motif is the catalytic base for ATP hydrolysis in the ATP-binding cassette transporter BmrA. Journal of Biological Chemistry *278*, 47002–47008.

Pannier, M., Veit, S., Godt, A., Jeschke, G., and Spiess, H. W. (2000). Dead-time free measurement of dipole–dipole interactions between electron spins. J. Magn. Reson. *142*, 331–340.

Polyhach, Y., Bordignon, E., and Jeschke, G. (2011). Rotamer libraries of spin labelled cysteines for protein studies. Phys Chem Chem Phys *13*, 2356–2366.

Procko, E., O'Mara, M. L., Bennett, W. F. D., Tieleman, D. P., and Gaudet, R. (2009). The mechanism of ABC transporters: general lessons from structural and functional studies of an antigenic peptide transporter. The FASEB Journal *23*, 1287–1302.

Ray, F. A., and Nickoloff, J. A. (1992). Site-specific mutagenesis of almost any plasmid using a PCR-based version of unique site elimination. BioTechniques *13*, 342–348.

Rees, D. C., Johnson, E., and Lewinson, O. (2009). ABC transporters: the power to change. Nat Rev Mol Cell Biol *10*, 218–227.

Rodionov, D. A., Hebbeln, P., Eudes, A., Beek, ter, J., Rodionova, I. A., Erkens, G. B., Slotboom, D. J., Gelfand, M. S., Osterman, A. L., Hanson, A. D., et al. (2009). A novel class of modular transporters for vitamins in prokaryotes. J Bacteriol *191*, 42–51.

Rodionov, D. A., Hebbeln, P., Gelfand, M. S., and Eitinger, T. (2006). Comparative and functional genomic analysis of prokaryotic nickel and cobalt uptake transporters: evidence for a novel group of ATP-binding cassette transporters. J Bacteriol *188*, 317–327.

Rodionov, D. A., Vitreschak, A. G., (null), and Gelfand, M. S. (2002). Comparative genomics of thiamin biosynthesis in procaryotes. New genes and regulatory mechanisms. J Biol Chem *277*, 48949–48959.

Ryan, R. M., Compton, E. L. R., and Mindell, J. A. (2009). Functional characterization of a Na+-dependent aspartate transporter from *Pyrococcus horikoshii*. J Biol Chem *284*, 17540–17548.

Sander, C., and Schneider, R. (1991). Database of homology-derived protein structures and the structural meaning of sequence alignment. Proteins *9*, 56–68.

Siche, S., Neubauer, O., Hebbeln, P., and Eitinger, T. (2010). A bipartite S unit of an ECF-type cobalt transporter. Res. Microbiol. *161*, 824–829.

Singh, U. C., and Kollman, P. A. (1984). An approach to computing electrostatic charges for molecules. J Comput Chem *5*, 129–145.

Slotboom, D. J., Konings, W. N., and Lolkema, J. S. (2001). Cysteine-scanning mutagenesis reveals a highly amphipathic, pore-lining membrane-spanning helix in the glutamate transporter GltT. J Biol Chem *276*, 10775–10781.

Steinhoff, H. J., Radzwill, N., Thevis, W., Lenz, V., Brandenburg, D., Antson, A., Dodson, G., and Wollmer, A. (1997). Determination of interspin distances between spin labels attached to insulin: comparison of electron paramagnetic resonance data with the X-ray structure. Biophys J *73*, 3287–3298.

van der Heide, T., Stuart, M. C. A., and Poolman, B. (2001). On the osmotic signal and osmosensing mechanism of an ABC transport system for glycine betaine. The EMBO Journal *20*, 7022–7032.

Vonrhein, C., Blanc, E., Roversi, P., and Bricogne, G. (2007). Automated structure solution with autoSHARP. Methods Mol. Biol. *364*, 215–230.

Wagner, S., Klepsch, M. M., Schlegel, S., Appel, A., Draheim, R., Tarry, M., Högbom, M., van Wijk, K. J., Slotboom, D. J., Persson, J. O., et al. (2008). Tuning *Escherichia coli* for membrane protein overexpression. Proc. Natl. Acad. Sci. U.S.A. *105*, 14371–14376.

Wang, B., Dukarevich, M., Sun, E. I., Yen, M. R., and Saier, M. H. (2009). Membrane porters of ATP-binding cassette transport systems are polyphyletic. J. Membr. Biol. *231*, 1–10.

Wang, J., Wolf, R. M., Caldwell, J. W., Kollman, P. A., and Case, D. A. (2004). Development and testing of a general Amber force field. J Comput Chem *25*, 1157–1174.

Wang, T., Fu, G., Pan, X., Wu, J., Gong, X., Wang, J., and Shi, Y. (2013). Structure of a bacterial energy-coupling factor transporter. Nature *497*, 272–276.

Xu, K., Zhang, M., Zhao, Q., Yu, F., Guo, H., Wang, C., He, F., Ding, J., and Zhang, P. (2013). Crystal structure of a folate energy-coupling factor transporter from *Lactobacillus brevis*. Nature *497*, 268–271.

Zhang, J., Lau, M. W., and Ferré-D'Amaré, A. R. (2010a). Ribozymes and Riboswitches: Modulation of RNA Function by Small Molecules. Biochemistry *49*, 9123–9131.

Zhang, P., Wang, J., and Shi, Y. (2010b). Structure and mechanism of the S component of a bacterial ECF transporter. Nature *468*, 717–720.

LIST OF PUBLICATIONS:

Maria Majsnerowska*, Inga Hänelt*, Dorith Wunnicke, Lars V. Schäfer,Heinz-Jurgen Steinhoff, and Dirk J. Slotboom, (2013). Substrate-Induced Conformational Changes in the S-Component ThiT from an Energy Coupling Factor Transporter. Structure / Folding and Design *21*, 861–867.

Ronnie P.-A. Berntsson*, Josy ter Beek*, **Maria Majsnerowska***, Ria H. Duurkens, Pranav Puri, Bert Poolman, and Dirk J. Slotboom. (2012). Structural divergence of paralogous S components from ECF-type ABC transporters. Proc. Natl. Acad. Sci. U.S.A. *109*, 13990–13995.

Guus B. Erkens, **Maria Majsnerowska**, Josy ter Beek, and Dirk J. Slotboom. (2012). Energy Coupling Factor-Type ABC Transporters for Vitamin Uptake in Prokaryotes. Biochemistry *51*, 4390–4396.

Guus B. Erkens, Ronnie P.-A. Berntsson, R. P.-A., Faizah Fulyani, **Maria Majsnerowska**, Andreja Vujičić-Žagar, Josy ter Beek, Bert Poolman, and Dirk J. Slotboom, (2011). The structural basis of modularity in ECF-type ABC transporters. Nat Struct Mol Biol *18*, 755–760.

*Authors contributed equally.

ACKNOWLEDGMENTS

After spending over four years on performing experiments and half a year on writing this thesis, the remaining task is to acknowledge people who supported and encouraged me during my PhD. I find it very difficult to express my gratitude in the right words, but I will do my best.

Dirk, I could not have imagined a better supervisor. Thank you for guiding me through my PhD, for your trust in me, support, understanding and patience. I'm grateful for all the freedom you gave me, your precious advice and great interest in all the results I obtained in the lab. Your door was always open to discuss all the smaller or bigger problems I encountered. I have learned a lot from you!

Inga and *Guus*, my paranymphs, I'm so happy that I will have you next to me during my defense. Thank you for coming back to Groningen specially for this occasion. You have been not only the best labmates ever- always helpful and involved but, what is even more precious to me, great friends. I could always be honest with you, talk to you when my motivation dropped and share all the successes and happy moments. I will miss you a lot here! (I already do...) I hope we will stay in touch wherever we go! *Guus*, thank you for translating my summary to Dutch!

Bert, thank you for all the helpful comments and suggestions and sharing your knowledge!

I would also like to thank the Dirk's ECF/Glt team and all the members of the Enzymology group: *Guus, Inga, Josy, Ronnie, Maarten, Jacek, Justyna, Ria, Dorith, Gemma, Tejas, Andreja, Frans, Duygu, Stephanie, Nobina, Gea, Pranav, Jan Peter, Anton, Jeanette, Arnold, Faizah, Astri, Petra, Karin, Siva, Sonja, Lotteke, Michael, Katja, Albert, Raj, Rianne, Jonas, Fabrizia, Armağan, Alicja, Joury, McDonald, Nadia, Anna, Liesbeth* thank you all for the pleasant atmosphere in the labs, during coffee/cake breaks, lunches and outside Nijenborgh 4 - Enzymology parties, dinners and BBQs in the park.

Josy, Ronnie, Maarten from the very beginning of my PhD you were great colleagues always willing to help with translating Dutch official letters to English, explaining the Dutch culture and rules. We had so much fun together outside the lab as well - birthday parties, dinners and many more.

Ria, thank you for all the experiments you've done for me in the isotope lab. I appreciate it a lot!

Dorith, you've been a great collaborator during the EPR project. I'm very happy that you've joined our team for the postdoc! I enjoyed sharing the office with you!

Jacek and *Justyna,* thank you for all the support, understanding and our Polish coffee breaks.

Anton – a god of cloning :) - thank you for all your helpful advice.

Karlien, Sanda and *Durkje,* thank you for all the administrative support.

My stay in Groningen would not be the same without my great Polish friends (and their non-Polish partners ;)): *Hania, Gosia, Sławek, Jagódka, Agata, Piotrek, Jacek, Wojtek, Justyna, Michiel, Pani Isia, Pani Zosia, Ewa, Łukasz, Milenka, Kasia, Maciek, Dawidek, Mariusz, Dorothy, Dropiu, Marta, Gabi, Kasia, Hendrik Jan i Oskarek*. Kochani, dziękuje Wam za wszystkie wspólne obiady, wycieczki, pikniki, imprezy, bez których weekendy i wieczory w Groningen byłyby bardzo smutne. Dzięki Wam czułam i czuję się tu jak w domu!

Haniu, dziękuję za to, że tak długo ze mną mieszkałaś: za Twoją cierpliwość i wyrozumiałość dla mojego bałaganiarstwa, wsparcie, wesołe wspólne gotowanie i długie wieczorne rozmowy. Te wszystkie spędzone razem chwile sprawiły, że stałaś się dla mnie bardzo bliska. Cieszę się, że zostajesz w Groningen na kolejne co najmniej dwa lata. Życzę Ci spełnienia wszystkich Twoich marzeń i planów.

Gosiu, Sławku, Agatko Wam również chciałam szczególnie podziękować za Wasze wsparcie w trudnych chwilach! Będzie mi tu Was bardzo brakowało! Mam nadzieję, że mimo tego, że nasze drogi się rozchodzą, pozostaniemy w kontakcie i będziemy się odwiedzać.

Pani Isiu, dziękuję za bycie naszą "groningeńską Mamą".

I would like to thank my friends who supported me from the distance: *Agata, Radek, Gosia, Malwina, Krzysiek, Julita, Kornel, Agnieszka, Paweł, Hania i Łukasz*. Bardzo się cieszę, że za każdym razem, kiedy się spotykamy, mamy sobie ciągle wiele do powiedzenia! Dziękuję za Waszą przyjaźń!

At last but definitely not least I thank my family! Kochani, *Mamo, Tato, Maćku, Asiu, Jadziu, Babciu, Mateuszu* i *Mamo Gabrysiu,* Wam dedykowana jest ta rozprawa.

Mamo i Tato, ciężko wyrazić słowami wdzięczność za wszystko to, co od Was dostałam. Tutaj dziękuję Wam za wsparcie na każdym etapie mojej edukacji. Bez tego nie doszłabym tak daleko!

Jadzia, dziękuje Ci za piękny projekt okładki!

Maćku, (mój najdroższy Misiu) dziękuję Ci za Twój bezgraniczny optymizm, wiarę we mnie, olbrzymie pokłady cierpliwości i miłości. Bez tego wszystkiego ta książka by nigdy nie powstała! Kocham Cię!

Marysia